Modeling and analysis of competing dynamic ecological systems

by

YAN KUANG

B.S., Tianjin University of Finance and Economics, 2011

AN ABSTRACT OF A DISSERTATION

submitted in partial fulfillment of the requirements for the degree

DOCTOR OF PHILOSOPHY

Department of Industrial and Manufacturing Systems Engineering
College of Engineering

KANSAS STATE UNIVERSITY
Manhattan, Kansas

2017

Abstract

The dynamic relationship between competing ecological systems has long been and will continue to be one of vital topics in both ecology and mathematical ecology because of its importance and universal existence. Mathematical modeling has become an effective tool to model and simulate the dynamic system, providing decision makers with strategy recommendations. Although a great amount of previous work has attempted to model the biological mechanisms including dispersal, only rarely has there been a systematic investigation on different spatial effects.

The author introduces spatial games as a modeling approach with different constructions towards different dynamic systems in order to benefit from the systematic research on spatial dynamics when studying the competing ecological systems. This research developed models of two systems: (1) two-spotted spider mite prey-predator system; (2) tomato spotted wilt virus (TSWV) and west flower thrips (WFT) vector-borne disease system.

For two-spotted spider mite system, the author presented four spatial mathematical models as well as a novel spatial game model to describe the spatial movement of two competing species.

For the TSWV-WFT system, a spatial game was introduced to describe the spatial dynamics of adult thrips and the novel model was validated with experimental data. The author also gave suggestions for efficiently controlling the vector-borne disease by performing sensitivity analysis towards parameters.

The major contribution of this research is to introduce spatial games as a tool to describe the dynamic schemes in ecological systems. Compared to a traditional dynamic model, a spatial game model is more expressive and informative. This approach uses a payoff function and a

movement probability function that can be adjusted based on habits, characteristics and mobility schemes of different competing entities, which has enriched its modeling power.

The methodology and modeling approach used in this dissertation can be applied to other competing species dynamic systems, and have a broad impact on research areas related to mathematical ecology, biology modeling, epidemiology, pest control, vector-borne disease control, and ecological decision-making processes.

Modeling and analysis of competing dynamic ecological systems

by

YAN KUANG

B.S., Tianjin University of Finance and Economics, 2011

A DISSERTATION

submitted in partial fulfillment of the requirements for the degree

DOCTOR OF PHILOSOPHY

Department of Industrial and Manufacturing Systems Engineering
College of Engineering

KANSAS STATE UNIVERSITY
Manhattan, Kansas

2017

Approved by:

Major Professor
David Ben-Arieh

Copyright

Abstract

The dynamic relationship between competing ecological systems has long been and will continue to be one of vital topics in both ecology and mathematical ecology because of its importance and universal existence. Mathematical modeling has become an effective tool to model and simulate the dynamic system, providing decision makers with strategy recommendations. Although a great amount of previous work has attempted to model the biological mechanisms including dispersal, only rarely has there been a systematic investigation on different spatial effects.

The author introduces spatial games as a modeling approach with different constructions towards different dynamic systems in order to benefit from the systematic research on spatial dynamics when studying the competing ecological systems. This research developed models of two systems: (1) two-spotted spider mite prey-predator system; (2) tomato spotted wilt virus (TSWV) and west flower thrips (WFT) vector-borne disease system.

For two-spotted spider mite system, the author presented four spatial mathematical models as well as a novel spatial game model to describe the spatial movement of two competing species.

For the TSWV-WFT system, a spatial game was introduced to describe the spatial dynamics of adult thrips and the novel model was validated with experimental data. The author also gave suggestions for efficiently controlling the vector-borne disease by performing sensitivity analysis towards parameters.

The major contribution of this research is to introduce spatial games as a tool to describe the dynamic schemes in ecological systems. Compared to a traditional dynamic model, a spatial game model is more expressive and informative. This approach uses a payoff function and a

movement probability function that can be adjusted based on habits, characteristics and mobility schemes of different competing entities, which has enriched its modeling power.

The methodology and modeling approach used in this dissertation can be applied to other competing species dynamic systems, and have a broad impact on research areas related to mathematical ecology, biology modeling, epidemiology, pest control, vector-borne disease control, and ecological decision-making processes.

Acknowledgements

Here, I owe my gratitude to all those who have made this dissertation possible and because of whom my journey to Ph.D. graduation is cherishable.

First, I would like to express my sincere gratitude to my advisor Dr. David Ben-Arieh, for the continuous support of my Ph.D. study, for his patience, motivation, understanding and immense knowledge. His guidance and support helped me throughout the research and study. I would never have been able to finish my dissertation without his guidance. Sincere thanks also go to my co-major advisor, Dr. Chih-Hang Wu, for his generous support and continuous supervision for my research and my study, especially for his encouragement and valued advice during hard times. His support is indispensable for completion of my Ph.D. study.

I would like to give my gratitude to my committee members Dr. David Margolies and Dr. James Nechols from the Department of Entomology for sharing experimental data and expert guidance on related research background, which makes this dissertation possible and valuable. I would also like to thank Dr. Todd Easton for serving as my committee member. His enthusiasm and rigorous scientific attitude for research and work inspired me. I would like to extend my thanks to Dr. Anthony Joern for serving as the outside chairperson for my final examination.

I would like to express my appreciation to my department head, Dr. Bradley Kramer, for the welcome, encouragement, and continuous support throughout my study. I would also like to thank Dr. Malgorzata Rys for her guidance and excellent assistance on teaching. I also thank Dr. E. Stanley Lee, Dr. Shuting Lei, Dr. Shing I. Chang, Dr. Jessica Heier Stamm and all the other faculty members for all they have taught me. My thanks go out to our department staff: Mrs. Vicky Geyer, Myra Peoples, Doris Galvan and Miss Lacey Brummer, for their warm and kind assistance.

I would like to express my gratitude to my colleagues and friends: Dr. Xiaoxu Song, Dr. Zhenzhen Shi, Dr. Qi Zhang, Dr. Meng Zhang, Dr. Mohammed Obeidat, Dr. Xinli Xiao, Mr. Fabio Vitor, Mr. Eric Carley, Mrs. Nibal Albashabsheh, Mrs. Hui Chen, Mrs. Weijia Jia, Mrs. Hongmin Li, Mrs. Xiuxiang Sun and Miss Hillary Hendricks and all others for their help and support for my study and my life. To my friends outside of the U.S., thank you for being there whenever I needed a friend.

Last but not the least, this dissertation is dedicated to my family, including my parents, Zhengke Kuang and Gengping He, my parents-in-law, Baozhong Zhao and Binmei Sun, my brother, Biao Kuang, for supporting me spiritually, having faith in me, and encouraging me to pursue this advanced degree. I must express my deep appreciation to the person who supports me more than anyone else: my husband, Songnian Zhao. Thank you for your love, patience, and devotion. I extend my thanks to my beloved daughter, Haley Zhao, for lighting the world and cheering me up.

Table of Contents

List of Figures

List of Tables

Chapter 1 - Introduction

1.1 Introduction and Background

The general purpose of modeling is to help explain the mechanics of real-world phenomenon. The process of modeling can be broken down to four main steps: 1) identifying the major variables that can explain the process, 2) identifying the main factors as physical parameters that are essential on governing the real-world situations, 3) building equations which describe and summarize the whole system, 4) validating the model [1]. It has been noted that an effective model should include the following features [2, 3]:

1. Simplicity. Models with fewer variables and parameters are always more favorable than complicated models, since they are easier to understand and test.
2. Reality. This is the core topic of modeling. Models should be able to illuminate the real-world situation.
3. Generality. Make the model general and expressive so that it can be adapted to other cases.
4. Accuracy. The purpose of the modeling is to predict the system, so validation is essential to test the accuracy of a model.

Mathematical biology is a powerful field which utilizes mathematical models to explore data-rich information sets analyzing complex biological mechanisms and to compute and simulate their associated dynamic systems. This type of modeling plays an important role in determining the interactions within a system which describes the properties of a physical system over time, such as the changes of a species population or its spatial movement pattern. An example is analyzing populations where the model attempts to link individual behaviors to population

dynamics. This type of approach provides insights on the biological processes and predicts changes to the total population system.

1.2 Research Motivation

Previous work has attempted to determine biological mechanisms including dispersal and the interaction between species. Studying the spatial effect of the biological process, which includes both dispersal and species interactions, offers researchers a critical view of movement within populations. Spatial effects are unique when considering the relationships between plants and insects. The challenge is accurately identifying and predicting their individual actions and reactions to their own interactions.

Cunniffe et al. [4] outlined thirteen specific challenges related to disease prediction and control in modeling plant diseases. The challenges include understanding temporal changes in host availability, from plant organs to populations and capturing host spatial structure, even when data are limited. Several methods have been attempted to reduce or prevent plant damage, such as releasing predators of the pest (in the case of insects), or treating with chemicals in the case of disease or pests. Hence, understanding the dynamics of a prey-predator system as well as the dynamics of the vector-borne disease system can be very important. Considerable research has sought efficient control strategies to help decision makers mitigate or control the plant damage. Developing useful strategies can direct the needs of general biological models and methodologies in future mathematical research.

For the sake of understanding the interaction mechanism of different systems to control plant pests, collaborative research with professors in the Department of Entomology at Kansas State University was developed. This research aims to develop new spatial models to study the

impacts of spatial movement and interaction among species, in order to systematically investigate different spatial schemes. This research includes two main ecology systems as follows:

1. **Two-Spotted Spider Mite system.** The two-spotted spider mite, *Tetranychus urticae*, is a species of plant eating mites which is widely regarded as a pest. Its predator, *Phytoseiulus persimilis*, effectively controls spider mite populations. There are quite a few models that have been discussed for this prey-predator system. Specific goals are:
    - Study the dynamic system with traditional system dynamics models, and compare and validate different methods
    - Develop a novel spatial game model to simulate the spatial transition of prey and predator, and compare the new model with traditional dynamics models discussed earlier
    - Perform stability analysis for the system
2. **Tomato Spotted Wilt Virus (TSWV) and West Flower Thrips (WFT) vector-borne disease system.** TSWV is a virus that infects more than 1000 plant species, which include agronomic and ornamental crops as well as weed hosts, causing significant financial loss. Western flower thrips (WFT) is considered the most efficient vector due to its wide distribution and the overlapping host ranges with TSWV [5, 6]. Studying the virus-vector-host plant dynamic system can be beneficial to controlling the thrips population and protecting the plants. For this system, specific goals are:
    - Develop mathematical models for TSWV-WFT

- Develop a novel spatial game model to simulate the movement of adult thrips, and validate the model with experiment data
- Identify key factors that impact plants infection level
- Discuss the proper intervention strategies and seek efficient control strategies

1.3 Proposed Methodologies

To understand the changes of species population and movement, a key task is to study their associated spatial effects. Different species have different preferences regarding where they travel. Hence, a general approach is required to describe each mobile behavior. In this research, a new methodology demonstrates an application of spatial game theory into two different competing biological systems. The spatial game perspective considers the benefits and costs at each location for the species and prompts their reactions, representing the dynamics of systems. Both modeling scenarios, two spotted spider mites vs. predators and TSWV vs. WFT, consist of three parts:

1. a payoff function, which assigns different payoff values according to the preference of players (different species),
2. a move probability function that controls the move likelihood and direction of the players based on the payoff values of each location,
3. an interaction function that describes the relationship between each subject species. For instance, the function could represent the predation process for prey-predator systems, or the virus transmission process along with the development of the vector for vector-borne disease systems.

Compared to a traditional dynamic model, a spatial game model is more general and informative. It can capture the different habits, characteristics and different mobility preferences of the different competing species. Thus, it can be extended to other systems.

This new methodology is applied separately to each of the case scenarios: one is for the prey-predator system; the other is for the vector-borne disease system. The new game-based model was compared with traditional dynamic models and validated with experimental data. The results of this research can be expanded and applied to other systematic investigations of biological systems with spatial dynamics.

1.4 Research Map

This research plan provides effective mathematical model for studying the spatial effect of biological dynamic systems. Figure 1.1 shows a research map that describes the research objective, research methodologies, and potential research contributions illustrating the use of the spatial game approach.

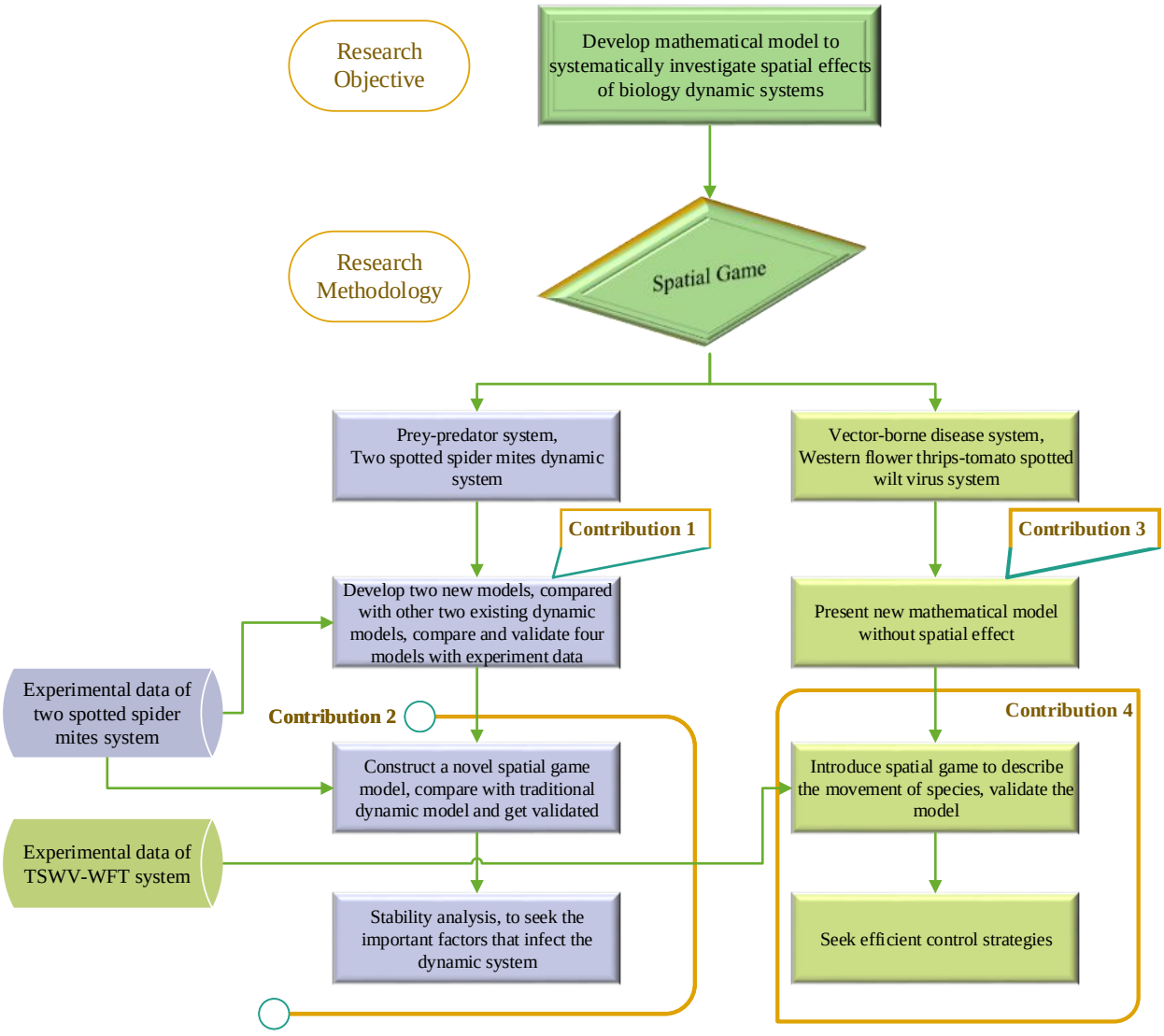

Figure 1.1 Research map

1.5 Outlines

This dissertation is organized into the following seven chapters:

Chapter 1) Introduction: interest in the research subject areas.

Chapter 2) Literature Review: for the study of prey-predator system and the vector-borne disease system, as well as the introduction to basic spatial evolutionary game.

Chapter 3) Mathematical Model for Two-Spotted Spider Mites System: Verification and Validation: two new models are developed and compared with traditional dynamic model, and are validated by using experiment data.

Chapter 4) Modeling Dynamic Evolutionary Systems Using Spatial Games: for the first time, the spatial game model for prey-predator system is developed and compared with traditional dynamic model.

Chapter 5) Using Spatial Games to Model and Simulate Tomato Spotted Wilt Virus-Western Flowers Thrip Dynamic: for the first time, the spatial game perspective is applied to vector-borne disease system with TSWV-WFT system, and the new model is validated with experiment data.

Chapter 6) Conclusions, Contributions, and Future Research: the main conclusions and contributions are summarized and the potential future works are discussed.

Chapter 2 - Literature Review

2.1 Spatial Game

In a classic game, there are three basic components: players, strategies, and payoffs. Each player rationally chooses the strategy independently based on the complete information they have about the game. The players should choose strategies that maximize their payoffs. Game theory, as a powerful tool for modeling the interaction of decision makers, has been applied to different areas, for instance, economics [7, 8], supply chain [9-11], network design [12-14], and epidemiology [15-17].

The spatial evolutionary game is a combination of classic game theory and spatial effects. In this type of game, players at different locations may have different information, and they make their decisions based on an updating rule that relates to the designed payoff functions [18]. Game theory was first applied to evolutionary biology by Lewontin [19]. He assumed that species were playing games against nature in order to seek strategies that can minimize the probability of being extinct. Since then, significant attention has been devoted to evolutionary game theory as a unifying framework for studying evolution in different disciplines such as animal dispersal [20], plant growth and reproduction [21]. May [22] extended this concept spatially to study the evolution of cooperative behavior by placing the players in a two-dimensional spatial array with ever-changing strategies. For spatial evolutionary game, several common updating rules and schemes are reviewed by Roca et al. [23] and Newth and Cornforth [24].

2.2 Previous Mathematical Models of Prey-predator System

2.2.1 General Models

Diffusion plays an important role in the system of prey and predators. In order to improve the interaction of prey and predators, it is important to understand the effect of diffusion (movement). Since the great work of Lotka [25] and Volterra [26], modeling predator–prey interaction has been one of the primary themes in mathematical ecology. The development and application of mathematical models become an important tool for investigating and quantifying such effects. The pioneering work on reaction diffusion model was introduced by Fisher [27] and Skellam [28]. Since then, diffusion effect in ecology and biology system has attracted much research attention [29-33].

For prey-predator systems, modeling approaches using either or both of self-diffusion model and the cross-diffusion model are commonly presented in literature. Self-diffusion has been taken into consideration by a number of studies when modeling prey-predator systems [34-36].

The general form of self-diffusion model of prey-predator is listed below.

$$\frac{\partial u}{\partial t} = f(u) - f_1(u, v) + D_u \nabla^2 u \tag{2.1}$$

$$\frac{\partial v}{\partial t} = f_2(u, v) - f(v) + D_v \nabla^2 v \tag{2.2}$$

where $f(u)$ is the birth rate function of prey and $f(v)$ is the death rate function of predator, $f_1(u, v)$ represents the interaction function which leads to a decreasing number of prey and $f_2(u, v)$ is the interaction function which contributes to the increases of predator. D_u, D_v is the self-diffusion coefficient, while $\nabla^2 u$ and $\nabla^2 v$ are the Laplacian operators in two dimensions, representing the species movement on a 2-D grid.

The self-diffusion model demonstrates the movement among each group. However, the prey may be able to recognize the predator, and thus the prey would keep away from predators to avoid being caught. On the other hand, predators tend to get closer to the prey. This phenomenon is called cross-diffusion, first introduced by Kerner [37], where both prey and predator are using opposing goals. Cross-diffusion has primarily been applied to competing population dynamic systems by Shigesada et at. [38]. The value of the cross-diffusion coefficient may be positive, negative or zero. The positive cross diffusion coefficient indicates the movement of the species in the direction of lower concentration of another species while negative cross-diffusion coefficient represents a situation when one species tends to diffuse in the direction of higher concentration of the other species. A variety of work has been done to investigate the prey-predator system through utilizing cross-diffusion [39-44].

The general form of cross-diffusion model of prey-predator is:

$$\frac{\partial u}{\partial t} = f(u) - f_1(u,v) + d_{11}\nabla^2 u + d_{12}\nabla^2 v \tag{2.3}$$

$$\frac{\partial v}{\partial t} = f_2(u,v) - f(v) + d_{21}\nabla^2 u + d_{22}\nabla^2 v \tag{2.4}$$

where $f(u)$ is the birth rate function of prey and $f(v)$ is the death rate function of predator, $f_1(u, v)$ stands for the interaction function causing the decrease of prey and $f_2(u, v)$ is the interaction function resulting in the increase of predator; d_{11} and d_{22} are the self-diffusion coefficients of prey and predator, respectively; d_{12}, and d_{21} are the cross-diffusion coefficients of predator and prey, respectively. If $d_{12} > 0$, and $d_{21} < 0$, it means that the prey species prefer to diffuse in the direction of lower density of the predator species, and the predator species tends to move to the direction with higher concentration of the prey species.

Cross-diffusion is able to generate many different kinds of spatiotemporal patterns. The interaction of self- and cross-diffusion is considered an vital mechanism for the appearance of

complex spatiotemporal dynamics in ecological models [45-47]. Recognizing and analyzing these complex dynamics allows for a more realistic understanding of the complete biological system's behavior.

Despite the successes of the self-diffusion model and cross-diffusion model, the prey-taxis effect model in one dimension has also been studied extensively. 'Taxis' describes the phenomenon that individuals change their movement due to a stimulus. Prey-taxis was first proposed by Kareiva and Odell [48]. Later it was defined as the movement of predators controlled by prey density [49]. As a result of these variations in the definitions in the literature, there are two different understandings of prey-taxis model. One assumes that the directed movement of predator density is proportional to the gradient of prey density [50-54], while the other assumption is that the directed movement of predator density is proportional to the gradient of some stimulus [55-57]. To resolve these possible modeling discrepancies, equations of the reaction–diffusion–advection type are used to obtain solutions for these prey-taxis models.

The general form of prey-taxis model in one dimension is presented below[57-60]:

$$\frac{\partial u}{\partial t} = f(u) - f_1(u,v) + d_1 \frac{\partial^2 u}{\partial x^2} \tag{2.5}$$

$$\frac{\partial v}{\partial t} = f_2(u,v) - f(v) - \frac{\partial (vw)}{\partial x} + d_2 \frac{\partial^2 v}{\partial x^2} \tag{2.6}$$

$$\frac{\partial w}{\partial t} = T \frac{\partial u}{\partial x} + d_3 \frac{\partial^2 w}{\partial x^2} \tag{2.7}$$

where $f(u)$ is the birth rate function of prey, $f(v)$ is the death rate function of predator, $f_1(u, v)$ stands for the interaction function that causes the decrease of prey and $f_2(u, v)$ is the interaction function that have effects on the increase of predator, $w(x, t)$ is the velocity of the predators, d_1 and d_2 are the non-negative diffusivity constants of the prey and predator, and d_3 is an effect of social behavior, T is the non-negative taxis coefficient that represents the sensitivity of the predators to the heterogeneous density distribution of prey.

2.2.2 Response Function

During the process of modeling prey-predator systems, a substantial element of the prey-predator relationship is the response function denoted by *f(u,v)* in the models. There are two common types of functional response: prey-dependent and predator-dependent. Prey-dependent means that the sole determining factor of the functional response is prey density, while the predator-dependent response function relies on both prey and predator densities. In most current research, the prey-dependent function plays a fundamental role in predator-prey theory, such as Holling's Type functional response [61-69], which includes Holling type I-III originally introduced by Holling [70, 71] and Holling type IV presented by Andrews [72]. The Holling type response function has attracted significant attention in population dynamics of prey-predator systems. The Holling- type II , III and Holling type IV response functions are listed here:

- $f(u,v) = \frac{mu}{1+bv}$, Holling- type II function;
- $f(u,v) = \frac{mu^2}{1+au^2}$, Holling- type III function;
- $f(u,v) = \frac{mu}{1+bu+au^2}$, Holling type IV function.

However, researchers have argued that the functional response should depend on both prey and predator densities when predators need to search for food and then share or compete for food. The predator-dependent functional response includes both predator and prey densities. There is substantial evidence indicating that predator-dependent functional responses are frequent occurrences, both in laboratory and natural systems [73], and they are more realistic than dependence only on absolute prey density [74]. A number of researchers have discussed the predator dependent response function for different systems [75-87]. One of the most popular functional responses is the Beddington-DeAngelis functional response [73, 88-93], which is

originally proposed by Beddington [78] and DeAngelis et al. [81]. The function is noted as: $f(u,v) = \frac{uv}{\partial+\beta u+\gamma v}$.

To resolve any concerns in the differences between the models, some scholars compare their model with different response functions, both prey-dependent and predator-dependent. For instance, the response functions that have been discussed by Chakraborty et al. [49] are listed here:

- $f(u,v) = \frac{u}{\emptyset+u}$; where ϕ is the level of prey at which half of the maximum consumption rate occurs.
- $f(u,v) = \frac{u}{\emptyset+u+\beta v}$; where β is the predator interference constant.
- $f(u,v) = \frac{u}{(\emptyset+u)(1+\beta v)}$;
- $f(u,v) = \frac{u}{(\emptyset+u)}(1-(1-\mu u)e^{-\mu u})$; where μ is a constant

2.2.3 Summary

Considerable research into prey-predator systems has created a foundation of effective modeling of these types of biological systems. What is clear is that such models must be customized to apply to their specific biological systems. As an extension of current research, there are unique characteristics when multiple species are involved in the same environment. The effort in this research was to uncover a more general predator-prey modeling approach that would be effective in simulating prey-predator dynamic systems. Also, the author compared four traditional dynamical models, which systematically discussed the different spatial effects that impact prey-predator systems.

2.3 Previous Mathematical Models of Tomato Spotted Wilt Virus and Western Flower Thrips System

Even though the tomato spotted wilt virus (TSWV) and western flower thrips (WFT) have created significant global economic loss, the mathematical modeling research for this specific plant disease system is very limited. There are only a few models that have considered the complex interactions among the virus-vector-host plant. Jones et al [94] summarized that there were only two published papers [95, 96] involving thrips vector when modeling the TSWV epidemics by 2010. Several models have been developed since then, but most of them only concentrated on biology perspective, such as the analysis of weather condition influences [97-101] and temperature influences [102, 103]. The work presented in Section 5.2 serves as the first study to model and simulate the TSWV-WFT systems which emphasized the transmission characteristics in the mutual interaction among virus-vector-host plants. Most recently, Ogada er al [104] proposed a predictive model that considered WFT's specific life cycle and preference of behavior of thrips towards host plants.

For the TSWV and WFT systems, the virus spread and transmission is impacted by a variety of factors such as development rate, mortality rate and preferential behavior of the vector [105-110]. Mathematical models help to quantify the virus-vector-host plant dynamic process. In this study, Chapter 5 is the first work that has attempted to construct mathematical models for this specific system and further employs the spatial game approach and validated using experimental data.

Chapter 3 - Mathematical Model for Two-Spotted Spider Mites System: Verification and Validation

Chapter 3 is based on the paper "Mathematical Model for Two-Spotted Spider Mites System: Verification and Validation" published in Open Journal of Modeling and Simulation (2017), 5: 13-31.

Abstract

This paper presents and compares four mathematical models with unique spatial effects for a prey-predator system, with *Tetranychus urticae* as prey and *Phytoseiulus persimilis* as predator. *Tetranychus urticae*, also known as two-spotted spider mite, is a harmful plant-feeding pest that causes damage to over 300 species of plants. Its predator, *Phytoseiulus persimilis*, a mite in the Family *Phytoseiidae*, effectively controls spider mite populations. In this study, we compared four mathematical models using a numerical simulation. These models include two known models: self-diffusion, and cross-diffusion, and two new models: chemotaxis effect model, and integro diffusion model, all with a Beddington-DeAngelis functional response. The modeling results were validated by fitting experimental data. Results demonstrates that interaction scheme plays an important role in the prey-predator system and that the cross-diffusion model fits the real system best. The main contribution of this paper is in the two new models developed, as well as the validation of all the models using experimental data.

3.1 Introduction

The two-spotted spider mite, *Tetranychus urticae*, is a species of plant-feeding mites generally considered to be a pest. It is the most widely known member of the Family *Tetranychidae*

and is a harmful pest in greenhouses and on field-grown crops. Previous reports have stated that *Tetranychus urticae* infests over 300 species of plants, including ornamental plants such as arborvitae, azalea, camellia, citrus, evergreens, hollies, ligustrum, pittosporum, pyracantha, rose, and viburnum; fruit crops such as blackberries, blueberries, and strawberries; and vegetable crops such as tomatoes, squash, eggplant, and cucumber [111].

Insects have three pairs of legs and three body regions (head, thorax, abdomen), but throughout most life stages, spider mites have four pairs of legs and one body region. *Tetranychus urticae* is distinguishable by two large dark green spots on the dorsal area of the abdomen. Depending on the host plant and other environmental factors, such as temperature and light, the color of *Tetranychus urticae* varies from light green, dark green, brown, black, and orange [60]. The population of *Tetranychus urticae* completes a generation every 7–10 days, depending on the temperature. They have five stages of development: egg, larva, protonymph, deutonymph, and adult [112].

Predators beneficially regulate spider mite populations. Five species of spider mite predators are commercially available in the United States for crop protection: *Phytoseiulus persimilis*, *Mesoseiulus longipes*, *Neoseiulus californicus*, *Galendromus occidentalis*, and *Amblyseius fallicus*. Predatory mites are distinguishable from spider mites due to longer legs, a more active life, and a faster pace of movement. Predators are often red or orange in color [111]. *Phytoseiulus persimilis*, the most common predator of all stages of mites, is thought to originate from the Mediterranean or South America, but, since the 1960s, it has been established worldwide as a biological control agent, primarily for two-spotted spider mites. *Phytoseiulus persimilis* tolerates hot climates if relative humidity remains between 60 and 90 percent. This predator can consume 20 eggs or five adults daily; females consume much more than immature and adult males. Each

female can produce 60 eggs in her lifetime. *Phytoseiulus persimilis* has five developmental stages: egg, nonfeeding larva, protonymph, deutonymph, and adult [112]. However, it often needs to be reintroduced because it relies exclusively on mites for food, eventually consuming all available prey. This beneficial mite is commercially available and commonly released against *Tetranychus urticae* [111].

Previous work has attempted to determine biological mechanisms, including dispersal, underlying mechanism of the spider mite-*Phytoseiulus persimilis* interaction. When diffusion is introduced into a prey-predator system, both species attain uniform distributions in the domain after certain time. Diffusion acts as a stabilizer in a reaction-diffusion system [113]. Under certain conditions, however, diffusion can destabilize the process, leading to non-uniform distribution in a prey-predator system. This destabilization is known as diffusion-driven instability [30].

Similar to predator interference and relative diffusion, another factor, called prey-taxis, introduce instability into this domain, and leading to the formation of spatial patterns. In the Lotka-Volterra logistic prey-predator model with prey-taxis, Sapoukhina et al [57]. demonstrated that "predators respond to the heterogeneity of the prey density by accelerating toward the localities where the prey is abundant, resulting in predator aggregation."

Phytoseiulus persimilis responds to odors released from leaves infested by *Tetranychus urticae*. Sabelis and Weel [114] discussed behavioral mechanisms of this predator by odor perception and how it contributes to prey identification. They observed the predators' walking paths in still air and in an air stream uniformly permeated with or without prey-related odor stimuli. According to Sabelis and Weel, "the anemotactic responses observed are therefore both odour-conditioned and (feeding) state-dependent." An anemotactic response of starved predators may help them find clusters of spider mite colonies [115].

This paper presents and compares four prey-predator models with distinctive spatial effects as they apply to a two-spotted spider mite and *Phytoseiulus persimilis* system. The paper is organized as follows. Section 3.2 presents the four models, i.e. self-diffusion model, cross-diffusion model, chemotaxis effect model, and integro-diffusion model for a *Tetranychus urticae* and *Phytoseiulus persimilis* prey-predator dynamic system. Section 3.3 presents simulation results, and Section 3.4 compares experimental data with simulated data from various models. Section 3.5 discusses numerical simulation and model validation.

3.2 Mathematical Models

The dynamic relationship between predator and prey is a central ecological matter and a primary concern when modeling prey-predator interactions. A significant component of the prey-predator relationship is the functional response, which indicates the average number of prey killed per predator per unit of time. Two types of functional response are common: prey-dependent and predator-dependent. Prey-dependent implies that the functional response depends only on prey density; in a predator-dependent response, the function of response depends on both prey and predator densities. In the literature, the prey-dependent function has served as the basis for predator-prey theory, such as Holling's Type II functional response [116]. However, researchers have argued that when predators must search for food and then share or compete for food, the functional response should depend on both prey and predator densities. Considerable evidence suggests that predator-dependent functional responses occur quite frequently in laboratory as well as in natural systems [117]. One of the most popular functional responses is the Beddington-DeAngelis functional response [89, 118], originally proposed by Beddington [78] and DeAngelis et al. [81]. The function is noted as $\frac{x_t y_t}{\alpha+\beta x_t+\gamma y_t}$. This paper employs the Beddington-DeAngelis response function under an assumption that the predator Phytoseiulus persimilis must search for

food. The logistic growth function is also employed for a prey system. The basic model is presented in Equation (3.1-3.2):

$$\frac{\partial u}{\partial t} = ru\left(1 - \frac{u}{K}\right) - \frac{auv}{b+u+cv} \tag{3.1}$$

$$\frac{\partial v}{\partial t} = \frac{eauv}{b+u+cv} - dv \tag{3.2}$$

Where

u(t), v(t): spider mite and Phytoseiulus persimilis densities at time t, respectively

r: intrinsic growth of spider mites

K: carrying capacity of spider mites

e: conversion rate of prey to predator

d: death rate of Phytoseiulus persimilis

a: maximum consumption rate

b: saturation constant

c: factor to scale the impact of predator interference.

Let $\alpha = \frac{cr}{a}$, $\beta = \frac{b}{K}$, $\gamma = ce$, $\delta = \frac{dc}{a}$.

After manipulation, the following polynomial form is obtained:

$$\frac{\partial u}{\partial t} = \alpha u(1-u)(\beta + u + v) - uv \tag{3.3}$$

$$\frac{\partial v}{\partial t} = \gamma uv - \delta v(\beta + u + v) \tag{3.4}$$

This dynamic relationship is demonstrated in Figures 3.1 and Figure 3.2 which present two snapshots of dynamic simulation with the parameter α = 0.5, δ= 0.3, γ= 0.8 and an initial density for prey of 0.209 while the initial density for predator is 0.2203; maximum simulation time is 2000. Figure 3.1(a) and Figure 3.2(a) demonstrate the density of prey and predator changes through time,

while the red line represents of density of prey, and the blue line represents the density of predator. Figure 3.1(b) and Figure 3.2(b) demonstrate the trajectory of the dynamical system.

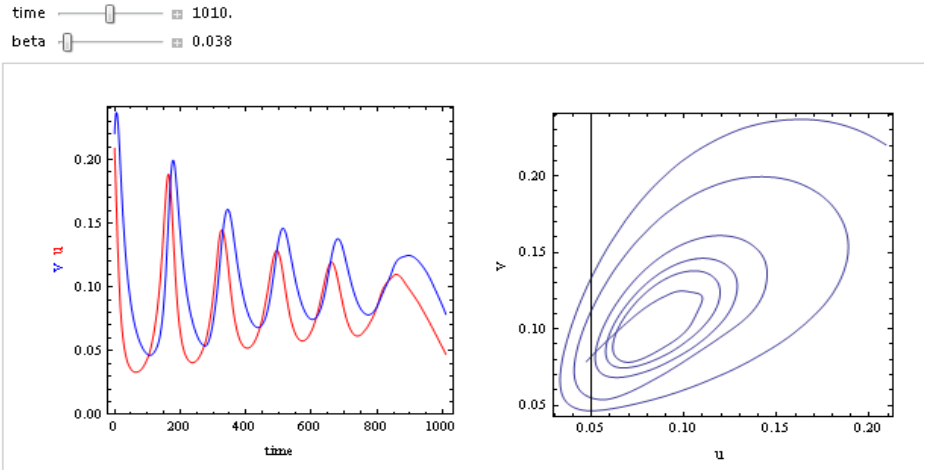

(a) (b)

Figure 3.1 Snapshot of dynamic simulation when t = 1010, β = 0.038.

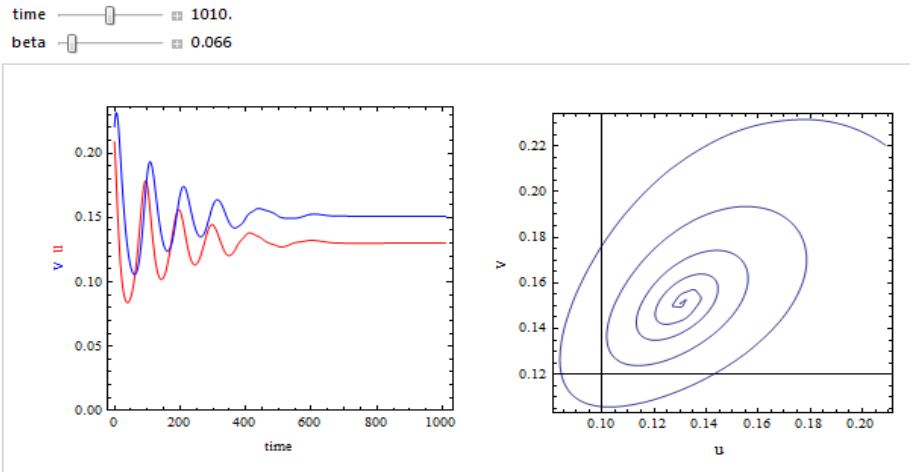

(a) (b)

Figure 3.2 Snapshot of dynamic simulation when t = 1010, β = 0.066.

According to Figure 3.1 and Figure 3.2, beta is correlated to the system stability. The system is unstable as shown in Figure 3.1 when β=0.038 and the system is stable when β=0.066.

This paper fits the dynamic system (3.3-3.4) into four models: self-diffusion model and cross-diffusion model which are based on existing formulations, and chemotaxis effect model and integro diffusion model which are part of the contribution of this paper. These models are presented in the following sections.

3.2.1 Self-Diffusion Model

The tendency for a species to move in the direction of lower species density is called self-diffusion [43]. A general form of a self-diffusion model for a prey and predator system is presented as follows:

$$\frac{\partial u}{\partial t} = f(u) - f_1(u,v) + d_1\nabla^2 u \tag{3.5}$$

$$\frac{\partial v}{\partial t} = f_2(u,v) - f(v) + d_2\nabla^2 v \tag{3.6}$$

Where:

f(u): birth rate function of prey

f(v): death rate function of predator

$f_1(u,v)$: interaction function effect on the decrease of prey

$f_2(u,v)$: interaction function effect on the increase of predator

d_1: self-diffusion coefficient for prey

d_2: self-diffusion coefficient for predator

∇^2: usual Laplacian operator in two dimensions.

For the Beddington-DeAngelis response function and logistic growth function, the corresponding polynomial form becomes:

$$\frac{\partial u}{\partial t} = \alpha u(1-u)(\beta + u + v) - uv + d_1 \nabla^2 u \tag{3.7}$$

$$\frac{\partial v}{\partial t} = \gamma uv - \delta v(\beta + u + v) + d_2 \nabla^2 v \tag{3.8}$$

3.2.2 Cross-Diffusion Model

Although the self-diffusion model demonstrates that the movement within a given species is independent of other species, prey may recognize predators and respond by moving away to avoid capture by predators in predator-prey systems. However, if predators recognize prey, this recognition may affect the rate or direction of their movement, thereby helping the predators find prey. This phenomenon, known as cross-diffusion, has recently received significant attention, as described in [39, 119-121]. Value of the cross-diffusion coefficient may be positive, negative, or zero. A positive cross-diffusion coefficient denotes species movement in the direction of lower concentration of another species. A negative cross-diffusion coefficient indicates that one species tends to diffuse in the direction of higher concentration of another species.

The general form of a cross-diffusion model for prey-predator interactions is presented as follows:

$$\frac{\partial u}{\partial t} = f(u) - f_1(u,v) + d_{11} \nabla^2 u + d_{12} \nabla^2 v \tag{3.9}$$

$$\frac{\partial v}{\partial t} = f_2(u,v) - f(v) + d_{21} \nabla^2 u + d_{22} \nabla^2 v \tag{3.10}$$

Where:

f(u): birth rate function of prey

f(v): death rate function of predator

$f_1(u,v)$: interaction function effect on the decrease of prey

$f_2(u,v)$: interaction function effect on the increase of predator

d_{11} and d_{22}: self-diffusion coefficients of prey and predator, respectively

d_{12} and d_{21}: cross diffusion coefficients of predator and prey, respectively.

If $d_{12} > 0$ and $d_{21} < 0$, then the prey species tends to diffuse in the direction of lower concentration of the predator species and the predator species tends to diffuse in the direction of higher concentration of the prey species. Using the Beddington-DeAngelis response function and logistic growth function, the corresponding polynomial form becomes:

$$\frac{\partial u}{\partial t} = \alpha u(1-u)(\beta + u + v) - uv + d_{11}\nabla^2 u + d_{12}\nabla^2 v \tag{3.11}$$

$$\frac{\partial v}{\partial t} = \gamma uv - \delta v(\beta + u + v) + d_{21}\nabla^2 u + d_{22}\nabla^2 v \tag{3.12}$$

3.2.3 Chemotaxis Effect Model

A large number of insects, animals, and humans rely on smell to convey information between species members. Predatory mites respond to volatile chemicals released by plants infested with spider mites, as shown in experiments using Y-tube olfactometers and chemical analyses [30]. Previous research work has investigated the attraction mechanism between *Phytoseiulus persimilis* and herbivore-induced plant volatiles [122-125]. For example, Michiel van Wijk confirmed that *P. persimilis* identifies chemical compounds in odor mixtures but the predators possess a limited ability to identify individual spider mite-induced plant volatiles in odor mixtures. Therefore, predatory mites have to learn to respond to prey-associated odor mixtures [125]. This section models this chemically-directed movement, or chemotaxis effect.

The predator-prey model with chemotaxis effect can be written as:

$$\frac{\partial u}{\partial t} = \alpha u(1-u)(\beta + u + v) - uv + d_1 \nabla^2 u \tag{3.13}$$

$$\frac{\partial v}{\partial t} = \gamma uv - \delta v(\beta + u + v) - \frac{\partial (vw)}{\partial x} - \frac{\partial \left(v\chi(a)\frac{\partial a}{\partial x}\right)}{\partial x} + d_2 \nabla^2 v \tag{3.14}$$

$$\frac{\partial w}{\partial t} = T\frac{\partial u}{\partial x} + d_3 \nabla^2 w \tag{3.15}$$

Where:

u(x, t): population density of prey

v(x, t): population density of predator

w(x, t): velocity of predators

a(x, t): presence of a gradient in an attractant

$\chi(a)$: function of the attractant concentration

d_3: effect of social behavior

T: sensitivity coefficient of predators to heterogeneous density distribution of prey.

3.2.4 Integro Diffusion Model

Integro-differential equations (IDEs) share continuous-space and continuous population assumptions of partial-differential equation (PDE) models. The PDE model focuses on localized movement (diffusion) of individuals, while IDE models focus on long-range movement. In this case, both prey and predator can move a long distance.

The predator-prey model with IDE can be written as:

$$\frac{\partial u(x)}{\partial t} = \alpha u(1-u)(\beta + u + v) - uv - \int_{y \in D} u(x) K_1(x-y)\, d_y + \int_{y \in D} u(y) K_1(x-y)\, d_y \quad (3.16)$$

$$\frac{\partial v(x)}{\partial t} = \gamma uv - \delta v(\beta + u + v) - \int_{y \in D} v(x) K_2(x-y)\, d_y + \int_{y \in D} v(y) K_2(x-y)\, d_y \quad (3.17)$$

Where $K_1(x-y) = K_2(x-y) = \frac{1}{4\pi\mu T} \exp\left[-\frac{x^2+y^2}{4\mu T}\right]$

Equation (3.16-3.17) considers movement from all points in space *D* (labeled y in the integral) to point *x*. *T* is the dispersal time of each species, and μ is a species parameter describing the diffusivity, or rate of dispersal, of each population. Movement rate, assumed to vary with distance, is described by kernel function K_1 and K_2. Kernel function defines how movement rate decreases with distance, thus offering greater flexibility than the PDE model. Therefore, predation can occur over a variety of scales instead of being a local event.

3.3 Numerical Simulation

In this section, dynamic simulations are performed with the four discussed models. The simulation is performed on a two-dimensional lattice with 100 x 100 cells. Spacing between each lattice cell was 1.25-unit distance, and the timing step was 0.05. Laplacian diffusion was calculated using finite difference, and Neumann boundary conditions were employed. The parameter used [43] was α = 0.5, β = 0.128, γ = 0.8, δ = 0.3, d_{11} (d_1) = 0.01, d_{22} (d_2) = 1, d_{12} = 0.005, and d_{21} = -0.001. Additional parameters for the chemotaxis effect model were d_3 = 0.005, *T* = 0.01, for integro diffusion model were μ=0.051, *T*=2.5.

3.3.1 Prey and Predator Density Simulation

Prey and predator densities were compared at fixed locations of (50, 50) and (90, 90) within a 100 x100 grid. The simulation ran 10000 iterations with initial prey density 0.5 and predator density 0.2. Results of the self-diffusion model, cross-diffusion model, chemotaxis effect model, and integro diffusion model are shown in Figures 3.3–3.6, respectively. In all four figures, the left subfigure (a) represents prey and predator densities at the location (50, 50) and the right subfigure (b) represents these densities at the location (90, 90).

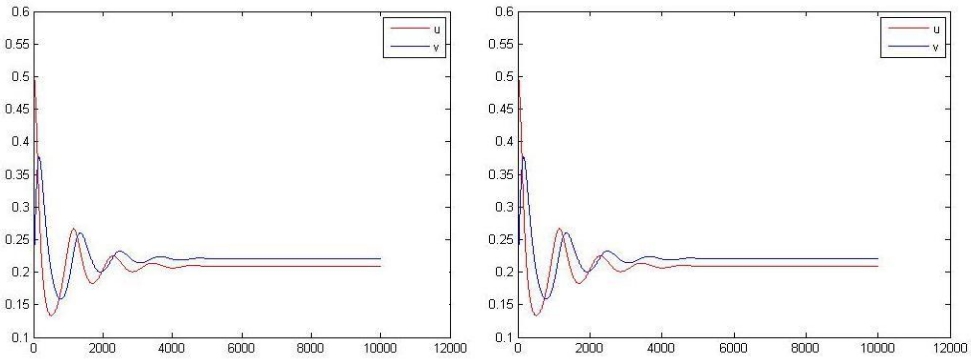

Figure 3.3 Prey and predator density for self-diffusion model, x axis is iteration time while y axis is the density of prey and predator.

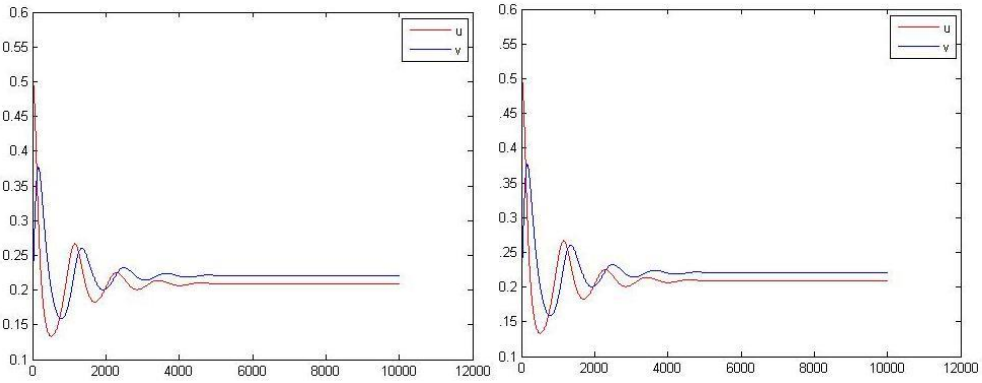

Figure 3.4 Prey and predator density for cross-diffusion model, x axis is iteration time while y axis is the density of prey and predator.

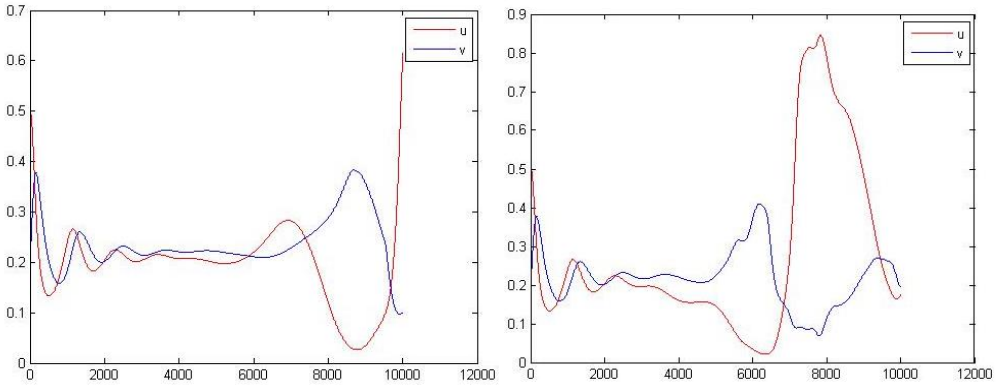

Figure 3.5 Prey and predator density for chemotaxis effect model, x axis is iteration time while y axis is the density of prey and predator.

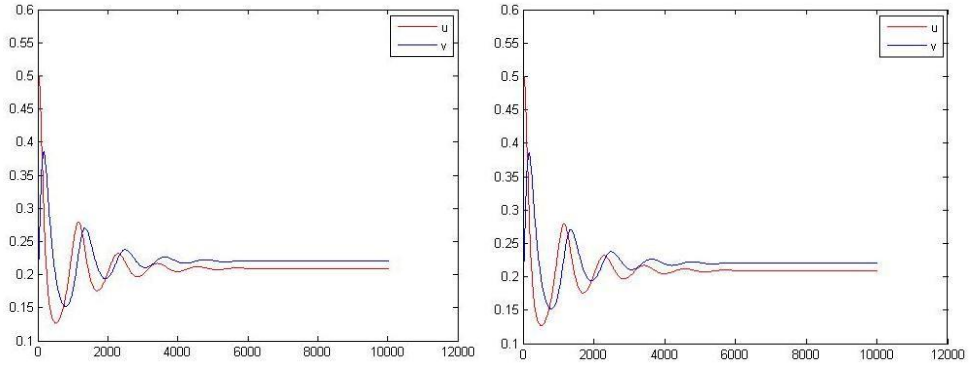

Figure 3.6 Prey and predator density for integro diffusion model, x axis is iteration time while y axis is the density of prey and predator.

Simulation results in Figures 3.3–3.6 show that the chemotaxis effect model differs significantly from the other three models. The chemotaxis effect system did not achieve steady state by 10000 iterations, while the other three dynamic systems achieved steady state at approximately 4000–6000 iterations. The reason for this could be predatory mites move faster toward the higher density of prey area when attraction odors are present for predatory mites, thereby weakening system stability.

3.3.2 Pattern Simulation

This section presents simulated patterns of formation among models. Using stable state as the initial condition, simulations were run with 0, 100000, and 20000 iterations. Corresponding results are shown in subfigure (a), subfigure (b), and subfigure (c) of Figures 3.7–3.10. Simulated results for self-diffusion, cross-diffusion, chemotaxis effect, and integro diffusion models are shown in Figures 3.7, 3.8, 3.9, and 3.10, respectively.

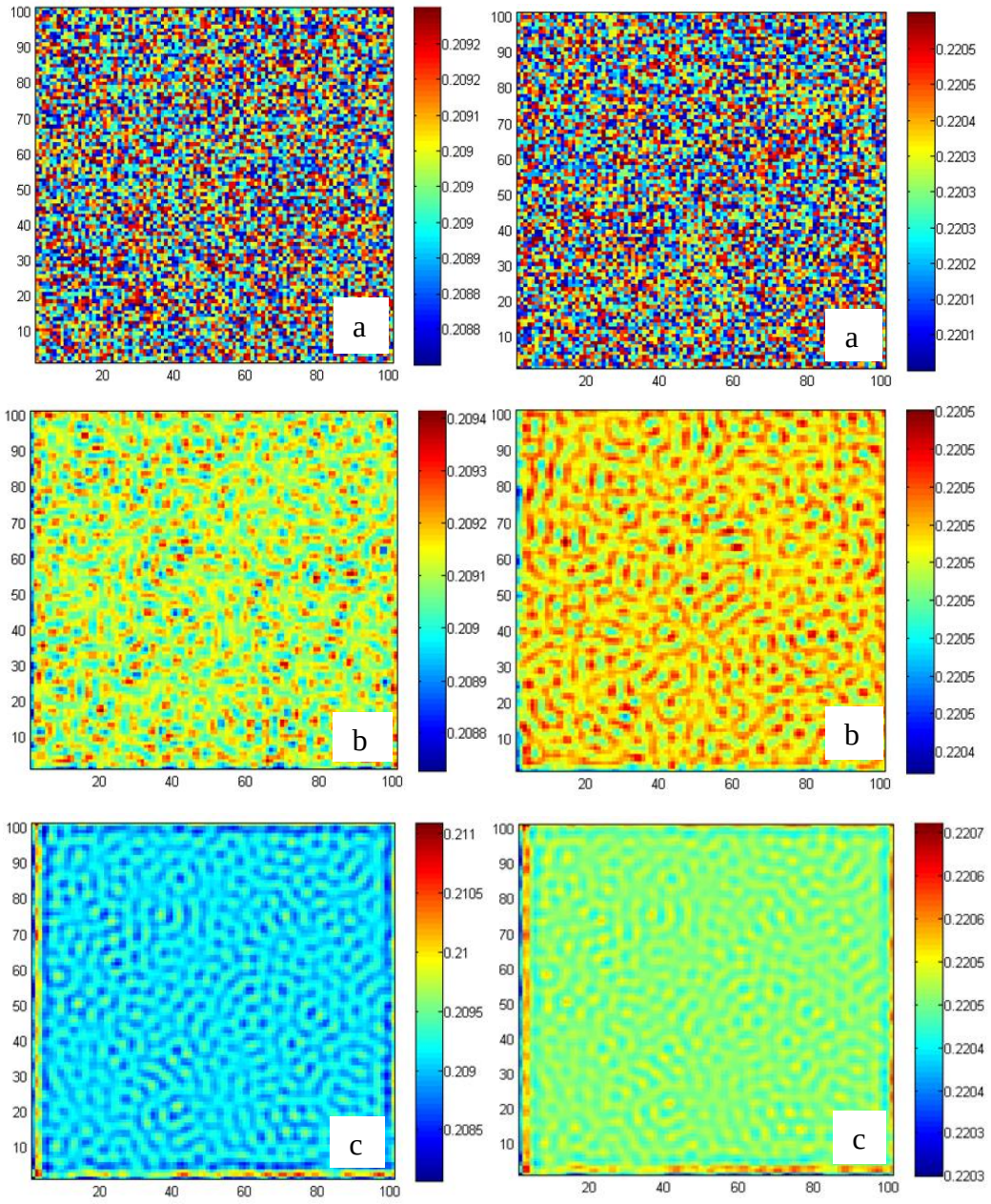

Figure 3.7 Patterns of prey and predator in self-diffusion model: (a) 0 iteration, (b) 10000 iterations, and (c) 20000 iterations. Prey population is shown on the left, and predator population is shown on the right.

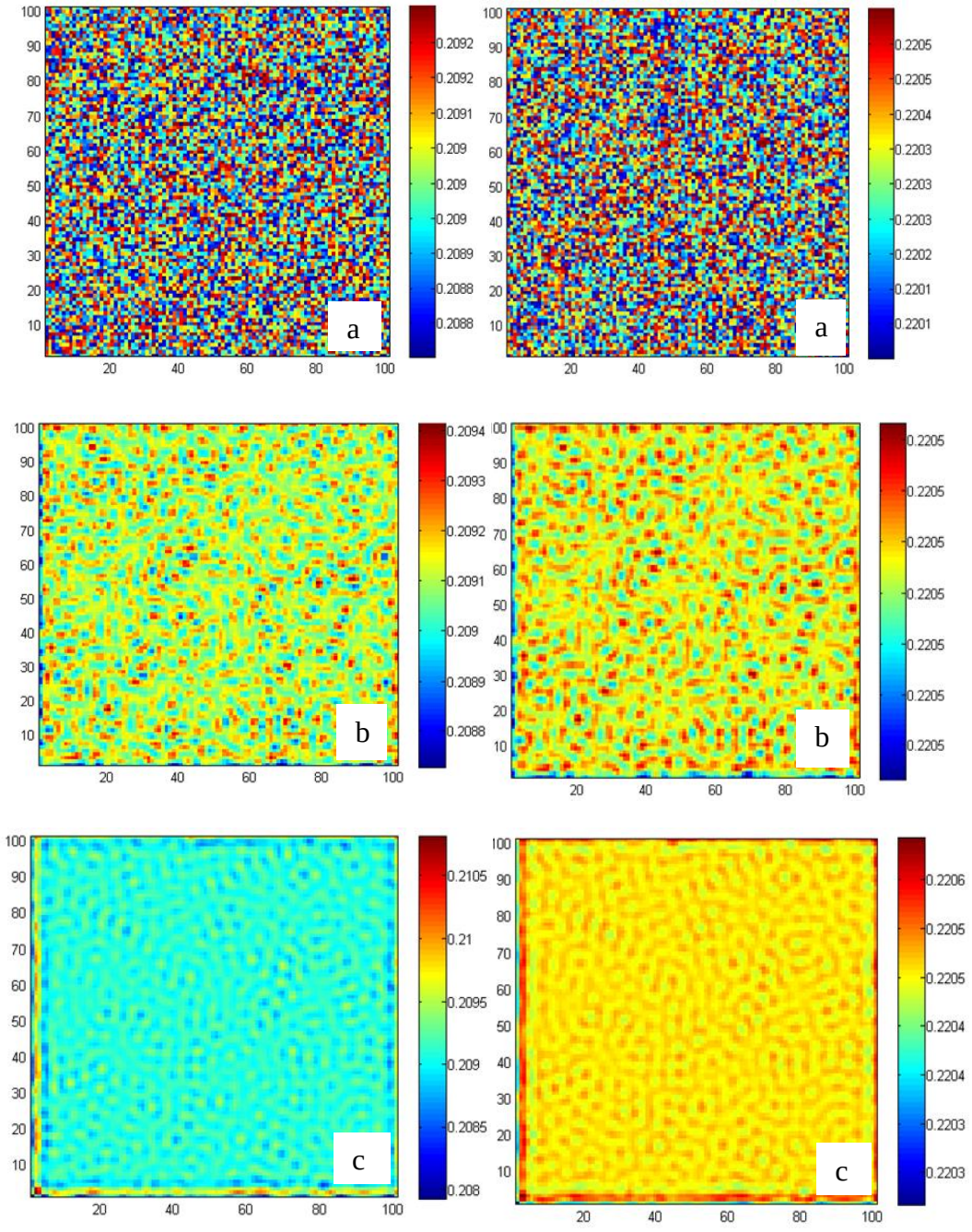

Figure 3.8 Patterns of prey and predator in cross-diffusion model: (a) 0 iteration, (b) 10000 iterations, and (c) 20000 iterations. Prey population is shown on the left, and predator population is shown on the right.

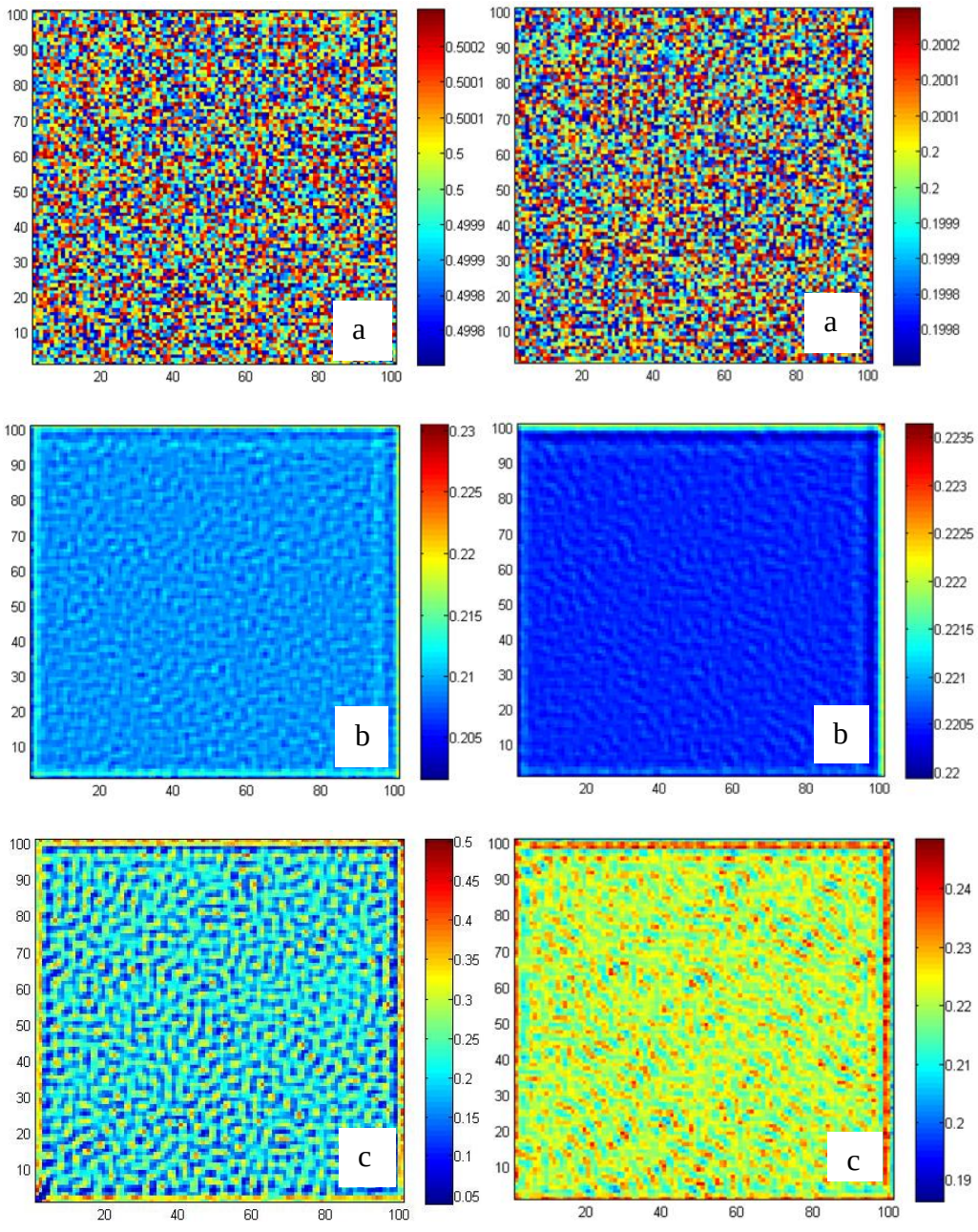

Figure 3.9 Patterns of prey and predator in chemotaxis effect model: (a) 0 iteration, (b) 10000 iterations, and (c) 20000 iterations. Prey population is shown on the left, and predator population is shown on the right.

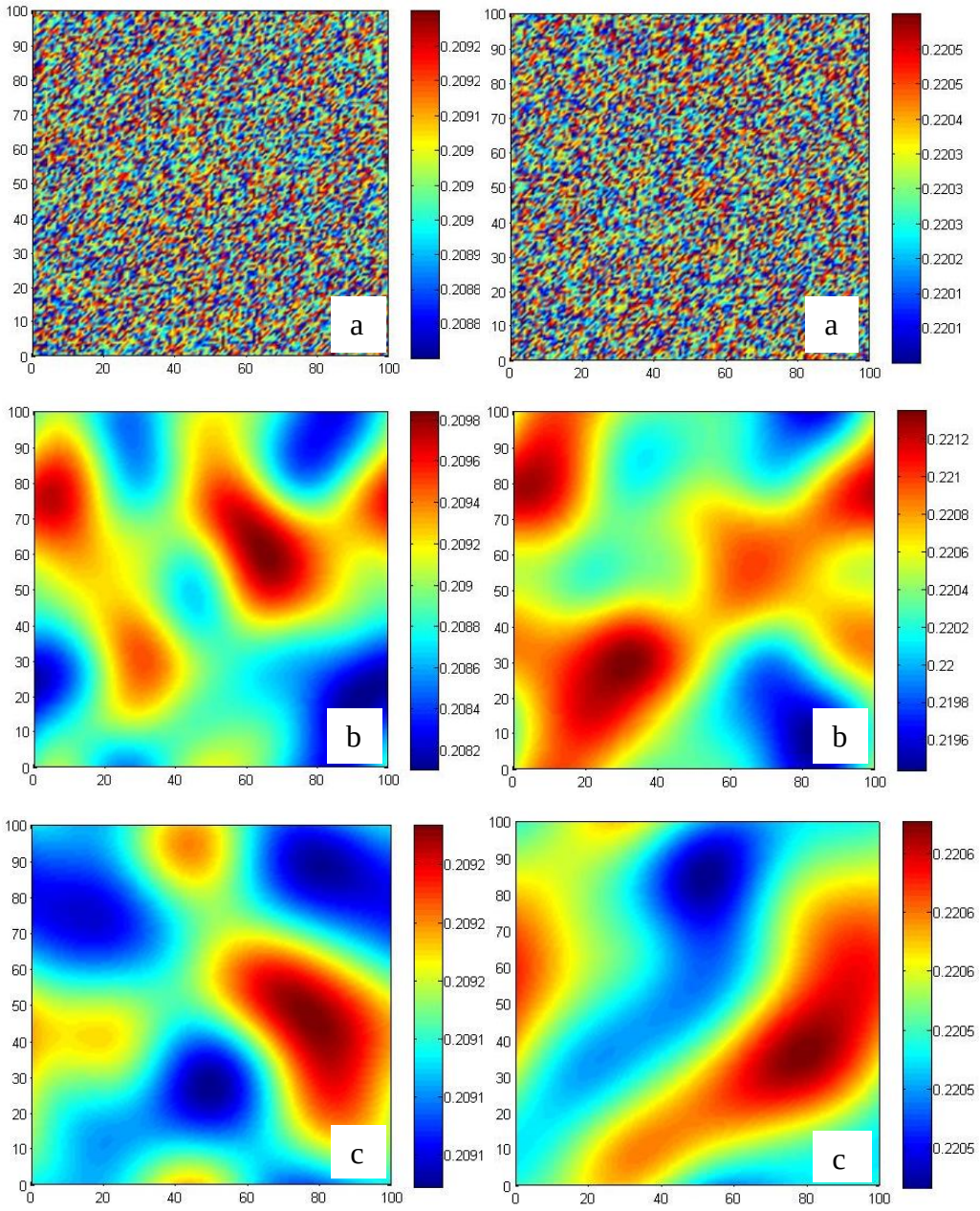

Figure 3.10 Patterns of prey and predator in integro diffusion model: (a) 0 iteration, (b) 10000 iterations, and (c) 20000 iterations. Prey population is shown on the left, and predator population is shown on the right.

From Figures 3.7 – 3.10, it could be concluded that different spatial effect played important role towards the dynamic system. Using the chemotaxis effect model shows a larger range of

density distributions of prey and predator than that of the other three models when they all began from the same steady state. For instance, after 20000 iterations, the difference of density distribution of prey is around 0.45 for chemotaxis effect model while that for other models is around 0.0045, and the density distribution difference of predator is about 0.05 for chemotaxis effect model while that of predator for other models is about 0.0005. This indicates that chemotaxis introduces more instability into the model. On the other side, the pattern for the integro diffusion model differed significantly from the other models, which is consistent with the model assumption that prey and predator system has long-range interaction during their movement. The simulation results verified the assumption of different spatial effect models and confirmed that different interaction scheme plays an important role in this prey-predator system.

3.4 Validation

3.4.1 Introduction of the Experiment

This experiment, conducted by the entomology department at Kansas State University, was carried out on 24 individually-potted lima beans plants set in 8x3 arrays, with *Phytoseiulus persimilis* as predator and *Tetranychus urticae* as prey. The experiment lasted four weeks, and the total number of two-spotted spider mites and predator were counted every six days. Table 3.1 lists the total number of observed prey (*Tetranychus urticae*) and predator numbers in 24 days.

Table 3.1 Total number of prey and predator every six days

Times/Days	Observations	
	Number of prey	Number of predator
0	64	6
6	458	6
12	490	13
18	2238	67
24	1954	239

3.4.2 Comparison of Total Number of Prey and Predator

This section compares the number of two-spotted spider mites and its predator using a simulated model with the experimental (actual) observations. Parameters in Equation (3.1) -(3.2) for simulation were $\alpha = 20$, $b = 105$, $c = 45$, $d = 0.3$, $e = 0.25$, $r = 0.38$, $K = 800$.

Simulation results are shown in Figure 3.11- Figure 3.14, where the dotted curve represents actual data from the experiment and the solid curve represents the number of prey and predator calculated from the simulated models. The number of prey comparison is presented on the subfigure (a) while the number of predator comparison is presented in the subfigure (b) of each figure.

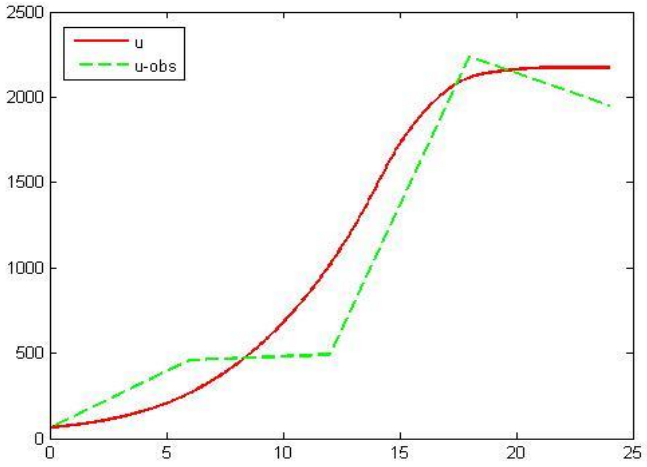

(a)

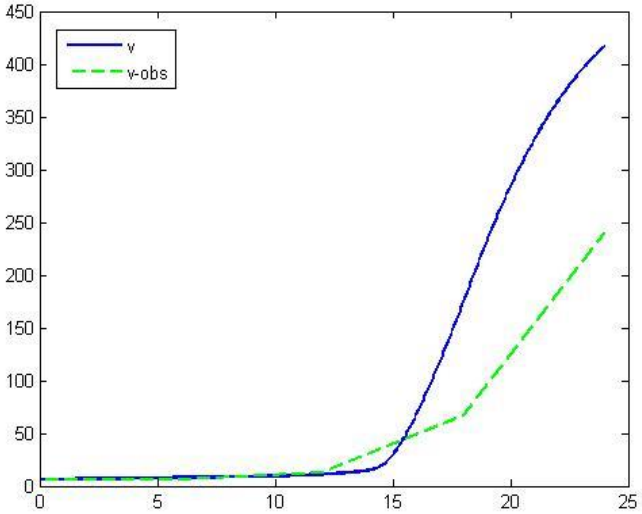

(b)

Figure 3.11 Comparison of simulated numbers from the self-diffusion model with experiment observations in 24 days

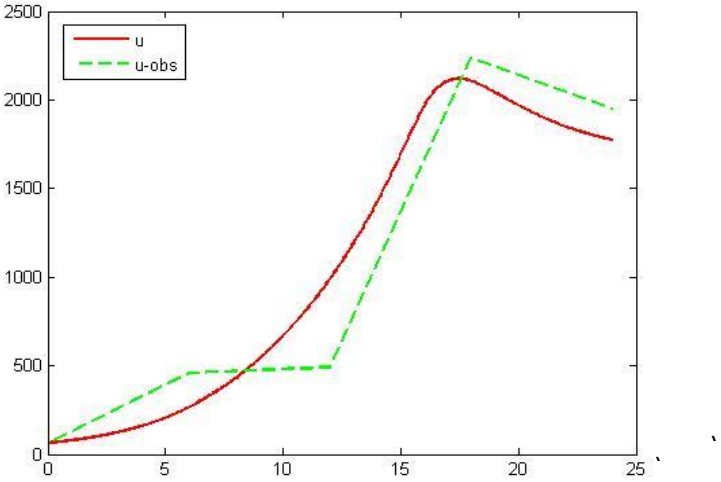

(a)

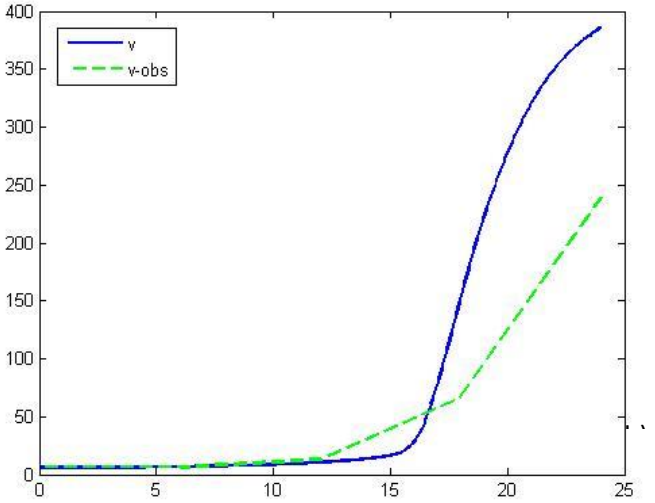

(b)

Figure 3.12 Comparison of simulated numbers from the cross-diffusion model with experiment observations in 24 days

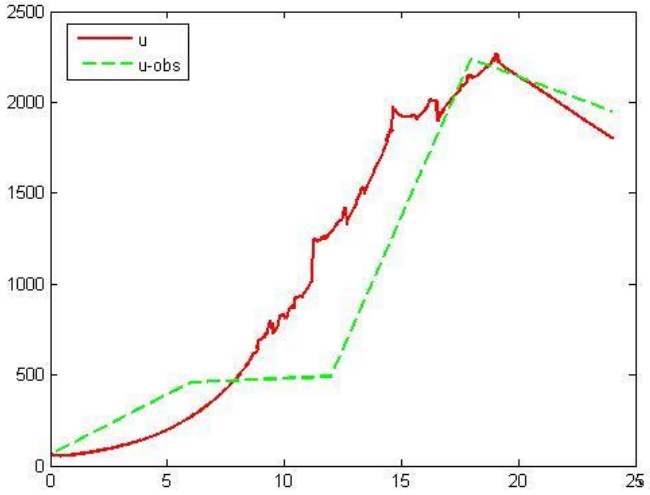

(a)

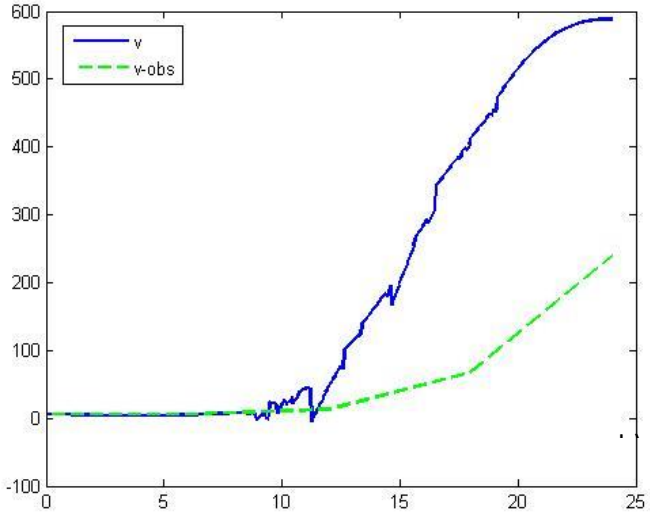

(b)

Figure 3.13 Comparison of simulated numbers from the chemotaxis effect model with experiment observations in 24 days

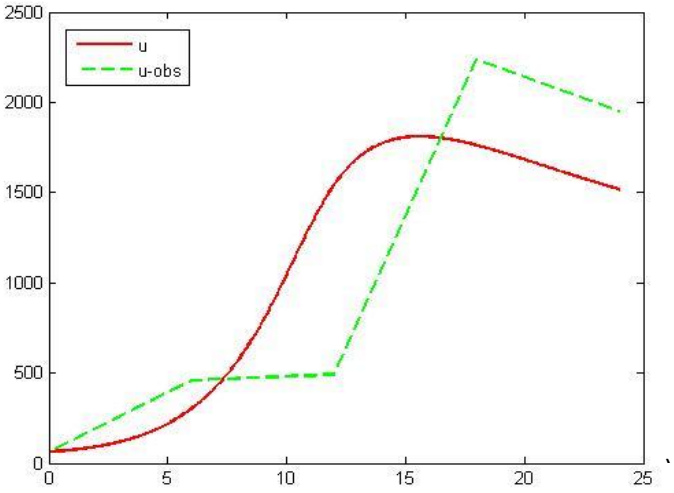

(a)

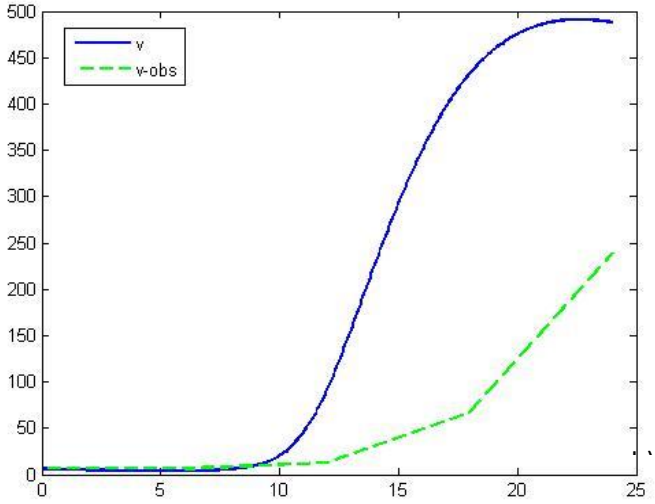

(b)

Figure 3.14 Comparison of simulated numbers from the integro diffusion model with experiment observations in 24 days

From Figure 3.11 to Figure 3.14, we can see that the total number of prey has good fit while the total number of predator does not have the same good fit. In order to compare the results numerically, we performed statistical analysis comparing the simulation results with observations. This analysis employs Root Mean Squared Error (RMSE). RMSE is a measure of how close a

fitted line is to data points. The use of RMSE is very common and makes an excellent general purpose error metric for numerical predictions. The statistical analysis is presented in Table 3.2 and Table 3.3.

Table 3.2 RMSE of the number of prey between predicted value and observations

Time/Days	Different Models				
	Observations of Prey	Self-Diffusion	Cross-Diffusion	Chemotaxis Effect	Integro Diffusion
0	64	64	64	64	64
6	458	266	267	268	301
12	490	1016	990	1285	1543
18	2238	2116	2107	2134	1761
24	1954	2171	1774	1802	1517
RMSE		306.59	**289.83**	418.93	622.49

Table 3.3 RMSE of the number of predator between predicted value and observations

Time/Days	Different Models				
	Observations of Predator	Self-Diffusion	Cross-Diffusion	Chemotaxis Effect	Integro Diffusion
0	6	6	6	6	6
6	6	8	7	5	4
12	13	11	11	48	93
18	67	175	152	412	433
24	239	417	386	588	488
RMSE		104.16	**84.85**	245.97	224.72

Results show that the cross-diffusion model fits the two-spotted spider mite system best, with the smallest RMSE compared to the other three models for both prey and predator number prediction. The integro diffusion model had the largest RMSE for prey number prediction while the chemotaxis effect model had the largest RMSE for predator number prediction.

3.5 Conclusions

This paper presented and analyzed four mathematical models with the Beddington-DeAngelis functional response [78, 81, 89, 118] for *Tetranychus urticae* and *Phytoseiulus persimilis* prey-predator system. The four models were the self-diffusion model, the cross-diffusion model, the chemotaxis effect model, and the integro-diffusion model. Simulation results were shown using a numerical example. One conclusion obtained from the results is that different spatial effects impact the prey-predator distribution, since the integro-diffusion model exhibit a significantly differently pattern than the other three models.

Another conclusion could be made is the two proposed models were theoretically reasonable. According to the simulation, the chemotaxis effect model was not as stable as the other three models, affirming that predator mites move faster and further when presented with attracting odors, thereby reducing system stability. The chemotaxis effect model lack of stability was also derived from the pattern formation simulation result. The result shows the range of density distribution of the chemotaxis effect model was much larger than that of the other three models when all models began from an identical steady state. On the other hand, the pattern for the integro diffusion model differed from the other models, which is consistent with the model assumption that prey and predator has long-range interaction during their movement.

In the validation process, results showed that all four models have good fit with the real system, with the cross-diffusion model having the best fit. For a future research, we plan to develop an agent-based model [126-128] to simulate interactions and predict the key parameters in order to offer suggestions on controlling the number of predators. Also, future expansion of this research can consider applying optimal control theory [129, 130] to provide decision makers with better policies of controlling the population of the two-spotted spider mites. Spatial games which have

been adopted to analyze various structure of populations [131, 132], also present a future expansion of our research.

Chapter 4 - Modeling Dynamic Evolutionary Systems using Spatial Games

Chapter 4 is based on the paper "Modeling Dynamic Evolutionary Systems using Spatial Games" submitted to Mathematical and Computer Modeling of Dynamical Systems.

Abstract

Modeling the dynamics of evolutionary competing species on a physical grid is a challenging modeling problem. This paper presents a novel modeling approach for synthesizing evolutionary dynamics of competing species using a spatial game perspective. This modeling approach describes the movement of players ('species' in our context) across a lattice. The model is based on a payoff function which controls the move likelihood and direction of the players ('predators' and 'preys'). Using simulated results, the paper provides a comparison between the spatial game model and an existing predator-prey dynamic model. Finally, a case study is presented to illustrate the applicability of this formalism and validate the model.

4.1 Introduction

Spatial games are a combination of traditional game models and cellular automata, representing strategies, players, payoff function, structure of population, and updating rules. This methodology has been adopted to analyze various structures of populations [131-133]. This paper introduces for the first-time spatial games as a modeling approach towards a system of evolutionary dynamics representing predator and prey.

The dynamic relationship between prey and its predator has long been and will continue to be one of the popular topics in both biology and mathematical biology because of its importance

and universal existence. A large body of research has been devoted to modeling the biological mechanisms of dispersal, and the underlying prey and predator interaction.

Traditional modeling approaches use mathematical formulations and include various diffusion models. Introducing diffusion into a prey-predator system usually results in both species eventually reaching homogeneous distributions in the domain. Thus, diffusion models act as a stabilizer in a reaction-diffusion system [113]. Under certain conditions, however, diffusion can destabilize the process, leading to non-uniform distribution in a prey-predator system. This destabilization is known as diffusion-driven instability [30]. Traditional models have also considered influences such as odor [57, 114, 115, 122-125] and mobility effect [134].

Compared to a traditional dynamic model, a spatial game model is more expressive and informative. It can capture the different habits and characteristics of the competing species and can be extended to other systems. It can also capture different mobility preferences of the species. For instance, the game-based perspective can be used to model the self-diffusion, cross-diffusion, chemo-taxis effect or even longer distance movement, that has previously discussed [135].

In this paper, the new approach is discussed and validated by comparing it with the more traditional cross-diffusion dynamic model and also validated with an actual field experiment. The paper is organized as follows: section 4.2 presents the new approach game-based model with payoff functions, probability move functions and interaction functions. Section 4.3 recalls the cross-diffusion model and section 4.4 demonstrates the numerical simulation of both modeling approaches. Section 4.5 presents a comparison between the two modeling approaches and an actual field experiment. Section 4.6 discusses the results considering validation of the models and presents future work.

4.2 Game-based Model

In this section, the mathematical model of the spatial game is introduced. The model includes payoff functions, probabilistic functions and interaction functions all acting on a square grid. The payoff functions describe quantitatively the benefits that each species in each cell location (i, j) gains from its surrounding cells. The probability functions calculate the likelihood of each member of cell location (i, j) to migrate to the neighboring cells, and the interaction functions describe the dynamic between prey and predator that coexist in each cell.

4.2.1 Payoff Function

Using the spatial game approach, it is assumed that prey and predator move in a reactionary way, meaning that the prey may be able to recognize the predator, and respond by moving away to avoid being caught. On the other hand, if predators recognize the prey, this may affect the rate and directions of their movement which may help them find prey. The payoff function of prey and predator at cell (i, j) is shown in Equation (4.1).

$$Pu(i,j) = \left(\frac{k_1}{u + c_1} + e_1\right)\left(\frac{k_2}{v + c_2} + f\right)$$
$$Pv(i,j) = \left(k_3(u + c_3) + g\right)\left(\frac{k_4}{v + c_4} + h\right) \quad (4.1)$$

Where Pu denotes the payoff of prey, Pv indicates the payoff of predator. Parameters c_1, c_2, c_3, k_1, k_2, k_3, k_4, e_1, f, g, and h scale the payoff affections. As can be seen the prey's function is inversely proportional to the number of prey (u) and predator (v) in cell (i, j). The predator's payoff, on the other hand, in proportion to the number of prey and inversely proportional to the number of other predators in cell (i, j). This implies that the prey prefers to move away from its own species

(reduce competition for food) and understandably also from predators. The predators are attracted to the prey but prefer to move away from other predators.

The behavior of the payoff functions is demonstrated in Figure 4.1 and Figure 4.2, using a small example corresponding to different numbers of prey and predators in cell (i, j). The parameters used here are: k_1=250; k_2=100; k_3=1; k_4=10; e_1=0.01; f=0.01; g=0.01; h=0.01; c_1=20; c_2=20; c_3=20; c_4=20; u=0 to100; v=0 to 100; Figure 4.1 denotes that prey will get higher payoff if there were less prey and less predator within its cell. Figure 4.2 indicates that predator will have higher payoff with more prey and less predator.

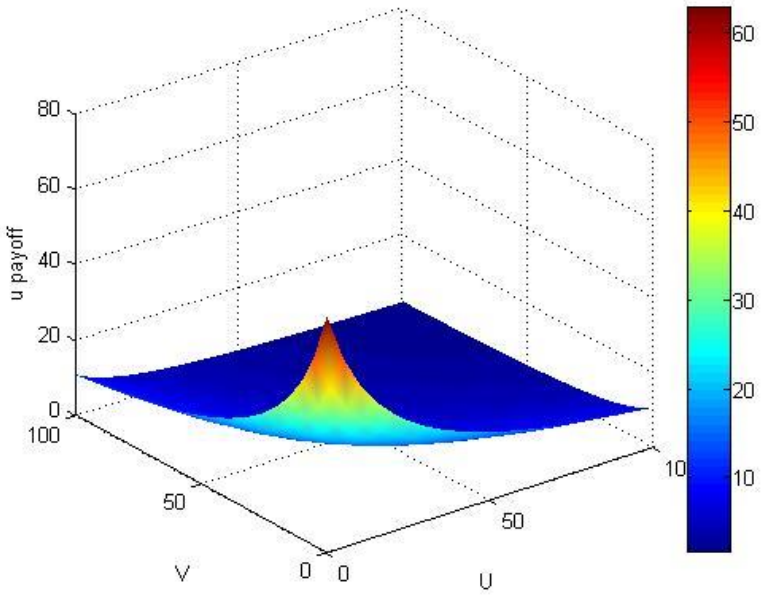

Figure 4.1 Behavior of payoff function of prey

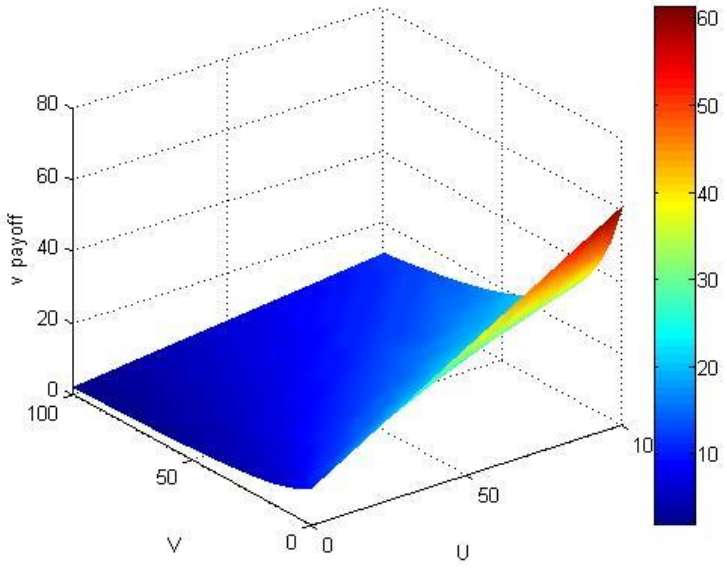

Figure 4.2 Behavior of payoff function of predator

4.2.2 Movement Probability Function

The payoff function discussed above define the payoff of each cell in a neighborhood. Based on those payoff values, the probability of the population in each cell to move can be calculated. This probability depends on the fraction of the total payoffs of the neighbors, compared to the cell's payoff as shown in Equations (4.2) – (4.6). Note that the movement of the prey is based on the prey payoffs and similarly the predators' movement depends on their payoff of each cell in a neighborhood.

4.2.2.1 The probability to stay at the same place

$$P_1 = \frac{P_{u,v}(i,j)}{\sum_{\substack{x=i-1,i+1 \\ y=i-1,j+1}} P_{u,v}(x,y)} \tag{4.2}$$

4.2.2.2 The probability to move one cell up

$$P_2 = \frac{P_{u,v}(i-1,\ j)}{\sum_{\substack{x=i-1,i+1 \\ y=i-1,\ j+1}} P_{u,v}(x, y)} \tag{4.3}$$

4.2.2.3 The probability to move one cell down

$$P_3 = \frac{P_{u,v}(i+1,\ j)}{\sum_{\substack{x=i-1,i+1 \\ y=i-1,\ j+1}} P_{u,v}(x, y)} \tag{4.4}$$

4.2.2.4 The probability to move one cell left

$$P_4 = \frac{P_{u,v}(i,\ j-1)}{\sum_{\substack{x=i-1,i+1 \\ y=i-1,\ j+1}} P_{u,v}(x, y)} \tag{4.5}$$

4.2.2.5 The probability to move one cell right

$$P_5 = \frac{P_{u,v}(i,\ j+1)}{\sum_{\substack{x=i-1,i+1 \\ y=i-1,\ j+1}} P_{u,v}(x, y)} \tag{4.6}$$

Based on the probabilities calculated, the number of entities (predators and preys) that move to the neighboring cells is calculated. This analysis is performed for each cell in the lattice to determine the population distribution, as shown in the example below.

4.2.3 Example of Game Execution

This example uses a 3*3 lattice to demonstrate the mechanism of the spatial game and the schedule of movements for prey or predator. Table 4.1 shows the current population of prey and predator on our grid. First, the payoffs of the prey and predator is calculated in each cell, using Equation (4.1), as depicted in Table 4.2 and Table 4.3.

Table 4.1 Initial distribution of prey and predator presented as (*u*,v)

(*10*, **20**)	(*9*,**2**)	(*8*,**2**)
(*7*, **4**)	(*30*, **2**)	(*5*, **2**)
(*4*, **2**)	(*3*, **3**)	(*2*, **1**)

Table 4.2 Payoff distribution of prey

1.86	3.42	3.52
3.33	2.12	3.88
4.01	3.98	4.51

Table 4.3 Payoff distribution of predator

122.50	188.55	183.00
165.33	305.00	166.36
160.82	149.74	155.57

Iteration I:

After the payoff is calculated, the probabilities to move are determined based on the movement probability functions. For example, the following equations present the move probability for prey in cell (2, 2).

- The probability to stay at the same place:

$$P_1 = \frac{Pu(i,j)}{\sum_{\substack{x=i-1,i+1 \\ y=i-1,j+1}} Pu(x,y)} = \frac{2.12}{3.42+2.12+3.98+3.33+3.88} = \frac{2.12}{16.73} = 0.126$$

This implies that 12.6% of the prey population in cell (2, 2) will not move.

- The probability to move one cell up:

$$P_2 = \frac{Pu(i-1, j)}{\sum_{\substack{x=i-1,i+1 \\ y=i-1,j+1}} Pu(x, y)} = \frac{3.42}{3.42+2.12+3.98+3.33+3.88} = \frac{3.42}{16.73} = 0.2044$$

- The probability to move one cell below:

$$P_3 = \frac{Pu(i+1, j)}{\sum_{\substack{x=i-1,i+1 \\ y=i-1,j+1}} Pu(x, y)} = \frac{3.98}{3.42+2.12+3.98+3.33+3.88} = \frac{3.98}{16.73} = 0.238$$

- The probability to move one cell left:

$$P_4 = \frac{Pu(i, j-1)}{\sum_{\substack{x=i-1,i+1 \\ y=i-1,j+1}} Pu(x, y)} = \frac{3.33}{3.42+2.12+3.98+3.33+3.88} = \frac{3.33}{16.73} = 0.199$$

- The probability to move one cell right:

$$P_5 = \frac{Pu(i, j+1)}{\sum_{\substack{x=i-1,i+1 \\ y=i-1,j+1}} Pu(x, y)} = \frac{3.88}{3.42+2.12+3.98+3.33+3.88} = \frac{3.88}{16.73} = 0.232$$

According to the calculations above, the movement of prey from cell (2, 2) to the neighboring cells could be obtained using the function $N \times P_i$ (i=1, 2, 3, 4, 5). The number of prey

is rounded to the nearest integer. For instance, the number would stay at the same place is: $N \times P_1 = 30 \times 0.126 = 3.8 \approx 4$. This movement of prey from cell (2, 2) is shown in Figure 4.3.

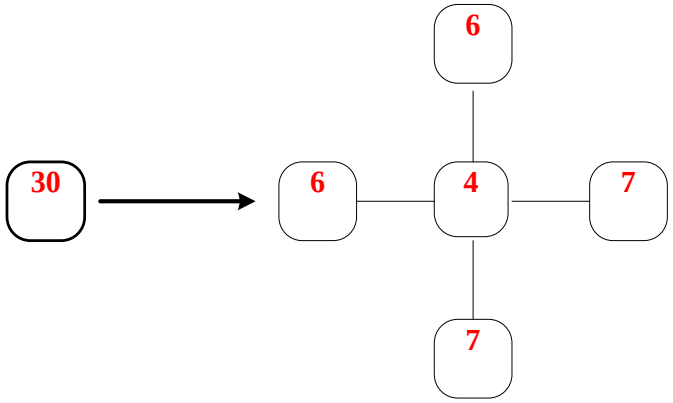

Figure 4.3 Move distribution of prey in cell (2, 2)

The same calculations are performed for each cell as well as for the predator population.

When all the cells and species complete their movements, the next iteration of the game is shown in Table 4.4. During the game movements process the total number of both species is kept the same, so at this point the total number of prey is 78, and the total number for predators is 38.

Table 4.4 The distribution of prey and predator (*u*, v) after exercising movement

(*5*, **6**)	(*15*, **9**)	(*7*, **2**)
(*13*, **9**)	(*8*, **5**)	(*12*, **2**)
(*5*, **2**)	(*10*, **2**)	(*3*, **1**)

4.2.4 Interaction Function

After moving and occupying neighboring cells, prey and predator have an interaction phase. In this case the same dynamics presented earlier is utilized, using the basic model with a

logistic growth function for prey and the Beddington and DeAngelis response function for the resources transfer [78, 81, 88, 89, 135], as shown in Equation (4.7-4.8).

$$\frac{\partial u}{\partial t} = ru\left(1 - \frac{u}{K}\right) - \frac{auv}{b+u+cv} \tag{4.7}$$

$$\frac{\partial v}{\partial t} = \frac{eauv}{b+u+cv} - dv \tag{4.8}$$

where:

$u(t)$, $v(t)$: the prey and predator densities at time t respectively

r: the birth rate of prey

K: the carrying capacity of prey

e: the conversion rate of prey to predator

d: the death rate of predator

a: the maximum consumption rate

b: the saturation constant

c: scales the impact of the predator interference.

Once predator and prey in each cell interact, some prey is consumed by the predators, some new prey is born and some predators die out. This step creates a new distribution of predators and prey in each cell, shown in Table 4.5. As shown in the table, the prey population has increased to 92 while the predator population has decreased to 33. This is the basis for the next iteration in which a new payoff is calculated, with a new probability to move and a new distribution of the species.

Table 4.5 The distribution of prey and predator (*u*, v) after interation

(*9*, **3**)	(*11*, **4**)	(*9*, **3**)
(*11*, **4**)	(*12*, **5**)	(*11*, **4**)
(*9*, **3**)	(*11*, **4**)	(*9*, **3**)

4.3 Cross-Diffusion Model

This section describes the more traditional spatial Cross Diffusion model that is used for comparison with the game-based spatial model. This well-known model describes a phenomenon that allows predators to recognize prey; this recognition may affect the rate or direction of their movement, thereby helping predators to find prey. This phenomenon, known as cross-diffusion, has recently received significant attention, as described in [39, 43, 119, 120].

4.3.1 General Cross-Diffusion Model

The general form of a cross-diffusion model for prey-predator interactions is

$$\frac{\partial u}{\partial t} = f(u) - f_1(u,v) + d_{11}\nabla^2 u + d_{12}\nabla^2 v \tag{4.9}$$

$$\frac{\partial v}{\partial t} = f_2(u,v) - f(v) + d_{21}\nabla^2 u + d_{22}\nabla^2 v \tag{4.10}$$

where:

$f(u)$: birth rate function of prey

$f(v)$: death rate function of predator

$f_1(u,v)$: interaction function effect on the decrease of prey

$f_2(u,v)$: interaction function effect on the increase of predator

d_{11} and d_{22}: self-diffusion coefficients of prey and predator, respectively

d_{12} and d_{21}: cross diffusion coefficients of predator and prey, respectively

Value of the cross-diffusion coefficient may be positive, negative, or zero. A positive cross-diffusion coefficient denotes species movement in the direction of lower concentration of another species. A negative cross-diffusion coefficient indicates that one species tends to diffuse in the direction of higher concentration. If $d_{12} > 0$ and $d_{21} < 0$, then the prey species tends to diffuse in

the direction of lower concentration of the predator species and the predator species tends to diffuse in the direction of higher concentration of the prey species.

4.3.2 Cross-Diffusion Model with Beddington-DeAngelis Function Response

Here the basic model Equation (4.7) -(4.8) presented earlier with Beddington-DeAngelis function response and the logistic growth function for prey is extended to include the cross-diffusion effect. The corresponding model is shown below:

$$\frac{\partial u}{\partial t} = ru(1 - \frac{u}{K}) - \frac{auv}{b+u+cv} + d_{11}\nabla^2 u + d_{12}\nabla^2 v \tag{4.11}$$

$$\frac{\partial v}{\partial t} = \frac{eauv}{b+u+cv} - dv + d_{21}\nabla^2 u + d_{22}\nabla^2 v \tag{4.12}$$

4.4 Model Comparison

To compare the performance of the different approaches on the dynamic system, simulation under critical conditions is conducted and compared.

We use bifurcation analysis to visualize the sensitivity of the system with respect to parameters *a*, which denoted the maximum consumption rate. Bifurcation points are defined as points where stability changes from stable to unstable. In our bifurcation diagram (Figure 4.4), there is a typical Hopf bifurcation point (marked as “H”).

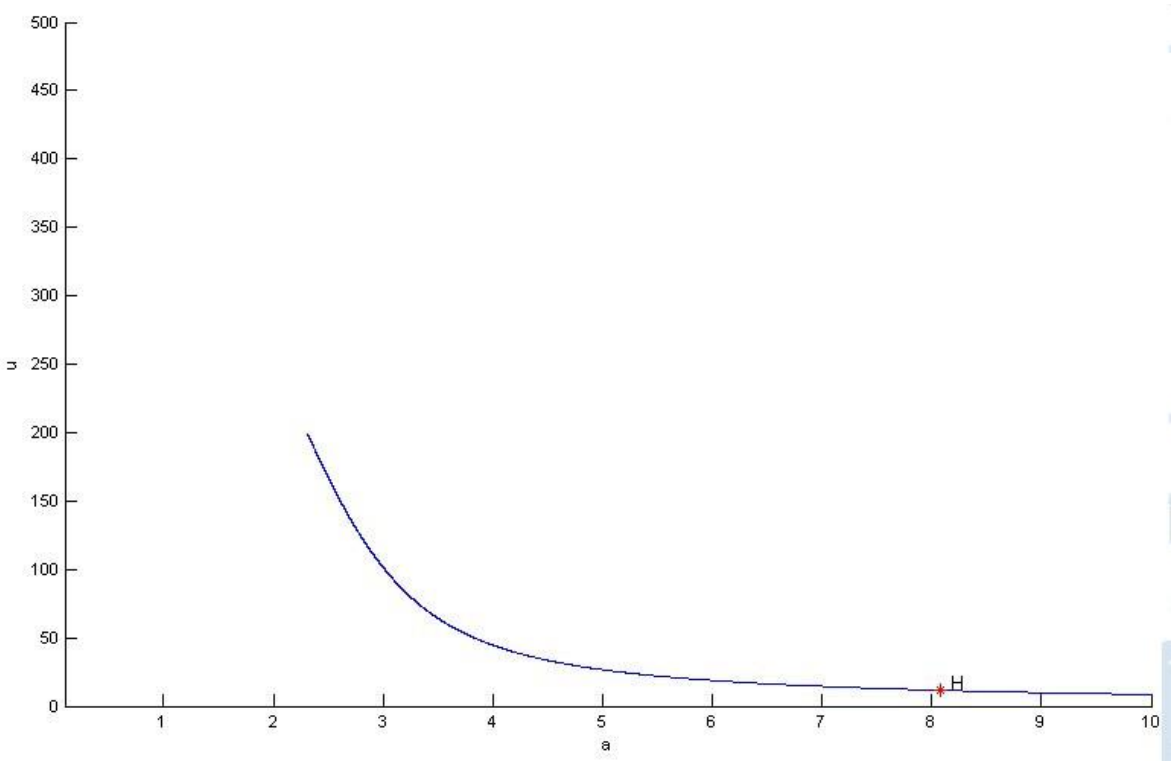

Figure 4.4 Computed equilibrium curve of prey population in relation to system parameter *a*

A Hopf bifurcation, identified in Figure 4.4, is a periodic bifurcation in which a new limit cycle is born from a stationary solution, and is detected when system parameter *a* changes. The parameters for the bifurcation analysis are: r=0.5, K=400, b=51.2, c=3.2, e=0.25, d=0.3 while a changed from 0 to 10 and have the bifurcation point of a=8.076 with u=11.54, and v=4.67. The dynamic system changes its stability while the maximum consumption rate a is equal to 8.076.

Figures 4.5-4.7 demonstrate the changes in the population of prey and predator through time near the bifurcation point, as well as the trajectory of the dynamic system from t=0 to t=500.

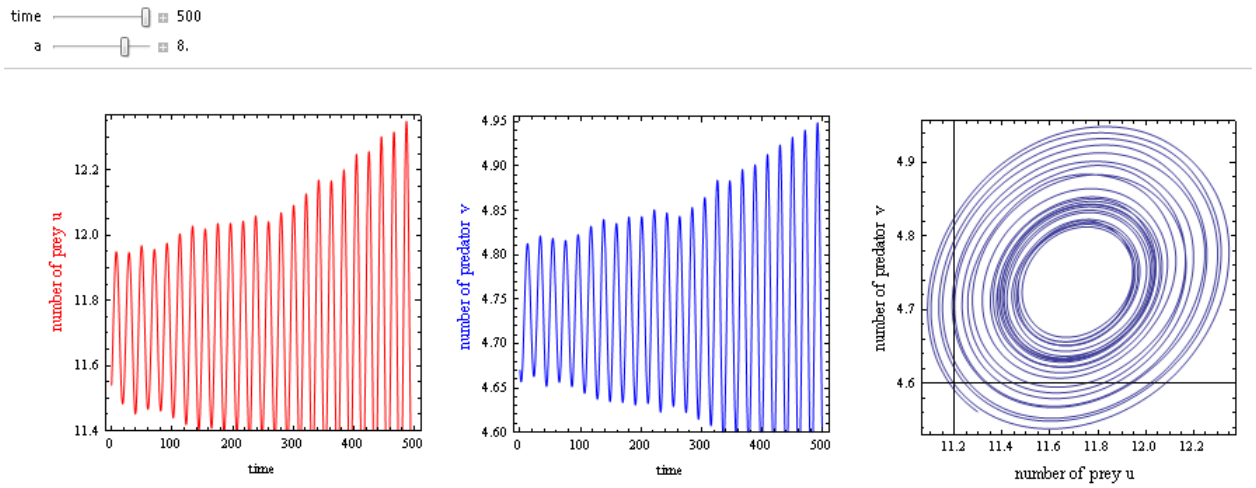

Figure 4.5 Snapshot of the dynamic simulation when t=500, *a*=8.0

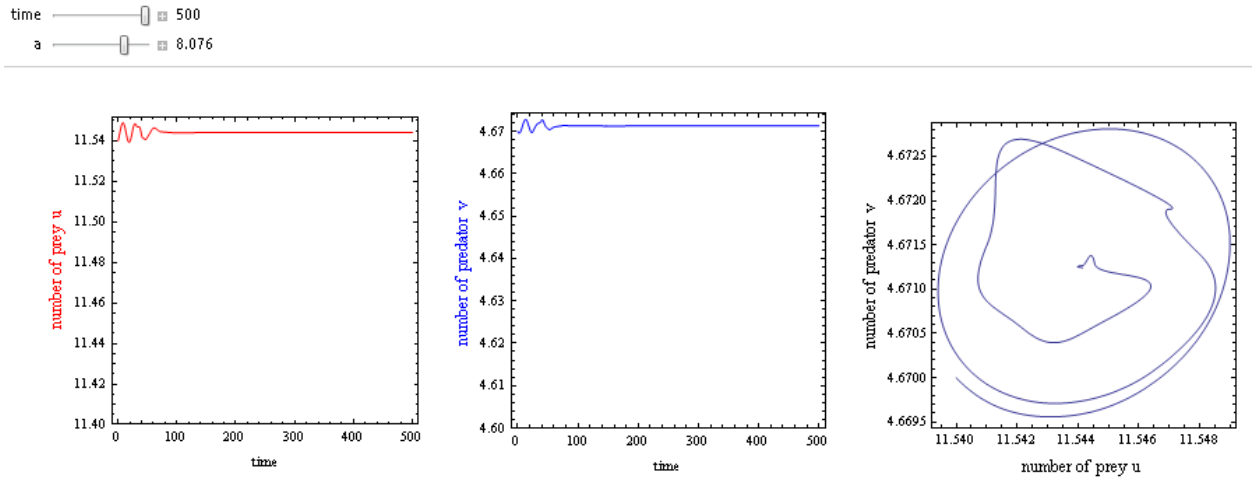

Figure 4.6 Snapshot of the dynamic simulation when t=500, *a*=8.076

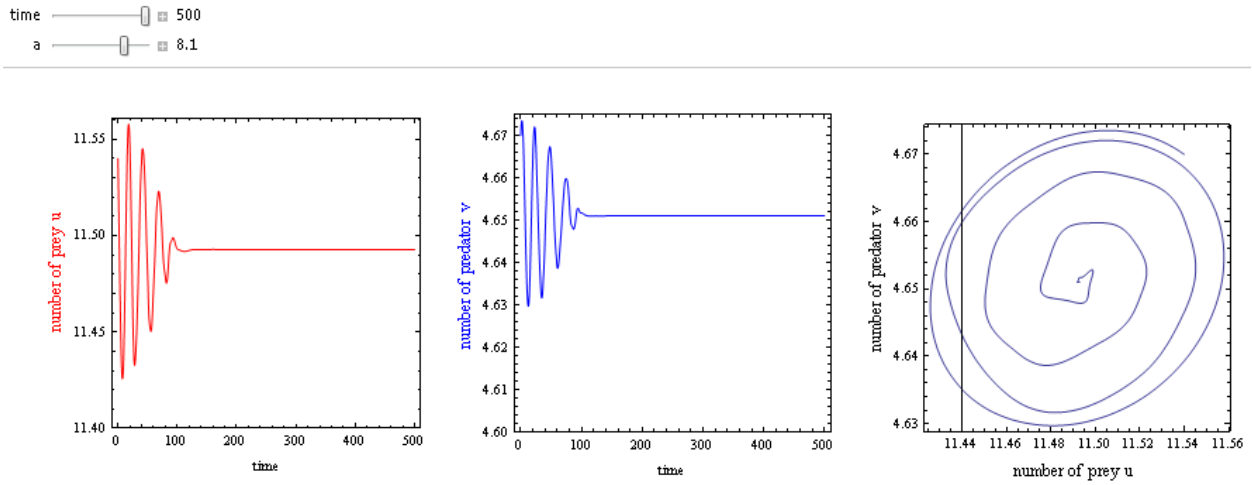

Figure 4.7 Snapshot of the dynamic simulation when t=500, *a*=8.10

Figure 4.5 presents an unstable system when *a*=8 while Figures 4.6 and 4.7 presents a stable state when *a*=8.076 and *a*=8.10, which indicates that the system stability changes at the bifurcation point.

In order to further compare the effect of the different approaches on the stability of the system, a simulation on a 100*100 grid is conducted. Figures 4.8-4.10 demonstrate the dynamics of the prey and predator as a function of the number of iterations (left hand side) and a function of both populations (right hand side) under the critical conditions of a = 8.076. Subfigure (a) shows the simulation when the initial distribution for prey and predator is at their stable state which is 11.54 and 4.67 respectively. Subfigure (b) shows the simulation when the initial distribution for prey and predator is not at a stable state (u= 4.67 and v=10). Subfigure (c) shows the simulation when the initial distribution for prey and predator is from the outside of the cycle in which u=100 and v=34. Figure 4.8 demonstrated the system performance for the basic model, while Figure 4.9 and Figure 4.10 demonstrated for game-based model and cross-diffusion model, respectively.

In addition, pattern formation simulations comparing the two models have also been conducted. Using the stable state as the initial condition, perturbation is introduced into the stable

state, in which there are 11.54 prey and 4.67 predators in each cell in the lattice. Simulations were run with 20000, 40000 and 60000 iterations. The simulated results for the game-based model and the cross-diffusion model are shown in Figures 4.11 and 4.12 respectively.

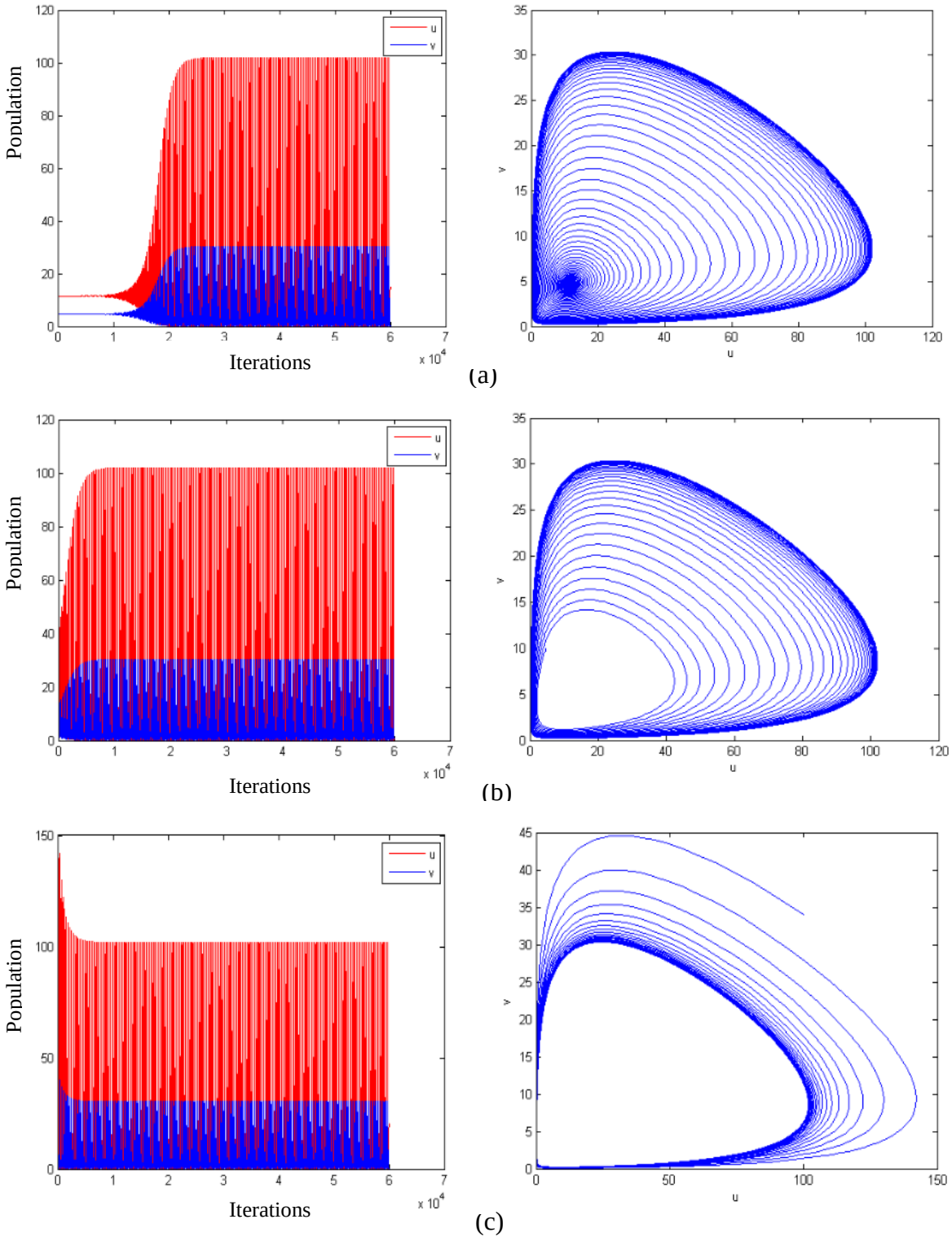

Figure 4.8 System performance for the basic model

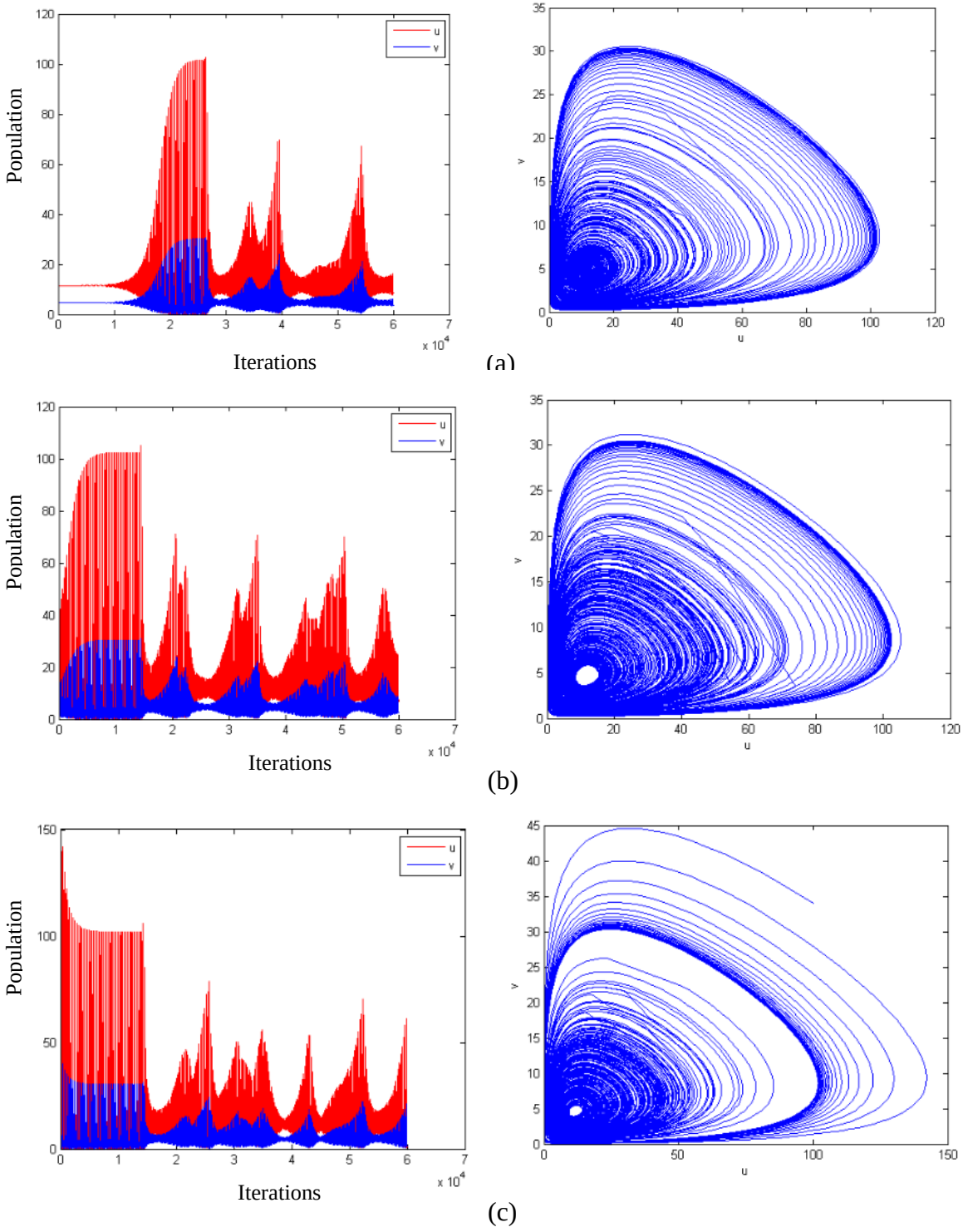

Figure 4.9 System performance for the game-based model

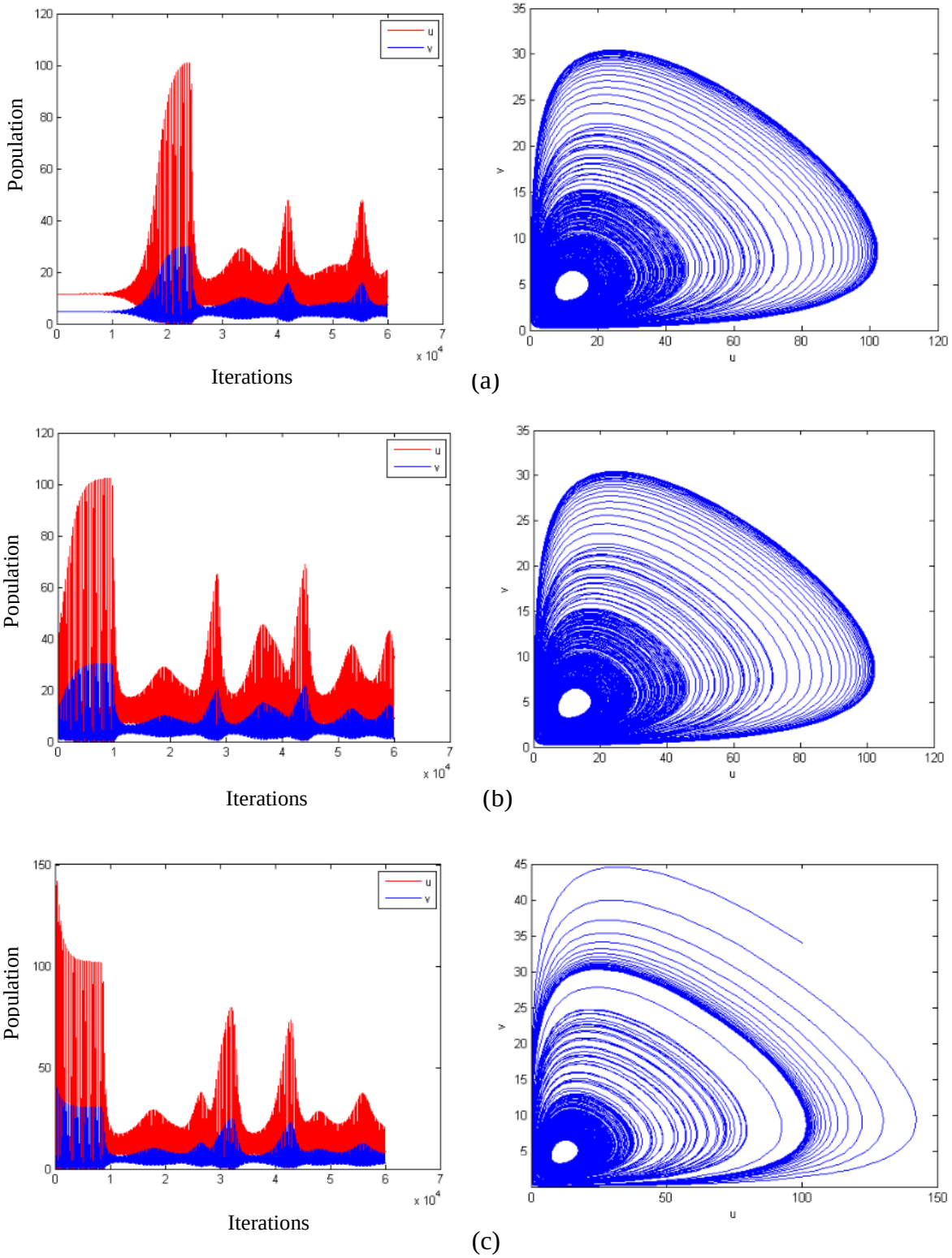

Figure 4.10 System performance for the cross-diffusion model

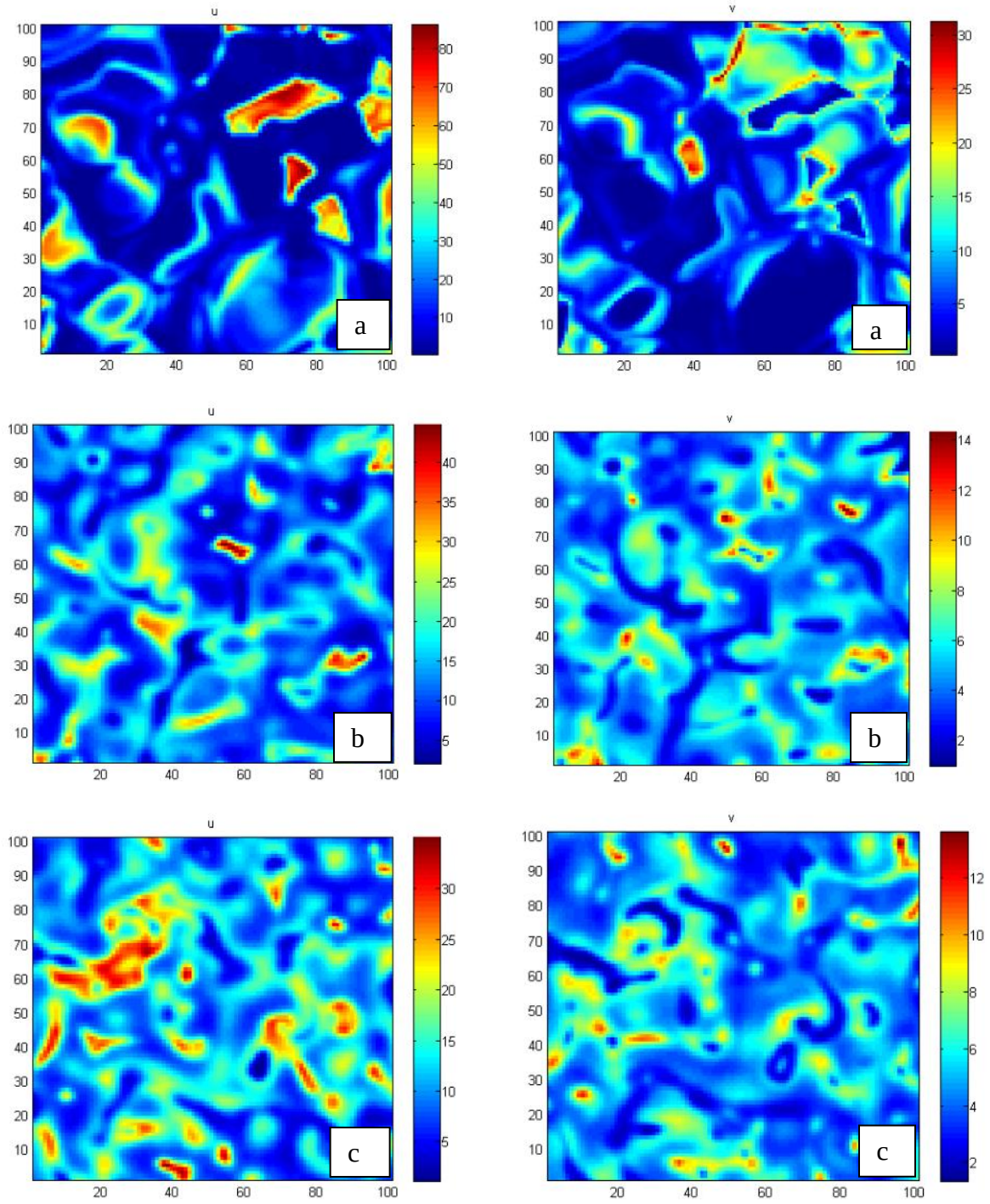

Figure 4.11 Pattern of Prey and Predator with game-based model. (a) 20000 iteration, (b) 40000 iterations, and (c) 60000 iterations. The prey population is shown on the left, and the predator population is on the right.

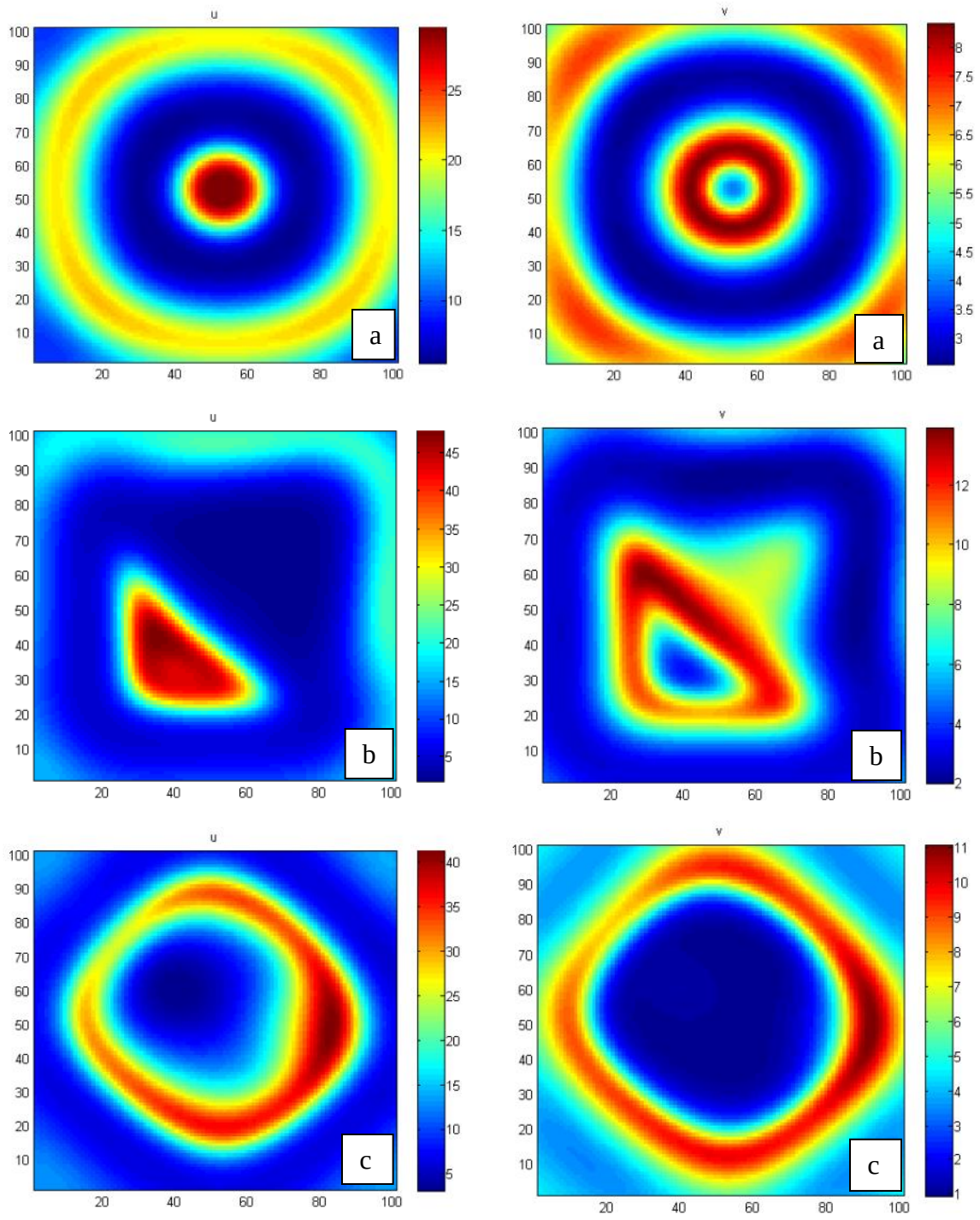

Figure 4.12 Pattern of Prey and Predator with cross-diffusion model. (a) 20000 iteration, (b) 40000 iterations, and (c) 60000 iterations. The prey population is shown on the left, and the predator population is on the right.

From the simulation results, Figure 4.8 shows that the system spirals towards the stable limit cycle when a=8.076 regardless of the initial conditions of prey and predator. In Figures 4.9 and Figure 4.10 we can see that both the game-based model and the cross-diffusion model are less stable than the basic model, demonstrating that the movement of prey and predators affects the stability of the system (the Basic Model is not spatial and does not capture movement of the population as is represented in Equation (4.7) -(4.8)). Also, we can see that the game-based model and cross-diffusion model act similarly in different scenarios. In subfigure (a) of Figure 4.9 and Figure 4.10, prey and predator stay in the stable state and then both populations grow reaching some peak point and then start to oscillate. In subfigure (b), prey and predator increased to a stable state and then fluctuate in both models. In subfigure (c), prey and predator decrease to stable state and then to fluctuate for both models. From the simulation result, the game-based model and cross-diffusion model act similarly in their density distribution but they differ when considering the pattern formation when starting from the same initial state. The game-based model looks more balanced than the cross-diffusion model.

4.5 Model Validation

This section presents an actual case with the two spotted spider mite and its predator *Phytoseiulus persimilis* illustrating the applicability of the game-based approach. This section describes the model's validation using the experimental data and compares the simulated results with the actual observed data using both modeling approaches.

4.5.1 Background

The two-spotted spider mite, *Tetranychus urticae* (*T. urticae*), is a species of plant-feeding mites generally considered to be a pest. Previous reports have stated that *T. urticae* infests over 300 species of plants, including ornamental plants such as arborvitae, azalea, and viburnum, fruit crops such as blackberries, blueberries and strawberries, vegetable crops such as tomatoes, squash, eggplant, and cucumber [111].

Predators are beneficial in regulating spider mite population, and there are several predators that can control the spider mite populations by feeding on the adults and the eggs. *Phytoseiulus persimilis* (*P. persimilis*) is the most popular predator for this pest. This beneficial mite is commercially available and commonly released against *T. urticae* [136].

4.5.2 Experimental Design

The data are taken from an actual study performed and published by the Entomology Department at Kansas State University.

The experimental unit consisted of 24 bean plants arranged in an 8*3 array with *Phytoseiulus persimilis* as predator and *Tetranychus urticae* as prey. Plants within the array were packed closely together to allow mites to move freely from plant to plant. This experiment lasted 24 days, and the total number of the two-spotted spider mites and the predator were counted every six days (6, 12, 18 and 24 days after the introduction of predators) during the experiment. The experiment ended after 24 days because many plants showed substantial damage and were no longer suitable hosts for the prey [112]. Table 4.6 lists the initial distribution of prey and predator, and Table 4.7 lists the total number of observed prey (*Tetranychus urticae*) and predator during the 24 days period. The distribution of prey and predator every 6 days is in Appendix A.

Table 4.6 Initial distribution of prey and predator presented as (*u*,v)

(*32*, **6**)	(*0*, **0**)	(*0*, **0**)
(*0*, **0**)	(*0*, **0**)	(*0*, **0**)
(*0*, **0**)	(*0*, **0**)	(*0*, **0**)
(*0*, **0**)	(*0*, **0**)	(*0*, **0**)
(*0*, **0**)	(*0*, **0**)	(*0*, **0**)
(*0*, **0**)	(*0*, **0**)	(*0*, **0**)
(*0*, **0**)	(*0*, **0**)	(*0*, **0**)
(32, **0**)	(*0*, **0**)	(*0*, **0**)

Table 4.7 Total number of observed prey and predators every six days

Time/Days	Number of prey	Number of predator
0	64	6
6	458	6
12	490	13
18	2238	67
24	1954	239

4.5.3 Comparison of Total Number of Prey and Predator

The total number of the two-spotted spider mites and its predator were counted every six days and compared with the simulated game model and the calculated cross-diffusion model. Basic parameters for the simulation were: $\alpha = 20$, $b = 105$, $c = 45$, $d = 0.3$, $e = 0.25$, $r = 0.38$, $K = 400$. While payoff parameters for the game-based model were: $k_1 = k_2 = k_3 = k_4 = 100$, $e_1 = f = g = h = 0.01$, $c_1 = 0.09$, $c_2 = c_3 = c_4 = 100$.

Figure 4.13 presents the comparison of the two species according to the game-based model and the observed data, and Figure 4.14 presents the comparison between the cross-diffusion model and the observed data.

In Figures 4.13-4.14, the dotted curve represents observed data, and the solid curve represents the number of prey and predator calculated based on the simulated models. Statistical results (Root Mean Square Error) are shown in Table 4.8 and Table 4.9.

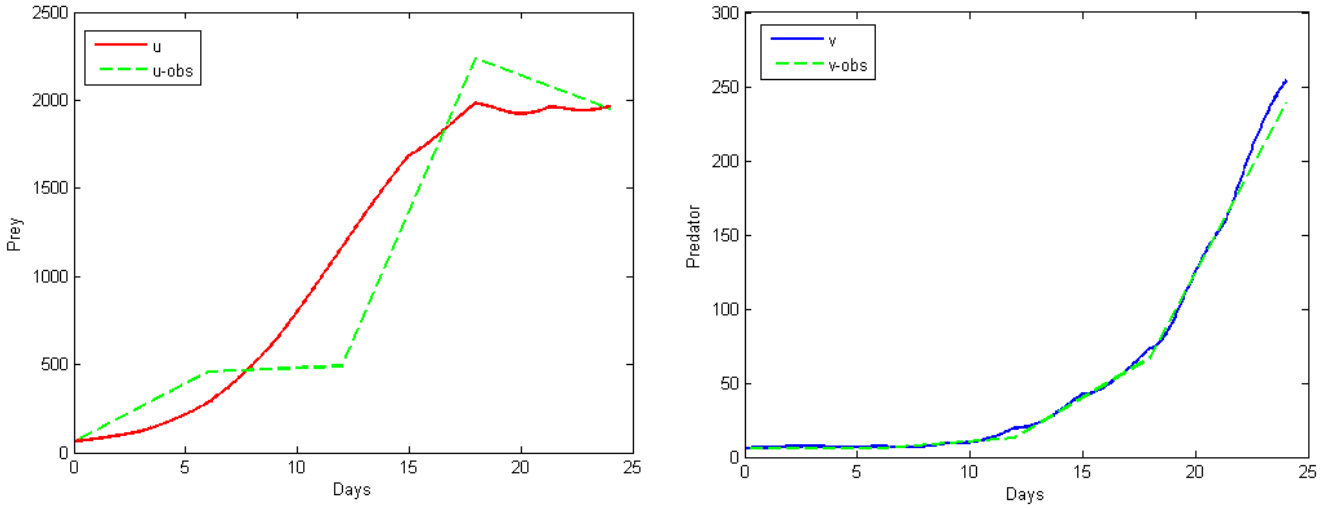

Figure 4.13 Comparison of game-based model with observed data

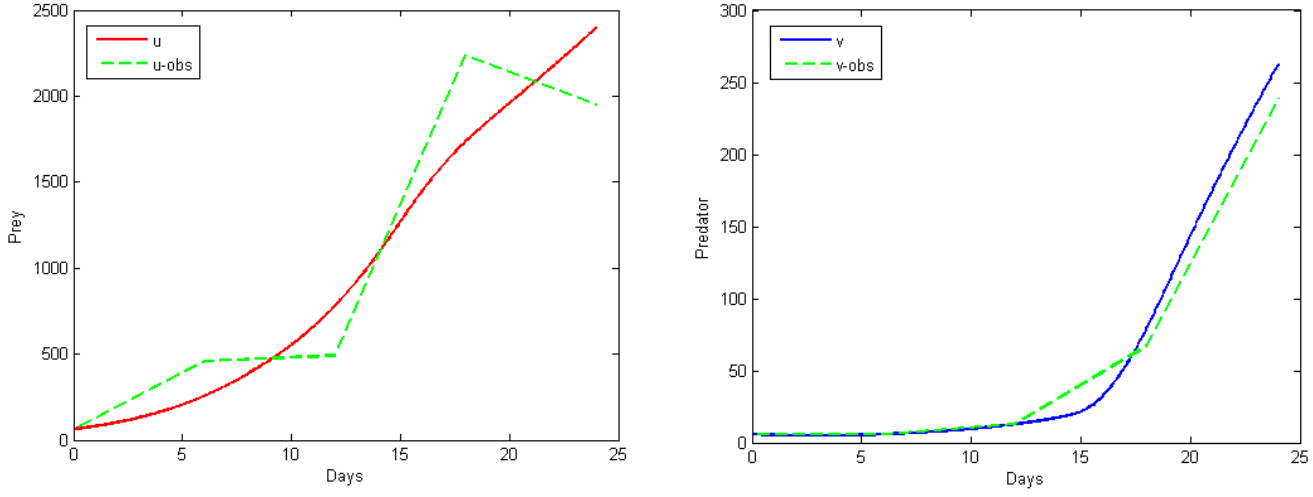

Figure 4.14 Comparison of cross-diffusion model with observed data

Table 4.8 RMSE of the simulated total number of prey and its observations

Time/Days	Observations of Prey	Model with game	Cross-Diffusion
0	64	64	64
6	458	284	258
12	490	1165	781
18	2238	1982	1737
24	1954	1965	2398
RMSE		**371.24**	**378.68**

Table 4.9 RMSE of the simulated total number of predators and its observations

Time/Days	Observations of Predator	Model with game	Cross-Diffusion
0	6	6	6
6	6	7	6
12	13	20	13
18	67	73	80
24	239	254	263
RMSE		**8.82**	**13.42**

The Root Mean Square Error (RMSE) is a frequently used measurement of the differences between values predicted by a model and the values actually observed. A smaller RMSE means a better fit of the model to the data. Comparison results show that the game-based model fits the observations more closely than the cross-diffusion model since it has a smaller RMSE for both prey and predator. Thus, we conclude that the game-based model has a good fit and can generate good predictions of the prey-predator populations.

4.5.4 Sensitivity Analysis

Sensitivity analysis is the study of the effect of uncertainty in input values that can impact the output of a mathematical model [137, 138]. For the game-based model, this section explores the impact of different parameters have on the total number of prey and predator, in order to recognize the significant factors and develop suggestions on controlling the population of two spotted spider mites.

In the sensitivity analysis presented in this section, the total number of two spotted spider mites and its predator acted as the response outputs. The uncertainty inputs tested (one at a time) are: the birth rate of prey, the conversion rate of prey to predator and the death rate of predator. This analysis follows the same initial conditions as in the experimental study (as stated in the previous section). Simulation results are shown in Figures 4.15-4.17. For each figure, subfigure (a) represents the total number of prey respond to different parameter values while subfigure (b) represents the total number of predator.

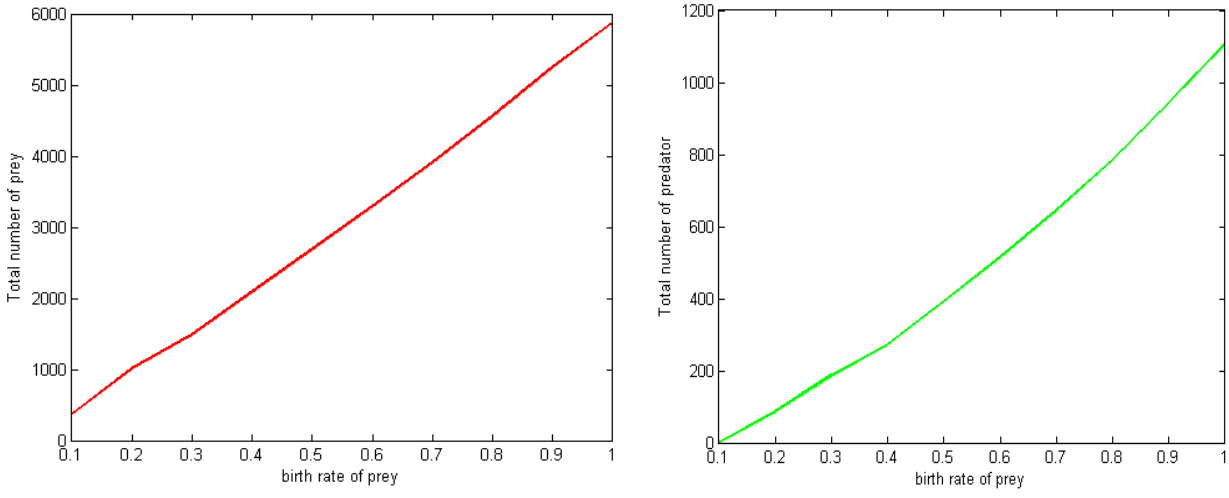

(a) (b)

Figure 4.15 Sensitivity to birth rate of prey

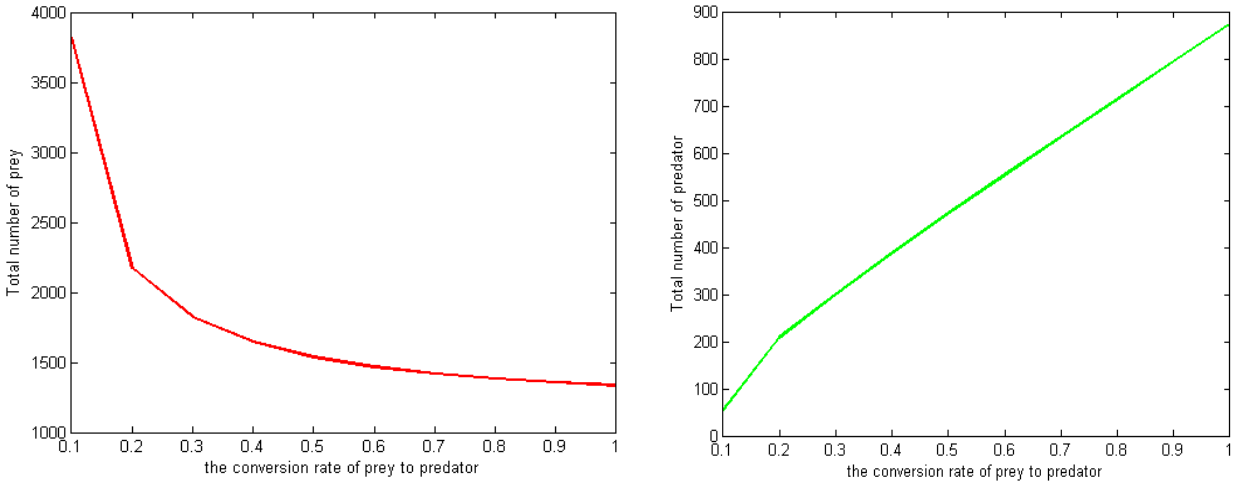

(a) (b)

Figure 4.16 Sensitivity to conversion rate of prey to predator

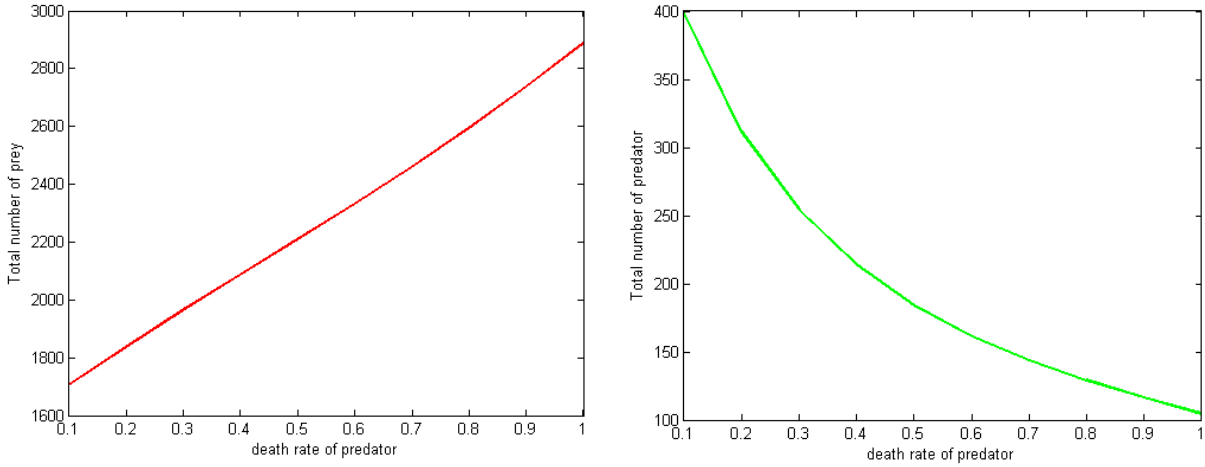

(a) (b)

Figure 4.17 Sensitivity to death rate of predator

Through the simulation, prey's birth rate and predator's death rate positively correlated with the total number of prey thus concluding that a higher birth rate of prey and a higher death rate of predator leads to higher economic loss. The conversion rate of prey to predator has a negative correlation with the total number of prey, which indicates that a higher conversion rate can reduce economic loss.

Thus, the suggested efficient control strategies should be to decrease the two spotted spider mites' birth rate and its predator's death rate, and to increase the conversion rate of prey to predator.

4.6 Conclusion and Discussion

This paper presents and analyzes a new modeling approach for spatial and dynamic evolutionary systems, specifically for two species prey-predator dynamics system. This new approach represents the spatial dynamics of both species as a game model which uses payoff functions that the players (the two species) can receive based on the populations in the surrounding cells. The values of the payoff for each player helps generate the probability that the players will migrate to or away from the neighboring cells. This interaction when carried out over many iterations represents the spatial dynamics of the two species. The game-based model is simulated and compared in this paper to a more traditional cross-diffusion dynamic model that was discussed earlier. In addition to the simulation, the game-based model is validated by using actual experimental data in which the two species were observed every six days over a period of 24 days.

In the numerical simulation section, one conclusion obtained from the results was that the game-based model performed similarly to the cross-diffusion model regarding population changes, while the pattern of the game-based model is more balanced than that of cross-diffusion model when they start from the same stable state.

In the model validation section, the paper presents a comparison of the population of prey and predator, taking two spotted spider mites and its predator- *Phytoseiulus persimilis* as an example. Results show that both the game-based model and the cross-diffusion model are a good fit for the actual experimental data and the game-based model fits the observations more closely

than the cross-diffusion model regarding the total number of prey and predator. Overall, we can conclude that the game-based model is a good fit and can generate good predictions of the prey-predator system.

The game-based modeling approach can be extended to other systems, such as competing commercial firms, logistic distribution systems and similar dynamic systems. The game-based approach uses a payoff function and a movement probability function that can be adjusted based on habits, characteristics and mobility schemes of different competing entities. Thus, this modeling approach can be applied to many other areas of science.

Overall, this modeling approach is more flexible and comprehensive. It can be easily extended to other systems, especially to biological and ecological dynamic systems, for instance to a virus-vector-host plant system. The game-based approach can capture complex interactions that go beyond the traditional system dynamics representation. These interactions can be modeled using the payoff functions, movement functions and other complex rules that control the interaction among the players. On the other hand, in traditional dynamic models the movement represented using a diffusion scheme is usually limited to simple movements of the players.

Future expansion of this research can include more sophisticated models, such as agent-based models [126, 127, 139, 140] and further validation of models using experimental systems with different spatial scales and different distributions of prey and predator. Also, optimal control theory could be considered [129, 130, 141]. This will provide decision makers with better policies for controlling the populations of evolutionary dynamic systems.

Chapter 5 - Using Spatial Games to Model and Simulate Tomato Spotted Wilt Virus – Western Flowers Thrip Dynamic System

Chapter 5 is based on the paper "Using Spatial Games to Model and Simulate Tomato Spotted Wilt Virus – Western Flowers Thrip Dynamic System" submitted to International Journal of Modeling and Simulation.

Abstract

Modeling a complex chain-effect of biological agents is of great interest to researchers and practitioners. The paper presents such a chain consisting of the Tomato Spotted Wilt Virus (TSWV) which is carried by the western flower thrips (WFT) as its vector, and infects tomato plants. The TSWV is a virus that infect more than 1000 plant species, including agronomic and ornamental crops as well as weed hosts, causing significant financial loss. This virus is transmitted by thrips, and the western flower thrips (*Frankliniella occidentalis*) is reported to be the most important vector due to its wide distribution. This paper introduces a new modeling approach based on a spatial game to model this dynamic system. The paper presents this approach along with simulations and validation using experimental data. This method has a broad descriptive power and is applicable to other vector-borne disease systems.

5.1 Introduction

Spotted wilt of tomato was first described by Brittlebank in 1919 [142]. The name Tomato Spotted Wilt Virus (TSWV) was first established by Samuel [143] for characterizing the pathogenic agent as a virus and it remains one of the most important plant viruses that are

distributed broadly around the world. Tomato spotted wilt virus, belongs to the genus *Tospovirus*, infects over 1000 plant species in over 85 families, including ornamentals, vegetables, and field crops [144], causing significant economic damage. The symptoms caused by TSWV varies from different species of infected host, weather condition and age of plants, including ringspots, mottling, and line patterns on leaves [145].

TSWV is unique since it is one of a few viruses known to be transmitted by thrips. There are nine species reported as vectors of TSWV [146] with the Western Flower Thrips (WFT) considered as the most efficient vector due to its wide distribution and the overlapping host ranges with TSWV [5, 147-149]. A large number of weed species in the family *Asteraceae* serve as common reservoirs for infected WFT that invade greenhouses [150-153].

Western flower thrips life cycle consists of six stages: egg, two larvae stages, two transformation stages (prepupae and pupae), and an adult stage. TSWV-WFT transmission happens in a continuous and spatially distributed mode. The TSWV must be acquired by thrips during the first larval stage. Thus, only immature thrips that acquire the TSWV when they are on the first larvae stage can grow into adults that can transmit the virus [5, 144, 154-156]. The WFT can get infected by the TSWV at the second larvae stage or at the adult stage but cannot transmit the virus to plants [157, 158]. Even though there is only a limited time for thrips to capture the virus, the widespread host range for both virus and thrips advances the spread of this virus. Infected thrips, primarily adults, move into greenhouses from outdoor plants and, thus, introduce plant infection [159].

This plant disease has been proven difficult to control, and even more difficult to predict the transmission effect among virus, vector and host plants due to the complexity of the disease interaction system. Mathematical models are of great importance serving as a valuable tool to

study this dynamic system and make predictions on the disease transmission. Some models for TSWV have been recently developed looking from both the biology perspective and from the vector perspective: some focused on the analysis of weather condition influences [95, 98, 100], temperature influences [160, 161], and analysis of parameters such as thrips age [162], time delay [153] and preference behavior [104, 108, 163] that may influence the whole system.

Since the adult thrips can fly and expedite the transmission of the disease within the greenhouse, spatial effect of this model needs to be considered. In this chapter, a spatial game model is used to capture this spatial dynamic. This model includes payoff functions, and move probability functions which define the mobility of adult thrips. The new approach is validated with experimental data and parametric simulation that provides sensitivity analysis and recommendations on the controlling this vector-borne disease.

This chapter is organized as follows. Section 5.2 presents the basic dynamic model considering the life development of the vector and transmission in the triangle virus-vector-host plant system. Section 5.3 proposes a more complex dynamic model considering the whole life cycle of the vector. Section 5.4 introduces the new game-based modeling approach and section 5.5 demonstrates preliminary results including a comparison between this new approach and experimental data, and a simulation to seek the significant factors that affect this disease system. Section 5.6 discusses the results and presents future work.

5.2 Basic Dynamic Model

One mathematical model is constructed based on the transmission principle of TSWV by WFT. The parameters used in the model are shown in Table 5.1.

Table 5.1 Parameters of the mathematical model

Parameter	Interpretation
ν_h	Birth rate of the host
β_v	Bite rate of the thrips
T_{hv}	Infection rate from vector to host
γ_h	Age at harvest of host
μ_h	Death rate of host
τ_h	Incubation period for exposed host
ν_v	Birth rate of the thrip
K_v	Carrying capacity of thrips population
T_{vh}	Infection transmission rate from host to vector
μ_v	Death rate of thrips adults
μ_L	Death rate of thrips larvae
γ_v	Age at maturity of WFT
τ_v	Incubation period for vector

The system diagram of TSWV transmission between the host and WFT is shown in Figure 5.1. In this section, we assume the population is homogeneous. A modified susceptible-exposed-infected (SEI) model is constructed for both of host and WFT (Eqs. (5.1)-(5.11)).

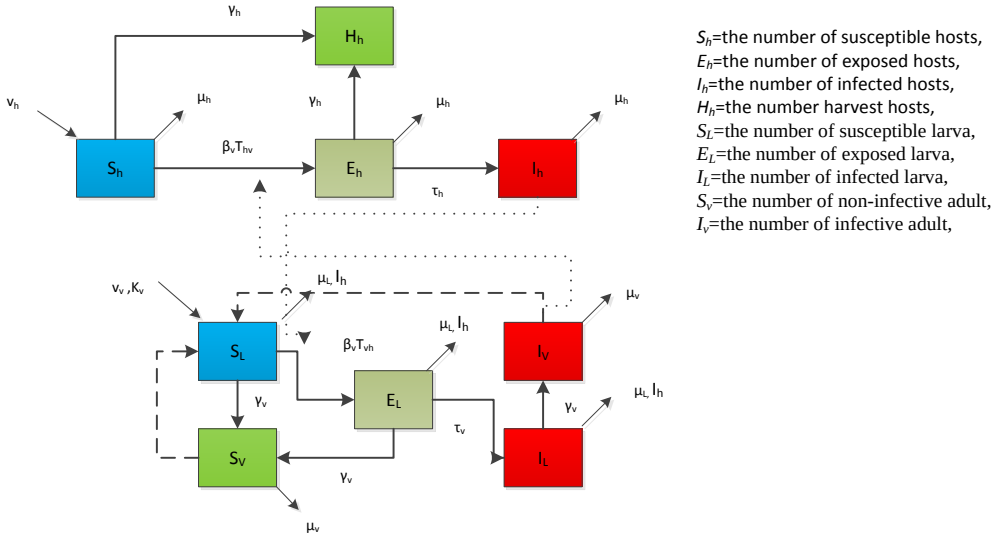

Figure 5.1 System Diagram of WFT-TSWV Model

Host Population

$$\frac{dS_h}{dt} = \nu_h - (\beta_v T_{hv} I_v S_h) / N_h - (1/\gamma_h) S_h - \mu_h S_h \tag{5.1}$$

$$\frac{dE_h}{dt} = (\beta_v T_{hv} I_v S_h) / N_h - (1/\tau_h) E_h - (1/\gamma_h) E_h - \mu_h E_h \tag{5.2}$$

$$\frac{dI_h}{dt} = (1/\tau_h) E_h - \mu_h I_h \tag{5.3}$$

$$\frac{dH_h}{dt} = (1/\gamma_h) S_h + (1/\gamma_h) E_h \tag{5.4}$$

$$\frac{dN_h}{dt} = \nu_h - \mu_h S_h - \mu_h E_h - \mu_h I_h \tag{5.5}$$

where

S_h: the number of susceptible hosts

E_h: the number of exposed hosts

I_h: the number of infected hosts

H_h: the number of harvested hosts

N_h: the total number of hosts

WFT Population

$$\frac{dS_L}{dt} = \nu_v (S_v + I_v)(1 - N_v / K_v) - (\beta_v T_{vh} I_h S_L) / N_h - (1/\gamma_v) S_L - \mu_L S_L \tag{5.6}$$

$$\frac{dE_L}{dt} = (\beta_v T_{vh} I_h S_L) / N_h - (1/\tau_v) E_L - (1/\gamma_v) E_L - \mu_L E_L \tag{5.7}$$

$$\frac{dI_L}{dt} = (1/\tau_v) E_L - (1/\gamma_v) I_L - \mu_L I_L \tag{5.8}$$

$$\frac{dS_v}{dt} = (1/\gamma_v) S_L + (1/\gamma_v) E_L - \mu_v S_v \tag{5.9}$$

$$\frac{dI_v}{dt} = (1/\gamma_v)I_L - \mu_v I_v \tag{5.10}$$

$$\frac{dN_v}{dt} = v_v(S_v + I_v)(1 - N_v / K_v) - \mu_v N_v \tag{5.11}$$

where

S_L: the number of susceptible larva

E_L: the number of exposed larva

I_L: the number of infected larva

S_v: the number of non-infective adult

I_v: the number of infective adult

N_v: total number of WFT

In this model, WFT are classified into two groups: larvae and adults. WFT larvae are distributed among susceptible S_L, exposed E_L, and infected I_L compartments and adults are distributed between non-infective S_v and infective I_v. Only susceptible larvae equation includes birth rate because the female WFT do not transmit TSWV vertically. Specifically, the susceptible larvae can either develop to non-infective adults or be transmitted to exposed larvae. The exposed larvae can either develop to non-infective adults successfully or be transferred to infected larvae. The infected larvae develop to infective adults. The hosts are distributed among susceptible S_h, exposed E_h, infected I_h, and harvest H_h. The susceptible host may either harvest or be infected by infective WFT adults. The exposed hosts may either be harvested before becoming infected or transfer to infected hosts. The infected hosts cannot recover or be harvested.

5.3 Complex Dynamic Model

In this section, a more complex dynamic model is presented. The key characteristics of the vector life process, such as development stages, development time, survival, daily death, as well as the virus transition and the mutual infection among virus-vector-host plants, forms the basis of the dynamic model. The model presented is an extension of the models presented in the literature, such as [104, 153].

5.3.1 Model Description and Assumption

The model describing the vector life process and disease transmission system is established based on the following assumptions:

- Infection transmission to host plants is subject to contact by infective vectors.
- The infection acquisition of the vector is by biting on infected host plants.
- Eggs are born as non-infected since this virus transmission does not belong to a vertically transmitted infection which uses mother-to-child transmission.
- Only the vector who got infected on Larvae 1 stage can transmit the virus during its development.
- The vectors on later stages (Larvae 2, Prepupa, Pupae and Adults) can acquire the virus but are not able to transmit the infection.
- The vectors on larvae stages (Larvae 1 and Larvae 2) are portable but restricted to the plant where they were born as eggs.
- Prepupae and Pupae are immobile and have no influence on the transmission process.
- Adults can move from plant to plant.

- Adults have preference for plants according to their infection status as well as the infective status of plants: infected adults prefer healthy host plants, while healthy adults prefer infected host plants.

  The development of WFT and the TSWV transmission process is clarified in Figure 5.2.

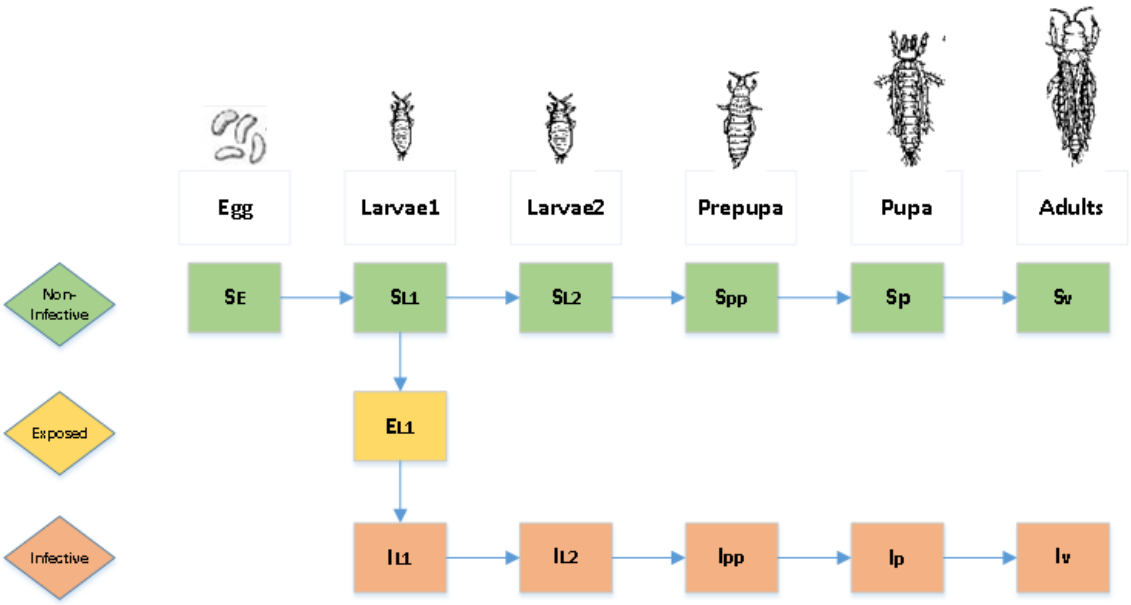

Figure 5.2 Flowchart of WFT life development and virus transmission

In this model, WFT have six developmental stages: egg-larvae1-larvae2-prepupae-pupae-adult. Susceptible-exposed-infected (SEI) framework is employed. As stated, all eggs are healthy, denoted as S_E. For larvae 1, susceptible vector (S_{L1}) get exposed (E_{L1}) and become infective (I_{L1}). For the other stages of WFT, only those developed from infective larvae 1 can transmit the virus, denoted as I_{L2}, Ipp, Ip and Iv. The other stages that are susceptive and are not able to transmit the virus, are denoted by S_{L2}, Spp, Sp and Sv.

5.3.2 Mathematical Model

Based on the principle of vector life development and TSWV transmission, the complex dynamic model is presented in Equations (5.12) - (5.24). For host plant, the infection level depends on the fraction of infective adults, meaning that with more infective adults on the plant, the higher the infection level that the host plant would get. The range of plant infection level is assumed to range from 0 to 1, (low to high). This model is an extension of the models reported in the literature, however, it is not capable of modeling the spatial effects of this complex interaction, such as movement of thrips and spread of the plant infections. All the variables and parameters are summarized in Table 5.2 and Table 5.3.

WFT Population:

Eggs

$$\frac{dS_E}{dt} = V_v(S_v + I_v) - \left({}^{1}/_{\gamma_{SL1}}\right)S_E - \mu_E S_E \tag{5.12}$$

Larvae 1

$$\frac{dS_{L1}}{dt} = \left({}^{1}/_{\gamma_{SL1}}\right)S_E - \beta_{L1} I_h S_{L1} - \left({}^{1}/_{\gamma_{SL2}}\right)S_{L1} - \mu_{SL1} S_{L1}\, {}^{N_v}/_{K_v} \tag{5.13}$$

$$\frac{dE_{L1}}{dt} = \beta_{L1} I_h S_{L1} - \left({}^{1}/_{\gamma_{IL1}}\right)E_{L1} - \mu_{EL1} E_{L1}\, {}^{N_v}/_{K_v} \tag{5.14}$$

$$\frac{dI_{L1}}{dt} = \left({}^{1}/_{\gamma_{IL1}}\right)E_{L1} - \left({}^{1}/_{\gamma_{IL2}}\right)I_{L1} - \mu_{IL1} I_{L1}\, {}^{N_v}/_{K_v} \tag{5.15}$$

Larvae 2

$$\frac{dS_{L2}}{dt} = \left(1/\gamma_{SL2}\right)S_{L1} - \left(1/\gamma_{SPP}\right)S_{L2} - \mu_{SL2}S_{L2}\,{}^{N_v}/_{K_v} \quad (5.16)$$

$$\frac{dI_{L2}}{dt} = \left(1/\gamma_{IL2}\right)I_{L1} - \left(1/\gamma_{IPP}\right)I_{L2} - \mu_{IL2}I_{L2}\,{}^{N_v}/_{K_v} \quad (5.17)$$

Prepupae

$$\frac{dS_{pp}}{dt} = \left(1/\gamma_{SPP}\right)S_{L2} - \left(1/\gamma_{SP}\right)S_{pp} - \mu_{Spp}S_{pp}\,{}^{N_v}/_{K_v} \quad (5.18)$$

$$\frac{dI_{pp}}{dt} = \left(1/\gamma_{IPP}\right)I_{L2} - \left(1/\gamma_{IP}\right)I_{pp} - \mu_{Ipp}I_{pp}\,{}^{N_v}/_{K_v} \quad (5.19)$$

Pupae

$$\frac{dS_p}{dt} = \left(1/\gamma_{SP}\right)S_{pp} - \left(1/\gamma_{Sv}\right)S_p - \mu_{Sp}S_p\,{}^{N_v}/_{K_v} \quad (5.20)$$

$$\frac{dI_p}{dt} = \left(1/\gamma_{IP}\right)I_{pp} - \left(1/\gamma_{Iv}\right)I_p - \mu_{Ip}I_p\,{}^{N_v}/_{K_v} \quad (5.21)$$

Adults

$$\frac{dS_v}{dt} = \left(1/\gamma_{Sv}\right)S_p - \mu_{Sv}S_v\,{}^{N_v}/_{K_v} \quad (5.22)$$

$$\frac{dI_v}{dt} = \left(1/\gamma_{Iv}\right)I_p - \mu_{Iv}I_v\,{}^{N_v}/_{K_v} \quad (5.23)$$

Where $Nv = (Sv + Iv)$ is the total number of adult thrips

Host Plants

$$\frac{dI_h}{dt} = \beta_I \frac{I_v}{S_v + I_v}(1 - I_h) \quad (5.24)$$

Table 5.2 Notations of the mathematical model

Parameter	Interpretation
S_E	Number of susceptible Eggs
S_{L1}	Number of susceptible Larvae1
E_{L1}	Number of exposed Larvae1
I_{L1}	Number of infective Larvae1
S_{L2}	Number of non-infective Larvae 2
I_{L2}	Number of infective Larvae 2
S_{pp}	Number of non-infective Prepupae
I_{pp}	Number of infective Prepupae
S_p	Number of non-infective Pupae
I_p	Number of infective Pupae
S_V	Number of interacting non-infective Adults
I_V	Number of interacting infective Adults
I_h	Infection level of host plants

Table 5.3 Parameters of the mathematical model

Parameter	Description
v_v	Birth rate of WFT
K_v	Carrying capacity of WFT population
γ_{SL1}	The average number of days required for eggs to develop to Larvae 1
μ_E	Daily death rate of thrip eggs
β_{L1}	Bite rate of the thrips
γ_{SL2}	The average number of days required for susceptible larvae 1to develop to non-infective Larvae 2
μ_{SL1}	Daily death rate of susceptible Larvae 1
γ_{IL1}	The average number of days required for exposed larvae 1to develop to infective Larvae 1
μ_{EL1}	Daily death rate of exposed Larvae 1
γ_{IL2}	The average number of days required for infective Larvae 1to develop to infective Larvae 2
μ_{IL1}	Daily death rate of infective Larvae 1
γ_{Spp}	The average number of days required for non-infective Larvae 2to develop to non- infective Prepupae
μ_{sL2}	Daily death rate of non-infective Larvae 2
γ_{Ipp}	The average number of days required for infective Larvae 2to develop to infective Prepupae
μ_{IL2}	Daily death rate of infective Larvae 2
γ_{Sp}	The average number of days required for non-infective Prepupae to develop to non-infective Pupae
μ_{Spp}	Daily death rate of non-infective Prepupae

γ_{Ip}	The average number of days required for infective Prepupae to develop to infective Pupae
μ_{Ipp}	Daily death rate of infective Prepupae
γ_{Sv}	The average number of days required for non-infective Pupae to develop to non-infective Adults
μ_{Sp}	Daily death rate of non-infective Pupae
γ_{Iv}	The average number of days required for infective Pupae to develop to infective Adults
μ_{Ip}	Daily death rate of infective Pupae
μ_{Sv}	Daily death rate of non-infective Adults
μ_{Iv}	Daily death rate of infective Adults
β_I	Coefficient on plants infection level

5.4 Spatial Game Model

The spatial evolutionary game is a combination of classic game theory and spatial effects, representing players, policies and dynamics. Generally the different players (plants, vectors and viruses) "make" their decisions based on an updating rule that depends on payoff functions [131]. Game theory was first applied to evolutionary biology by Lewontin [19] and has been adopted to analyze a variety of population problems [133, 164]. For spatial evolutionary game, several common updating rules and schemes are reviewed by Roca et al [23] and Newth and Cornforth [24].

Since the adult thrips have the ability to fly and thus spread the virus to different plants, spatial effect has to be taken into consideration for the distribution of the Tomato Spotted Wilt Virus dynamic system. This unfortunately enhances the speed of transmission of the virus. The robust approach of the spatial game provides this spatial dynamic. The model proposed here is comprised of payoff functions denoting the payoff for each player type and of probability functions which decided on the possibility of adult thrips next movements. This spatial dynamic is enacted on a grid representing the area of interest.

5.4.1 Payoff Function for Adult Thrips

Prior work denoted that the adult thrips, either uninfected or infected, has different preference towards plants that are in different infection status. That is, the non-infective adults show preference for infected plants over healthy plants, while the infective adults show fondness for healthy plants over infected plants [104, 108, 163]. Furthermore, like most thrips, western flower thrips is a competitive species that tends to fly to plants that have smaller thrips populations [165]. Taking these two factors into account makes the payoff for non-infective and infective adults different due to its different preference. For non-infective adults, the payoff is higher with plants that are more severely infected and have smaller population of adult thrips. For infective adults, the payoff is higher with plants that are heathier and have smaller population of adult thrips. The payoff of cell (*i,j*) is calculated as shown in Equation (5.25).

$$P_{Sv}(i,j) = k_1 * I_h(i,j) + \frac{k_2}{Sv(i,j) + Iv(i,j)}$$
$$P_{Iv}(i,j) = k_3 * (1 - I_h(i,j)) + \frac{k_2}{Sv(i,j) + Iv(i,j)} \quad (5.25)$$

Where P_{Sv} denotes the payoff of non-infective adults, P_{Iv} indicates the payoff of infective adults, and $I_h(i,j)$ represents the infection level of host plants within cell (*i, j*). $S_v(i,j)$ and $I_v(i,j)$ represent the noninfective and infective thrips in cell *(i,j)*. Parameters k_1, k_2, k_3 scale the payoff affections. As discussed, the payoff for non-infective adults is proportional to the infection level of plants, while, on the other hand, the payoff for infective adults is inversely proportional to the infection level of the plants. All adult thrips prefer to fly away from high concentration of their own species. The behavior of the payoff functions is demonstrated in Figure 5.3 and Figure 5.4

using the parameters: $k_1 = k_2 = k_3 = 100$, $I_h = [0:1]$, $(Sv + Iv) = 0$ to 40. The level of plant infection I_h goes from 0 to 1, and the total number of adult thrips on each plant changes from 0 to 40.

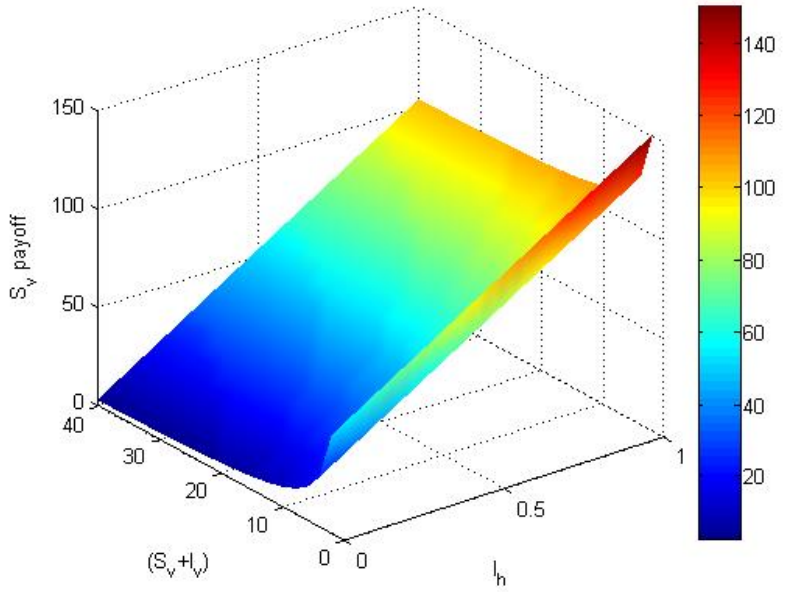

Figure 5.3 Value of payoff function of uninfected adult thrips

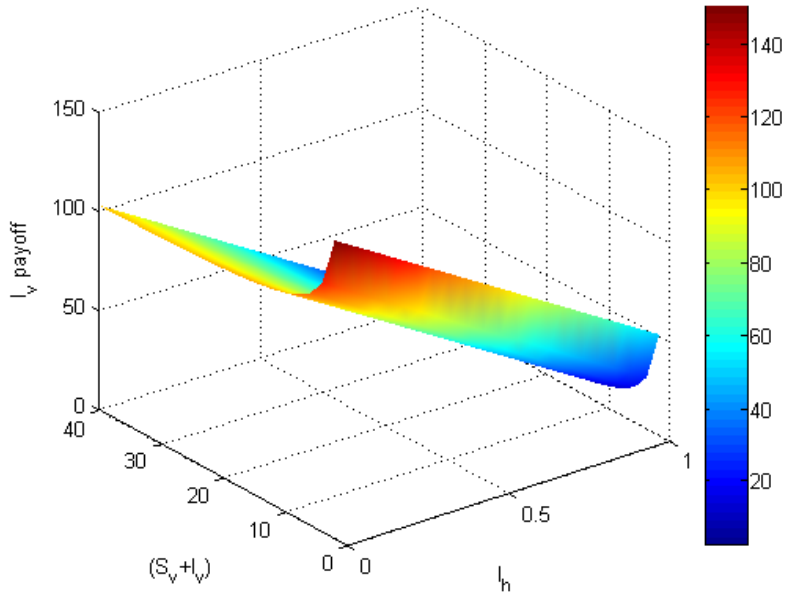

Figure 5.4 Value of payoff function of infected adult thrips

Figure 5.3 denotes that uninfected adult thrips will get higher payoff with the plants that have higher infection level and lower population of adult thrips. Figure 5.4 indicates that infected adult thrips will have higher payoff with the host plants that have lower infection level and lower population of adult thrips.

5.4.2 Move Probability Function

The payoff function presented above defines the payoff of each of the two players: (the healthy adult thrips and infective adult thrips) in the domain of interest (our grid). Based on those payoff values, the probability of the adult thrips to move can be calculated. Western flower thrips is not a strong flyer as discussed in [166]. Thus, it is assumed that adult thrips can move up to two adjacent cells in one move step. The probability of the direction and distance of each movement depends on the fraction of the total payoffs of the accessible region (Eqs. (5.26)- (5.34)).

5.4.2.1 The probability to stay at the same place

$$P_{(i,j)} = \frac{P_{Sv,Iv}(i,j)}{\sum_{\substack{x=i-2,i+2 \\ y=j-2,j+2}} P_{Sv,Iv}(x,y)} \tag{5.26}$$

5.4.2.2 The probability to move one cell up

$$P_{(i-1,j)} = \frac{P_{Sv,Iv}(i-1,j)}{\sum_{\substack{x=i-2,i+2 \\ y=j-2,j+2}} P_{Sv,Iv}(x,y)} \tag{5.27}$$

5.4.2.3 The probability to move two cells up

$$P_{(i-2,j)} = \frac{P_{Sv,Iv}(i-2,j)}{\sum_{\substack{x=i-2,i+2 \\ y=j-2,j+2}} P_{Sv,Iv}(x,y)} \tag{5.28}$$

5.4.2.4 The probability to move one cell down

$$P_{(i+1,\,j)} = \frac{P_{Sv,Iv}(i+1,\,j)}{\sum_{\substack{x=i-2,i+2 \\ y=j-2,\,j+2}} P_{Sv,Iv}(x,y)} \tag{5.29}$$

5.4.2.5 The probability to move two cells down

$$P_{(i+2,\,j)} = \frac{P_{Sv,Iv}(i+2,\,j)}{\sum_{\substack{x=i-2,i+2 \\ y=j-2,\,j+2}} P_{Sv,Iv}(x,y)} \tag{5.30}$$

5.4.2.6 The probability to move one cell left

$$P_{(i,\,j-1)} = \frac{P_{Sv,Iv}(i,\,j-1)}{\sum_{\substack{x=i-2,i+2 \\ y=j-2,\,j+2}} P_{Sv,Iv}(x,y)} \tag{5.31}$$

5.4.2.7 The probability to move two cells left

$$P_{(i,\,j-2)} = \frac{P_{Sv,Iv}(i,\,j-2)}{\sum_{\substack{x=i-2,i+2 \\ y=j-2,\,j+2}} P_{Sv,Iv}(x,y)} \tag{5.32}$$

5.4.2.8 The probability to move one cell right

$$P_{(i,\,j+1)} = \frac{P_{Sv,Iv}(i,\,j+1)}{\sum_{\substack{x=i-2,i+2 \\ y=j-2,\,j+2}} P_{Sv,Iv}(x,y)} \tag{5.33}$$

5.4.2.9 The probability to move two cells right

$$P_{(i,\,j+2)} = \frac{P_{Sv,Iv}(i,\,j+2)}{\sum_{\substack{x=i-2,i+2 \\ y=j-2,\,j+2}} P_{Sv,Iv}(x,y)} \tag{5.34}$$

Based on the probabilities calculated for each cell in the domain, the transition distribution is decided each time. Below is an example showing this dynamics under the spatial game mechanism.

5.4.3 Example of Game Execution

This example uses a 5x5 lattice to demonstrate the movement of adult thrips during one iteration. Table 5.4 shows the current population of uninfected adult thrips and infected adult thrips. Table 5.5 shows the current infection level of host plants. First, using Equation (5.25), the payoff in each cell for two players (the healthy adult thrips and infective adult thrips) is calculated, which is depicted in Table 5.6 and Table 5.7.

Table 5.4 Initial distribution of healthy and infected adult thrips denoted as (*Sv*, Iv)

(*51*, **12**)	(*60*, **18**)	(*23*, **18**)	(*36*, **21**)	(*55*, **29**)
(*32*, **12**)	(*47*, **30**)	(*46*, **29**)	(*39*, **7**)	(*44*, **28**)
(*29*, **23**)	(*57*, **31**)	(*42*, **17**)	(*31*, **13**)	(*31*, **31**)
(*35*, **8**)	(*54*, **29**)	(*34*, **25**)	(*31*, **39**)	(*31*, **22**)
(*58*, **22**)	(*35*, **29**)	(*29*, **16**)	(*38*, **13**)	(*38*, **26**)

Table 5.5 Initial infection level of host plants

0.5508	0.8963	0.0299	0.5909	0.2835
0.7081	0.1256	0.4568	0.0240	0.6931
0.2909	0.2072	0.6491	0.5589	0.4405
0.5108	0.0515	0.2785	0.2593	0.1569
0.8929	0.4408	0.6763	0.4151	0.5446

Table 5.6 Payoff distribution for healthy adult thrips

56.6671	90.9114	5.4266	60.8407	29.5430
73.0875	13.8572	47.0167	4.5721	70.7027
31.0136	21.8607	66.6093	58.1581	45.6583
53.4083	6.3515	29.5436	27.3538	17.5736
90.5447	45.6435	69.8477	43.4709	56.0274

Table 5.7 Payoff distribution for infected adult thrips

46.5075	11.6527	99.4514	42.6681	72.8380
31.4579	88.7402	55.6500	99.7757	32.0751
72.8326	80.4121	36.7805	46.3873	57.5675
51.2428	96.0581	73.8462	75.5033	86.2000
11.9553	57.4815	34.5967	60.4507	47.0976

After the payoff is calculated, the probabilities for players to move are determined based on the movement probability functions (Eqs. (5.26)-(5.34)) that are dependent on the payoff values. For example, the following equations present the move probability for 42 healthy adult thrips in cell (3, 3).

- The probability to stay at the same place:

$$P_{(3,3)} = \frac{P_{Sv,Iv}(3,3)}{\sum_{\substack{x=1,5 \\ y=1,5}} P_{Sv,Iv}(x,y)} = \frac{66.6093}{5.4266+47.0167+66.6093+29.5436+69.8477+31.0136+21.8607+58.1581+45.6583} = \frac{47.0167}{375.1346}$$

=0.177561

This implies that 17.7561% of the healthy adult thrips population in cell (3, 3) will not move.

- The probability to move one cell up:

$$P_{(2,3)} = \frac{P_{Sv,Iv}(2,3)}{\sum_{\substack{x=1,5 \\ y=1,5}} P_{Sv,Iv}(x,y)} = \frac{47.0167}{5.4266+47.0167+66.6093+29.5436+69.8477+31.0136+21.8607+58.1581+45.6583} = \frac{47.0167}{375.1346}$$

=0.12533

- The probability to move two cells up:

$$P_{(1,3)} = \frac{P_{Sv,Iv}(1,3)}{\sum_{\substack{x=1,5 \\ y=1,5}} P_{Sv,Iv}(x,y)} = \frac{5.4266}{5.4266+47.0167+66.6093+29.5436+69.8477+31.0136+21.8607+58.1581+45.6583} = \frac{5.4266}{375.1346}$$

=0.014466

The same calculations are performed for the probability to move to other cells. The entire set of move probabilities is presented in Figure 5.5, showing the probabilities to move from the center cell to the adjacent cells.

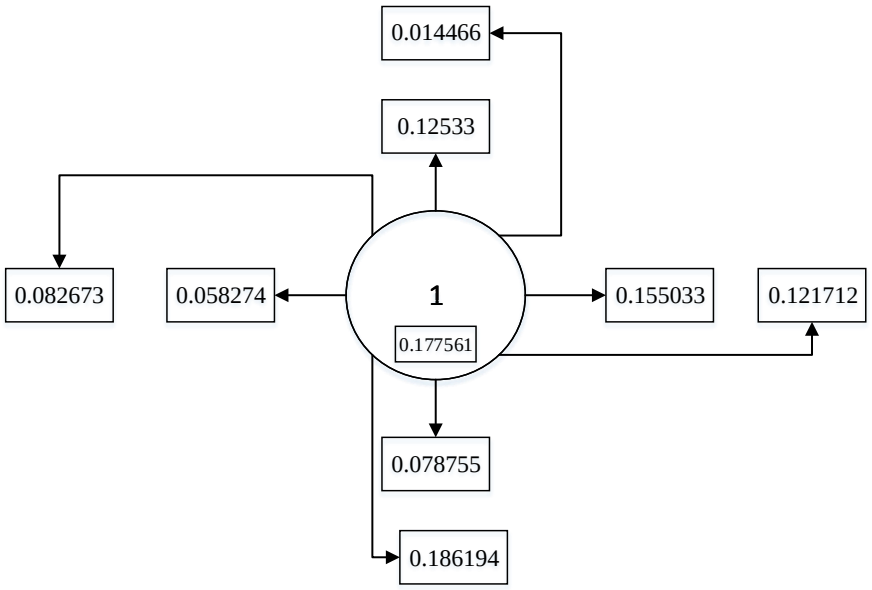

Figure 5.5 Move probability for cell (3,3)

According to the calculations above, the movement of healthy adult thrips from cell (3, 3) to the neighboring cells could be obtained using the function $N \times P$ while rounding up the numbers to the nearest integer. For instance, the 7 healthy thrips will not move ($42 \times 0.177561 = 7.457565 \approx 7$); and 5 will move one cell up ($42 \times 0.125333 = 5.263981 \approx 5$). The same calculations are performed for the other neighboring cells producing the distribution of the 42 healthy adult thrips. The movements from cell (3,3) is shown in Figure 5.6.

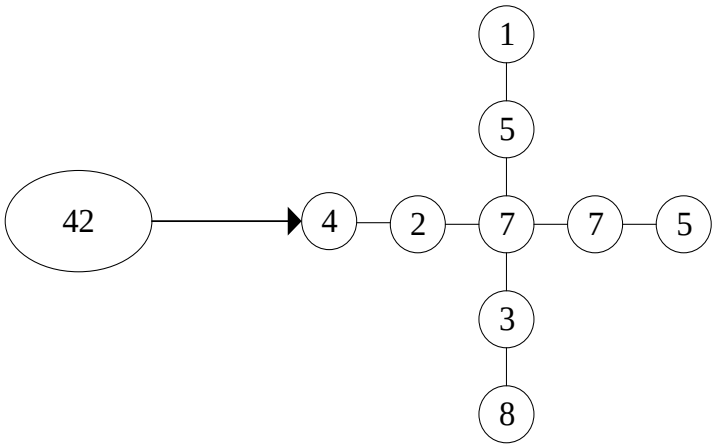

Figure 5.6 Move distribution of healthy adult thrips in cell (3,3)

The same calculations are performed for the infected adult thrips in each cell. After one iteration, the distribution of healthy and infected adult thrips is shown in Table 5.8. During the game mobility phase the populations of the two species is kept the same: there are 1006 heathy adult thrips and 548 infected adult thrips in the whole domain.

Table 5.8 The distribution of healthy and infected adult thrips after exercising movement

(*39*, **12**)	(*91*, **4**)	(*6*, **38**)	(*57*, **12**)	(*23*, **26**)
(*62*, **9**)	(*18*, **30**)	(*50*, **21**)	(*5*, **36**)	(*68*, **12**)
(*31*, **27**)	(*28*, **36**)	(*62*, **17**)	(*61*, **18**)	(*48*, **26**)
(*48*, **17**)	(*7*, **40**)	(*33*, **29**)	(*28*, **24**)	(*15*, **36**)
(*54*, **4**)	(*44*, **22**)	(*63*, **15**)	(*33*, **12**)	(*32*, **15**)

5.4.4 Interaction

After moving to the new cells, the virus, vector and plants interact in the manner formulated in Equations (5.12) - (5.24). The mutual interactions in the triangle virus-vector-plant and the movement of adult thrips captures the whole vector-borne disease dynamic interaction. This interaction defines how many more eggs are laid, how many thrips move between the stages of development, how many plants got infected and all the other parameters that completely define the system.

5.5 Numerical Simulation

This section presents the validation of the game-based model by comparing it with actual observed data from the Entomology Department at Kansas State University. This section also presents sensitivity analysis that the total number of infected host plants as a function of the birth rate of the WFT, biting rate of larva and death rate of infected WFT. This can help predict the transmission of the virus and can suggest potential strategies to control this plant disease.

5.5.1 Experiment and Data Introduction

The base data was collected using a physical study of the TSWV-WFT dynamic system with tomato plants. The experiment used a greenhouse with 80 tomato plants which were distributed in 8 rows and 10 columns [105]. In the experiment, 500 uninfected adult thrips were released in a uniform fashion into the greenhouse, in which 16 tomato plants were already infected (the rest 64 tomato plants were heathy). The initial status of tomato plants is presented in Table 5.9, while H is healthy plants and I is infected plants.

During the experiment, individual tomato plants were checked for visual indication of TSWV infection on a weekly basis for 8 weeks. When a plant was observed, it was recorded as

"uninfected", "questionable infection" or "confirmed infection". The experiment results are shown in Table 5.10. Detailed infection status of tomato plants is in Appendix B.

Table 5.9 Initial status of tomato plants

	1	2	3	4	5	6	7	8	9	10
1	H	H	H	H	H	I	H	H	H	I
2	I	H	H	H	H	I	H	H	H	H
3	H	H	H	I	I	H	H	H	H	H
4	I	H	H	H	H	H	H	H	H	I
5	I	H	H	I	H	H	H	H	H	H
6	H	H	H	H	H	H	H	H	I	I
7	H	H	H	I	H	H	I	H	H	H
8	H	I	I	H	H	H	H	H	H	H

Table 5.10 Experiment results of infected plants number

	Week 1	Week 2	Week 3	Week 4	Week 5	Week 6	Week 7	Week 8
Uninfected	64	64	64	64	52	32	0	0
Questionable	0	0	0	0	12	30	33	0
Infected	16	16	16	16	16	18	47	80

5.5.2 Comparison with Experimental Data

The simulation using the game-based approach represented the greenhouse as closely as possible. The simulation started with the same initial distribution of 64 healthy plants and 16 infected plants, as shown in Table 5.9. For thrips, 500 uninfected thrips are evenly distributed as initial condition. The game-based model was simulated for 8 weeks using the parameters shown in Table 5.11 and game parameters of $k_1 = k_2 = k_3 = 100$. Table 5.11 also provides references to the suggested values of these parameters. The simulated results are shown in Table 5.12.

Table 5.11 Parameter values for numerical simulations

Parameter	Description	Units	Ranges	Value	Source
v_v	Birth rate of the thrips	1/day	(4, 10)	5	[19, 153]
K_v	Capacity of thrips population	-	-	500	Estimated
γ_{SL1}	The average number of days required for eggs to develop to Larvae 1	day	(2, 4)	3	[19, 104, 133, 164]
μ_E	Daily death rate of thrip eggs	1/day	0.2	0.2	[104]
β_{L1}	Bite rate of the thrips	-		0.6	[153]
γ_{SL2}	The average number of days required for susceptible larvae 1 to develop to non-infective Larvae 2	day	(1, 2)	1.5	[19, 104, 133, 164]
μ_{SL1}	Daily death rate of susceptible Larvae 1	1/day	0.2	0.2	[104]
γ_{IL1}	The average number of days required for exposed larvae 1 to develop to infective Larvae 1	day	(1, 2)	1	Estimated
μ_{EL1}	Daily death rate of exposed Larvae 1	1/day	(0.1, 0.2)	0.15	Estimated
γ_{IL2}	The average number of days required for infective Larvae 1 to develop to infective Larvae 2	day	1	1	[104, 108]
μ_{IL1}	Daily death rate of infective Larvae 1	1/day	0.1	0.1	[104]
γ_{Spp}	The average number of days required for non-infective Larvae 2 to develop to non-infective Prepupae	day	(2, 4)	3	[19, 104, 133, 164]
μ_{sL2}	Daily death rate of non-infective Larvae 2	1/day	(0.1, 0.2)	0.2	[104]
γ_{Ipp}	The average number of days required for infective Larvae 2 to develop to infective Prepupae	day	2	2	[104, 108]
μ_{IL2}	Daily death rate of infective Larvae 2	1/day	0.1	0.1	[104]
γ_{Sp}	The average number of days required for non-infective Prepupae to develop to non-infective Pupae	day	(1, 2)	1.5	[19, 104, 133, 164]
μ_{Spp}	Daily death rate of non-infective Prepupae	1/day	(0.1, 0.2)	0.2	[104]
γ_{Ip}	The average number of days required for infective Prepupae to develop to infective Pupae	day	1	1	[104, 108]
μ_{Ipp}	Daily death rate of infective Prepupae	1/day	0.1	0.1	[104]
γ_{Sv}	The average number of days required for non-infective Pupae to develop to non-infective Adults	day	(1, 3)	2	[19, 104, 133, 164]
μ_{Sp}	Daily death rate of non-infective Pupae	1/day	(0.1, 0.2)	0.2	[104]
γ_{Iv}	The average number of days required for infective Pupae to develop to infective Adults	day	(1, 2)	1.5	[104, 108]
μ_{Ip}	Daily death rate of infective Pupae	1/day	0.1	0.1	[104]
μ_{Sv}	Daily death rate of non-infective Adults	1/day	(1/45, 1/30)	1/37.5	[19, 104]
μ_{Iv}	Daily death rate of infective Adults	1/day	(1/51, 1/42)	1/46.5	[19, 104]

Table 5.12 Simulated results of infected plants number

	Week 1	Week 2	Week 3	Week 4	Week 5	Week 6	Week 7	Week 8
Uninfected	64	64	64	57	23	5	0	0
Questionable	0	0	0	7	41	57	31	0
Infected	16	16	16	16	16	18	49	80

Figure 5.7 and Figure 5.8 presents the comparison of total number of uninfected plants and infected plants respectively, with the dotted line shows the simulated results while the solid line represents the actual observed experimental results. Also, the infection level distribution map for plants from the experiment and from the simulated model is presented in Figure 5.9 and Figure 5.10, respectively, for the time table of week 1 to week 8.

For the game-based model simulated results a plant is defined as uninfected if its infection level is less than 0.2, and the plant is classified as infected if its infection level is larger than 0.5, otherwise, it is defined as questionable infection. In Figures 5.9-5.10, a green cell indicates uninfected plant, yellow cell indicates questionable plant and a red cell represents a confirmed infected plant in that cell.

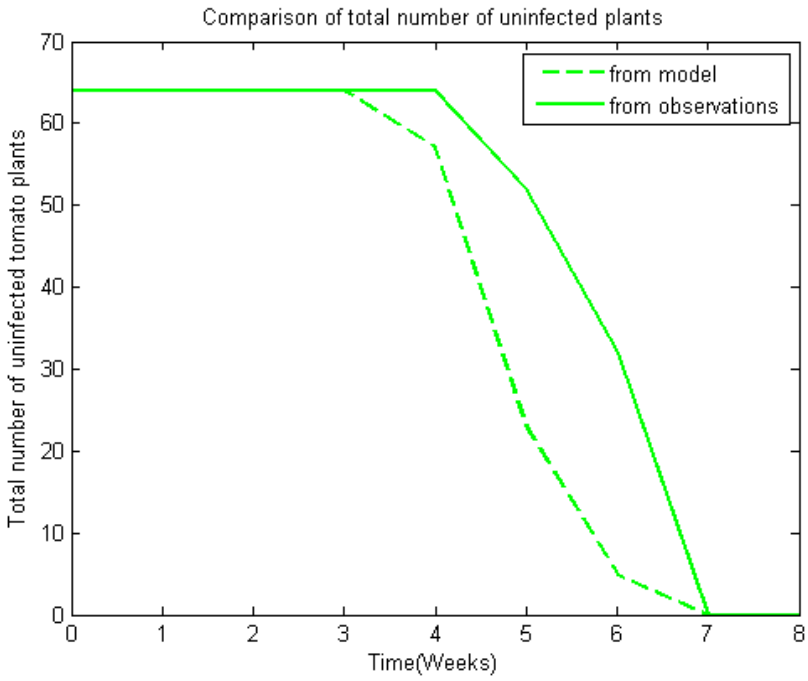

Figure 5.7 Comparison of total number of uninfected plants from simulation and experiment

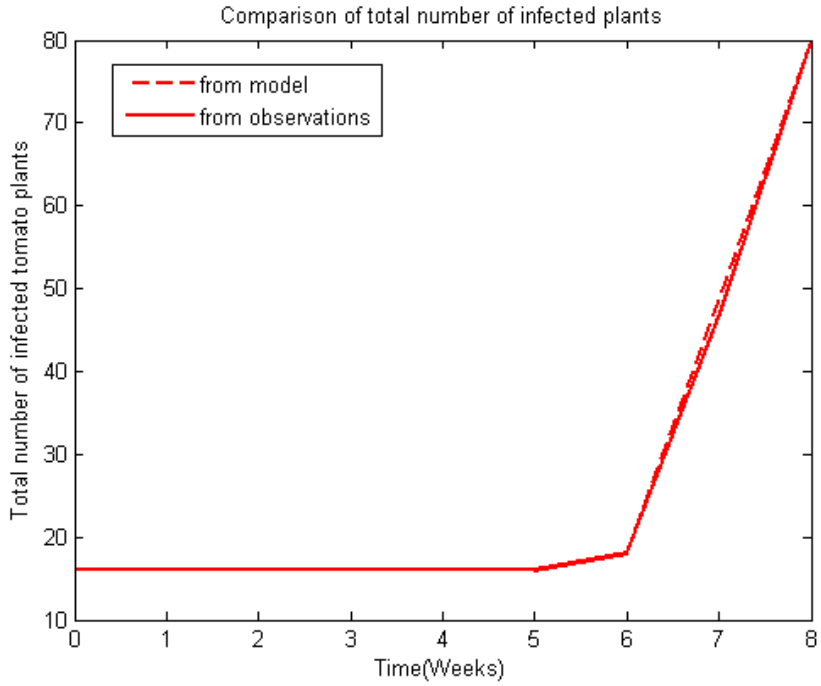

Figure 5.8 Comparison of total number of infected plants from simulation and experiment

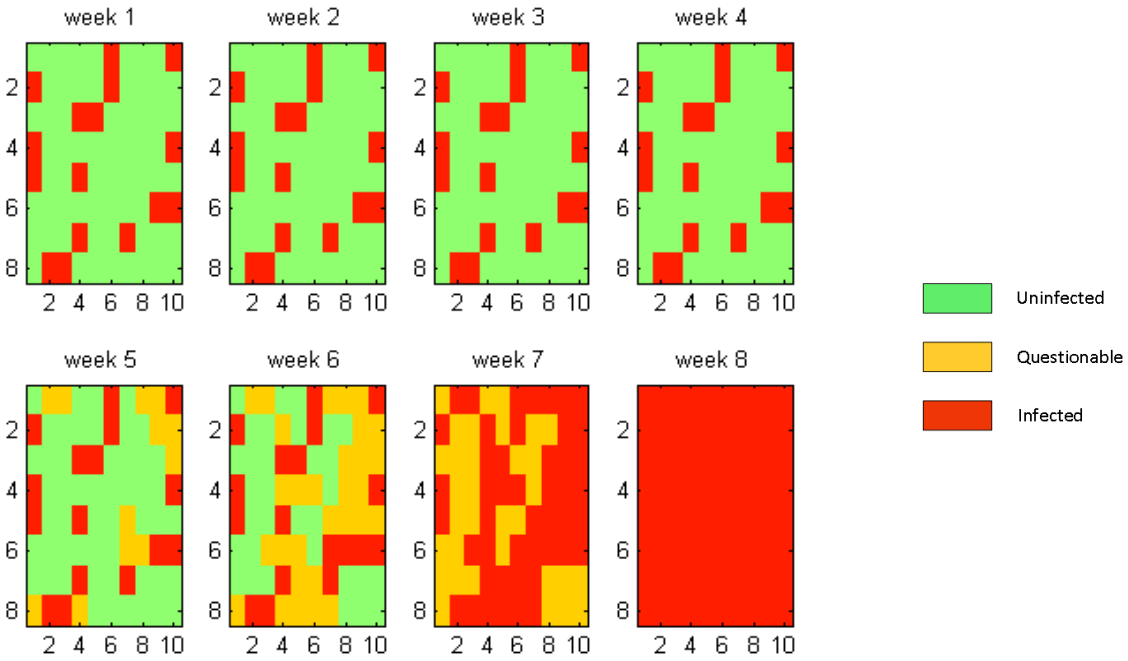

Figure 5.9 Plants Infection level distribution from experiment

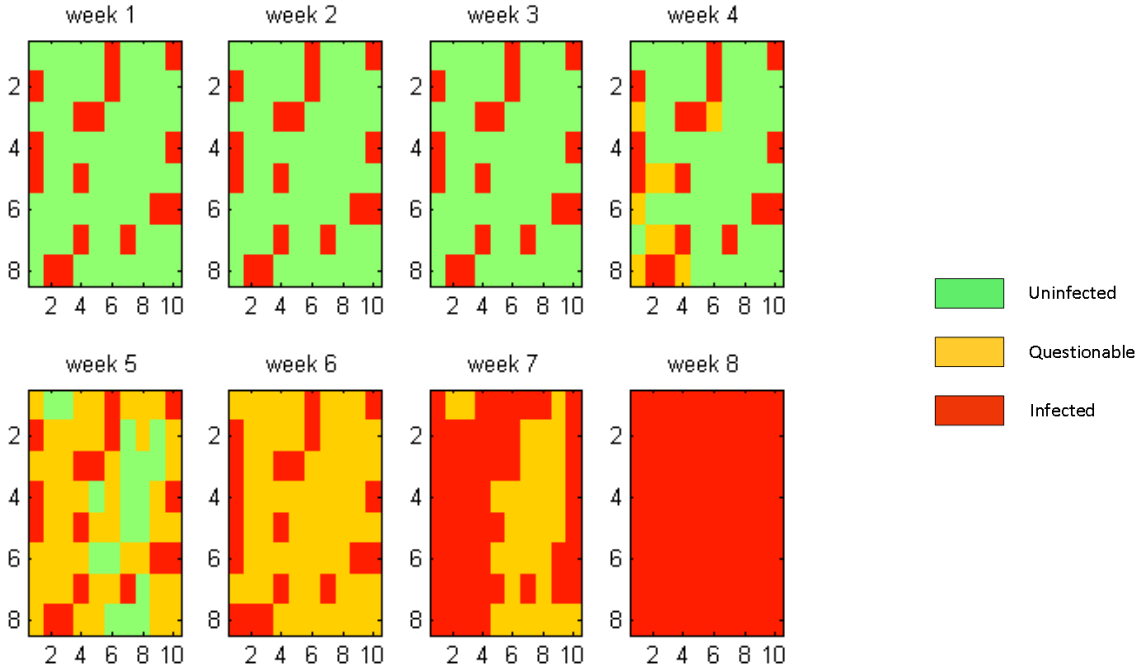

Figure 5.10 Plants Infection level distribution from simulated model

When comparing the simulation with the observation one can notice that the total number of uninfected plants decreased a little faster in the simulation in comparison with the observed data, while the total number of infected plants have a very good fit with the observations.

Looking at the comparison of pattern of infection, the first three weeks has a very similar pattern to the initial pattern in both the simulation and the actual data. From week 4, the simulated model has more healthy plants that become questionable while in the observed data this trend is not as evident. The same trend continues for week 5 and week 6 with the simulated model has more uninfected plants transferred to unhealthy plants. During week 7 all the plants became infected (either questionable or confirmed) and in week 8 all the plants were confirmed as infected. In all, we can conclude that game-based model has a good fit and can generate good predictions for the TSWV- WFT system.

5.5.3 Sensitivity Analysis

Sensitivity analysis is a technique used to study how different values that can impact the response output of a mathematical model [137, 138]. This section explores the impact of different parameters have on the total number of infected plants, in order to recognize the significant factors and develop suggestions on controlling the vector disease.

In a practical sense, the objective of studying this TSWV-WFT system is to control the total number of infected plants, and minimize the economic loss. In the sensitivity analysis presented in this section, the total number of infected host plants acted as the response output. The uncertainty inputs tested (one at a time) are: WFT birth rate, WFT larvae 1 biting rate, and the daily death rate of infected WFT adults. This analysis follows the same initial conditions as in the experimental study (as stated in the previous section). Simulation results are shown in Figures 5.11-5.13.

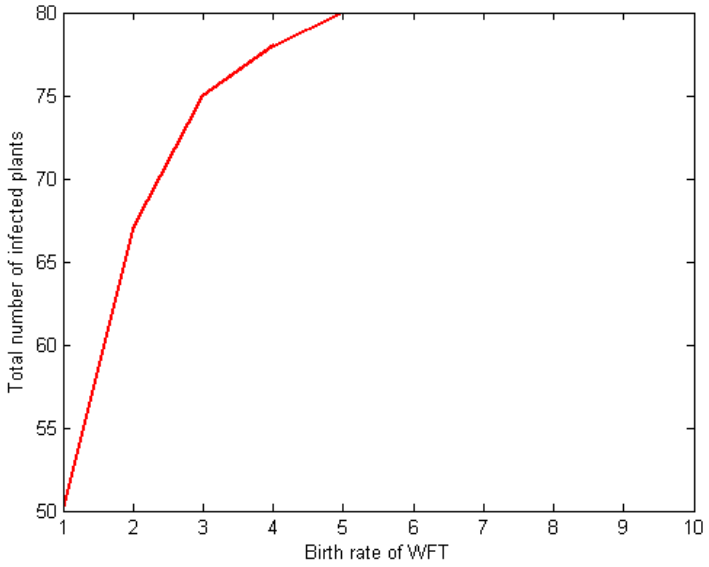

Figure 5.11 Sensitivity to WFT birth rate

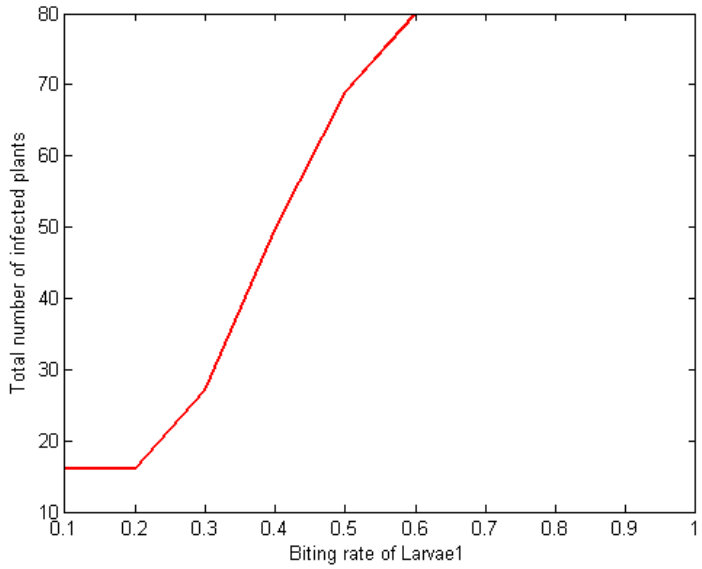

Figure 5.12 Sensitivity to WFT Larvae 1's biting rate

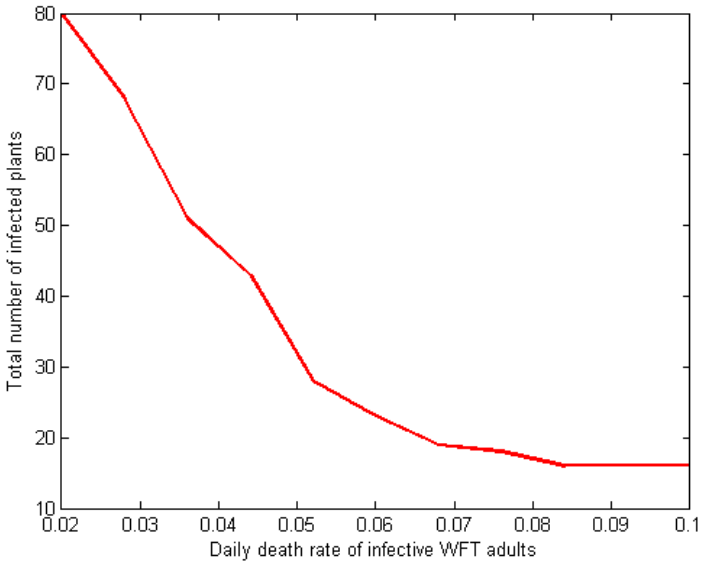

Figure 5.13 Sensitivity to daily death rate of infected WFT adults

Through the simulation, WFT birth rate and Larvae 1's biting rate positively correlated with the total number of infection plants thus concluding that a higher birth rate and a higher biting rate of WFT leads to higher economic loss. Daily death rate of infected WFT has a significant negative correlation with the total number of infected plants, which indicates that a higher death rate of infected WFT adults can reduce economic loss. Thus, our goal could be to decrease the WFT birth rate and WFT Larvae 1's biting rate, and also to increase the daily death rate of infected WFT adults. To change the biting rate of WFT some chemical control might be used to stimulate plant self-defense; or to improve resistance to the herbivore [153]. To impact the birth rate of WFT and daily death rate of infected WFT, temperature control in greenhouse may be a useful method as well as biological control such as introducing predator mites (*Amblyseius cucumeris* for example) to control WFT or using pesticide [105, 146, 167].

5.6 Conclusion and Discussion

This paper introduces and analyzes a new modeling approach for the Tomato Spotted Wilt Virus – western flower thrips – host plant disease system. This new perspective describes the spatial dynamics of adult thrips as a spatial game model which uses payoff functions that the players (the uninfected adult thrips and infected adult thrips) can receive based on the infection level of plants and the number of adult thrips population in the grid used for the spatial model. The values of the payoff from each cell helps generate the probability that the adult thrips will migrate to that cell. In each cell the basic dynamic model is used to analyze the development stages of thrips and transmission of infection representing the triangle interaction for virus-vector-host plant system. This interaction along with the spatial game dynamic carried out over many iterations represents the whole spatial dynamics for TSWV-WFT.

The game-based model is simulated and validated using actual experimental data in which the infection status of host plants was recorded every week for 8 weeks. The total number of uninfected plants, questionable plants, and confirmed infected plants has been compared between the simulated results and experiment results. The distribution of infected level of plants has been also compared for each week. Comparison results shows that this new approach has a good fit with the experimental data and indicates that the model can generate good predications of the TSWV-WFT system.

Moreover, a sensitivity analysis is performed studying the impact of different parameters on the infection of host plants. This allows to generate suggestions for controlling the vector-borne disease and minimize the total number of infected plants. Results show that WFT's birth rate, WFT larvae 1's biting rate and the daily death rate of infected WFT adults have a significant impact on the plants infection status. Strategies such as biological control, chemical control or

temperature control that can decrease the birth rate, biting rate or increase the daily death rate of infected WFT adults could be recommended.

The game-based approach can have wide applications in other research areas such as competing commercial firms, prey-predator systems, logistic distribution systems and similar dynamic systems. The payoff function and move probability function can be adjusted based on different habits, characteristics and mobility preferences of the different players or species. Thus, this modeling approach can be useful in many other areas of science.

Future expansion of this research can include more sophisticated models, such as agent based models [126, 127, 140] and use the optimal control theory [129, 141], which will provide decision makers with better policies for controlling the vector-borne disease. Also, further validation of models with TSWV-WFT experiment could be performed with different spatial scales and different initial distributions.

Chapter 6 - Conclusions, Contributions, and Future Works

6.1 Conclusions

In this research, spatial effects have been investigated and discussed for two competing dynamic ecological systems: a prey-predator system (two spotted spider mites and its predator), and a vector-borne disease system (tomato spotted wilt virus (TSWV) vs western flower thrips (WFT)). The author developed a novel methodology to these systems as well as compared the new model with traditional dynamic models. The resulting analytical and numerical simulation help us better understand the system behaviors and recommend the corresponding control strategies.

Main conclusions drawn from this dissertation are:

1. Different spatial assumptions impact the prey-predator distribution. The integro-diffusion model exhibits a significantly different pattern when compared to the other three models: self-diffusion, cross-diffusion and chemotaxis effect model.
2. For two spotted spider mite system, cross-diffusion model has the best fit with experimental data when compared with other three models: self-diffusion, chemotaxis effect model and integro-diffusion model.
3. For prey-predator system, the novel game-based model performed similarly to the cross-diffusion model regarding population changing. This similarity between models suggests that the game-based model is a valid approach for modeling the prey-predator dynamic system.
4. For two spotted spider mite system, the game-based model fits the observations more closely than the cross-diffusion model regarding the total number of prey and predator, indicating the game-based model is a good fit and can generate good predictions of the prey-predator systems.

5. For TSWV-WFT system, the game-based model has a good fit with the experimental data, which satisfied the fidelity requirement of the proposed new methodology.
6. In order to efficiently control the spread of TSWV, strategies such as biological control, chemical control or temperature control that can decrease the birth rate, biting rate, or increase the daily death rate of infected WFT adults is recommended.

6.2 Contributions

Major contributions of this dissertation to the area of biological systems modeling, decision making on pest control, and plant disease epidemiology are listed as follows:

1. For the first time, this research compared four dynamic models for two spotted spider mites vs. predators system from two perspective: numerical simulation and validation with observations. The four models including two well-known models in literature and two new models developed by the author.
2. For the first time, this research applied the spatial evolutionary game theory to the prey-predator system model. By defining a payoff function and a probability function, a spatial dynamic scheme is demarcated. This novel game-based model was successfully compared with the more traditional biological dynamic model.
3. For the first time, this research developed new mathematical models to study TSWV-WFT system which emphasized the life cycle of vector and transmission characteristics of the specific system.
4. For the first time, this research introduced spatial effect to TSWV-WFT system. Spatial game as an effective tool is applied to reveal the spatial movement of adult

thrips. This novel model was successfully validated with real-world experimental data. Sensitivity analysis is performed to suggest efficient controlling strategies.

5. The spatial game methodology developed in this research can be applied to other research areas with spatial dynamics.

6.3 Future Works

Major future works in the area of analysis of specific dynamic systems are listed as follows:

1. Further analytical study into the TSWV-WFT dynamic system, such as stability analysis and bifurcation analysis, should be conducted to better understand the behavior of the dynamic system.
2. In order to increase understanding of the variation of individuals' responses, an agent-based model could be developed as a tool to study the complex system with interactions among different species.
3. To seek more cost-effective control strategies, optimal control theory could be employed for these ecology systems. For both systems in this research, actual control costs in various scenarios should be discussed and compared.
4. Further validation of models for two spotted spider mites and TSWV-WFT using experimental systems, including discussion of different spatial scales and different predator and prey spatial distributions.

References

[1] Berryman AA, Kindlmann P. Population systems: a general introduction. Springer Science & Business Media; 2008.

[2] Gilpin ME, Ayala FJ. Global models of growth and competition. Proceedings of the National Academy of Sciences. 1973;70(12):3590-3.

[3] SALISBURY A. No title. Mathematical models in population dynamics. 2011.

[4] Cunniffe NJ, Koskella B, Metcalf CJE, Parnell S, Gottwald TR, Gilligan CA. Thirteen challenges in modelling plant diseases. Epidemics. 2015;10:6-10.

[5] Whitfield AE, Ullman DE, German TL. Tospovirus-thrips interactions. Annu.Rev.Phytopathol. 2005;43:459-89.

[6] PETERS D. An anatomical perspective of tospovirus transmission. Virus-insect-plant Interactions. 2001;5:51.

[7] Friedman JW. Game theory with applications to economics. Oxford University Press New York; 1990.

[8] Cable DM, Shane S. A prisoner's dilemma approach to entrepreneur-venture capitalist relationships. Academy of Management Review. 1997;22(1):142-76.

[9] Cachon GP, Netessine S. Game theory in supply chain analysis. In: Models, Methods, and Applications for Innovative Decision Making. INFORMS; 2006. p. 200-33.

[10] Hennet J, Arda Y. Supply chain coordination: A game-theory approach. Eng Appl Artif Intell. 2008;21(3):399-405.

[11] Esmaeili M, Aryanezhad M, Zeephongsekul P. A game theory approach in seller–buyer supply chain. Eur J Oper Res. 2009;195(2):442-8.

[12] Han Z. Game theory in wireless and communication networks: theory, models, and applications. Cambridge University Press; 2012.

[13] Manshaei MH, Zhu Q, Alpcan T, Bacşar T, Hubaux J. Game theory meets network security and privacy. ACM Computing Surveys (CSUR). 2013;45(3):25.

[14] Kim S. Game theory applications in network design. IGI Global; 2014.

[15] Funk S, Salath M, Jansen VA. Modelling the influence of human behaviour on the spread of infectious diseases: a review. Journal of the Royal Society Interface. 2010:rsif20100142.

[16] Chapman GB, Li M, Vietri J, Ibuka Y, Thomas D, Yoon H, et al. Using game theory to examine incentives in influenza vaccination behavior. Psychological science. 2012;23(9):1008-15.

[17] Shim E, Kochin B, Galvani A. Insights from epidemiological game theory into gender-specific vaccination against rubella. Mathematical biosciences and engineering: MBE. 2009;6(4):839-54.

[18] Zhao S, Wu J, Ben-Arieh D. Modeling infection spread and behavioral change using spatial games. Health Systems. 2015;4(1):41-53.

[19] Lewontin RC. Evolution and the theory of games. J Theor Biol. 1961;1(3):382-403.

[20] Hamilton WD, May RM. Dispersal in stable habitats. Nature. 1977;269(5629):578-81.

[21] Mirmirani M, Oster G. Competition, kin selection, and evolutionary stable strategies. Theor Popul Biol. 1978;13(3):304-39.

[22] Nowak MA, May RM. Evolutionary games and spatial chaos. Nature. 1992;359(6398):826-9.

[23] Roca CP, Cuesta JA, Snchez A. Evolutionary game theory: Temporal and spatial effects beyond replicator dynamics. Physics of life reviews. 2009;6(4):208-49.

[24] Newth D, Cornforth D. Asynchronous spatial evolutionary games. BioSystems. 2009;95(2):120-9.

[25] Lotka AJ. Elements of physical biology. . 1925.

[26] Volterra V. Variations and fluctuations of the number of individuals in animal species living together. J.Cons.Int.Explor.Mer. 1928;3(1):3-51.

[27] Fisher RA. The wave of advance of advantageous genes. Annals of eugenics. 1937;7(4):355-69.

[28] Skellam JG. Random dispersal in theoretical populations. Biometrika. 1951;38(1/2):196-218.

[29] Britton NF. Reaction-diffusion equations and their applications to biology. Academic Press; 1986.

[30] Murray JD. Mathematical Biology. II Spatial Models and Biomedical Applications {Interdisciplinary Applied Mathematics V. 18}. Springer-Verlag New York Incorporated; 2001.

[31] Cantrell RS, Cosner C. Spatial ecology via reaction-diffusion equations. John Wiley & Sons; 2004.

[32] Smoller J. Shock waves and reaction—diffusion equations. Springer Science & Business Media; 2012.

[33] Okubo A, Levin SA. Diffusion and ecological problems: modern perspectives. Springer Science & Business Media; 2013.

[34] Sherratt JA. Periodic travelling waves in cyclic predator–prey systems. Ecol Lett. 2001;4(1):30-7.

[35] Sun G, Zhang G, Jin Z, Li L. Predator cannibalism can give rise to regular spatial pattern in a predator–prey system. Nonlinear Dyn. 2009;58(1):75-84.

[36] Melese D, Gakkhar S. Stability analysis of a prey–predator model with Beddington–DeAngelis functional response. J.Int.Acad.Phys.Sci. 2011;15:1-6.

[37] Kerner EH. A statistical mechanics of interacting biological species. Bull Math Biophys. 1957;19(2):121-46.

[38] Shigesada N, Kawasaki K, Teramoto E. Spatial segregation of interacting species. J Theor Biol. 1979;79(1):83-99.

[39] Dubey B, Das B, Hussain J. A predator–prey interaction model with self and cross-diffusion. Ecol Model. 2001;141(1):67-76.

[40] Kuto K. Stability of steady-state solutions to a prey–predator system with cross-diffusion. Journal of Differential Equations. 2004;197(2):293-314.

[41] Pang PY, Wang M. Strategy and stationary pattern in a three-species predator–prey model. Journal of Differential Equations. 2004;200(2):245-73.

[42] Sun G, Zhang G, Jin Z, Li L. Predator cannibalism can give rise to regular spatial pattern in a predator–prey system. Nonlinear Dyn. 2009;58(1):75-84.

[43] Xue L. Pattern formation in a predator–prey model with spatial effect. Physica A: Statistical mechanics and its applications. 2012;391(23):5987-96.

[44] Guin LN, Haque M, Mandal PK. The spatial patterns through diffusion-driven instability in a predator–prey model. Appl Math Model. 2012;36(5):1825-41.

[45] Li L, Zhen J, Gui-Quan S. Spatial pattern of an epidemic model with cross-diffusion. Chinese Physics Letters. 2008;25(9):3500.

[46] Upadhyay RK, Thakur NK. Spatiotemporal pattern induced by self and cross-diffusion in a spatial Holling-Tanner model. Computational Ecology and Software. 2012;2(1):1-25.

[47] Rao F. Spatiotemporal pattern in a self-and cross-diffusive predation model with the Allee effect. Discrete Dynamics in Nature and society. 2013;2013.

[48] Kareiva P, Odell G. Swarms of predators exhibit" preytaxis" if individual predators use area-restricted search. Am Nat. 1987;130(2):233-70.

[49] Chakraborty A, Singh M, Lucy D, Ridland P. Predator–prey model with prey-taxis and diffusion. Math Comput Model. 2007;46(3):482-98.

[50] Turchin P. Quantitative analysis of movement. Sinauer. Inc., Sunderland, Massachusetts, USA. 1998.

[51] Grnbaum D. Using spatially explicit models to characterize foraging performance in heterogeneous landscapes. Am Nat. 1998;151(2):97-113.

[52] Czrn T. Spatiotemporal models of population and community dynamics. Springer Science & Business Media; 1998.

[53] Berezovskaya FS, Karev GP. Bifurcations of running waves in population models with taxis. Uspekhi Fizicheskikh Nauk. 1999;9:1011-24.

[54] Berezovskaya FS, Davydova NV, Isaev AS, Karev GP, Khlebopros RG. Migration waves and the spatial dynamics of phytophagous insects. Siber.Ecol.J. 1999;4:347-57.

[55] Govorukhin VN, Morgulis AB, Tyutyunov YV. Slow taxis in a predator-prey model. DOKLADY MATHEMATICS C/C OF DOKLADY-AKADEMIIA NAUK; MAIK NAUKA; 2000.

[56] Arditi R, Tyutyunov Y, Morgulis A, Govorukhin V, Senina I. Directed movement of predators and the emergence of density-dependence in predator–prey models. Theor Popul Biol. 2001;59(3):207-21.

[57] Sapoukhina N, Tyutyunov Y, Arditi R. The role of prey taxis in biological control: a spatial theoretical model. Am Nat. 2003;162(1):61-76.

[58] Harrison GW. Comparing predator-prey models to Luckinbill's experiment with didinium and paramecium. Ecology. 1995;76(2):357-74.

[59] Chakraborty A, Singh M, Lucy D, Ridland P. Predator–prey model with prey-taxis and diffusion. Math Comput Model. 2007;46(3):482-98.

[60] Chakraborty A, Singh M, Ridland P. Effect of prey-taxis on biological control of the two-spotted spider mite—A numerical approach. Math Comput Model. 2009;50(3):598-610.

[61] Abrams PA, Ginzburg LR. The nature of predation: prey dependent, ratio dependent or neither? Trends in Ecology & Evolution. 2000;15(8):337-41.

[62] Skalski GT, Gilliam JF. Functional responses with predator interference: viable alternatives to the Holling type II model. Ecology. 2001;82(11):3083-92.

[63] Malchow H, Hilker FM, Petrovskii SV. Noise and productivity dependence of spatiotemporal pattern formation in a prey-predator system. parameters. 2004;14:15.

[64] Chen Y. Multiple periodic solutions of delayed predator–prey systems with type IV functional responses. Nonlinear Analysis: Real World Applications. 2004;5(1):45-53.

[65] Ko W, Ryu K. Coexistence states of a predator–prey system with non-monotonic functional response. Nonlinear Analysis: Real World Applications. 2007;8(3):769-86.

[66] Gakkhar S, Singh B. The dynamics of a food web consisting of two preys and a harvesting predator. Chaos, Solitons & Fractals. 2007;34(4):1346-56.

[67] Estep D, Neckels D. Fast methods for determining the evolution of uncertain parameters in reaction-diffusion equations. Comput Methods Appl Mech Eng. 2007;196(37):3967-79.

[68] Zhang S, Tan D, Chen L. Chaos in periodically forced Holling type IV predator–prey system with impulsive perturbations. Chaos, Solitons & Fractals. 2006;27(4):980-90.

[69] Zhang W, Zhu D, Bi P. Multiple positive periodic solutions of a delayed discrete predator–prey system with type IV functional responses. Applied Mathematics Letters. 2007;20(10):1031-8.

[70] Holling CS. The components of predation as revealed by a study of small-mammal predation of the European pine sawfly. The Canadian Entomologist. 1959;91(05):293-320.

[71] Holling CS. Some characteristics of simple types of predation and parasitism. The Canadian Entomologist. 1959;91(07):385-98.

[72] Andrews JF. A mathematical model for the continuous culture of microorganisms utilizing inhibitory substrates. Biotechnol Bioeng. 1968;10(6):707-23.

[73] Fan M, Kuang Y. Dynamics of a nonautonomous predator–prey system with the Beddington–DeAngelis functional response. Journal of Mathematical Analysis and applications. 2004;295(1):15-39.

[74] Zimmermann B, Sand H, Wabakken P, Liberg O, Andreassen HP. Predator-dependent functional response in wolves: from food limitation to surplus killing. J Anim Ecol. 2015;84(1):102-12.

[75] Arditi R, Ginzburg LR. Coupling in predator-prey dynamics: ratio-dependence. J Theor Biol. 1989;139(3):311-26.

[76] Arditi R, Akakaya HR. Underestimation of mutual interference of predators. Oecologia. 1990;83(3):358-61.

[77] Arditi R, Callois J, Tyutyunov Y, Jost C. Does mutual interference always stabilize predator–prey dynamics? A comparison of models. Comptes Rendus Biologies. 2004;327(11):1037-57.

[78] Beddington JR. Mutual interference between parasites or predators and its effect on searching efficiency. The Journal of Animal Ecology. 1975:331-40.

[79] Crowley PH, Martin EK. Functional responses and interference within and between year classes of a dragonfly population. J N Am Benthol Soc. 1989;8(3):211-21.

[80] Cosner C, DeAngelis DL, Ault JS, Olson DB. Effects of spatial grouping on the functional response of predators. Theor Popul Biol. 1999;56(1):65-75.

[81] DeAngelis DL, Goldstein RA, O'neill RV. A model for tropic interaction. Ecology. 1975;56(4):881-92.

[82] Funston PJ, Mills M, Biggs HC. Factors affecting the hunting success of male and female lions in the Kruger National Park. J Zool. 2001;253(4):419-31.

[83] Hassell MP, Varley GC. New inductive population model for insect parasites and its bearing on biological control. Nature. 1969;223(5211):1133.

[84] Holekamp KE, Smale L, Berg R, Cooper SM. Hunting rates and hunting success in the spotted hyena (Crocuta crocuta). J Zool. 1997;242(1):1-15.

[85] Lima SL. Predators and the breeding bird: behavioral and reproductive flexibility under the risk of predation. Biological reviews. 2009;84(3):485-513.

[86] Packer C, Ruttan L. The evolution of cooperative hunting. Am Nat. 1988;132(2):159-98.

[87] Creel S, Creel NM. Communal hunting and pack size in African wild dogs, Lycaon pictus. Anim Behav. 1995;50(5):1325-39.

[88] Haque M. A detailed study of the Beddington–DeAngelis predator–prey model. Math Biosci. 2011;234(1):1-16.

[89] Li H, Takeuchi Y. Dynamics of the density dependent predator–prey system with Beddington–DeAngelis functional response. Journal of Mathematical Analysis and Applications. 2011;374(2):644-54.

[90] Hwang T. Global analysis of the predator–prey system with Beddington–DeAngelis functional response. Journal of Mathematical Analysis and Applications. 2003;281(1):395-401.

[91] Cantrell RS, Cosner C. On the dynamics of predator–prey models with the Beddington–DeAngelis functional response. Journal of Mathematical Analysis and Applications. 2001;257(1):206-22.

[92] Liu Z, Yuan R. Stability and bifurcation in a delayed predator–prey system with Beddington–DeAngelis functional response. Journal of mathematical analysis and applications. 2004;296(2):521-37.

[93] Hwang T. Uniqueness of limit cycles of the predator–prey system with Beddington–DeAngelis functional response. Journal of Mathematical Analysis and Applications. 2004;290(1):113-22.

[94] Jones RA, Salam MU, Maling TJ, Diggle AJ, Thackray DJ. Principles of predicting plant virus disease epidemics. Annu Rev Phytopathol. 2010;48:179-203.

[95] Olatinwo RO, Paz JO, Brown SL, Kemerait Jr RC, Culbreath AK, Beasley Jr JP, et al. A predictive model for spotted wilt epidemics in peanut based on local weather conditions and the tomato spotted wilt virus risk index. Phytopathology. 2008;98(10):1066-74.

[96] Yudin LS, Tabashnik BE, Cho JJ, Mitchell WC. Disease-prediction and economic models for managing tomato spotted wilt virus disease in lettuce. Plant Dis. 1990;74(3):211-6.

[97] De Wolf ED, Isard SA. Disease cycle approach to plant disease prediction. Annu.Rev.Phytopathol. 2007;45:203-20.

[98] Magarey RD, Fowler GA, Borchert DM, Sutton TB, Colunga-Garcia M, Simpson JA. NAPPFAST: an internet system for the weather-based mapping of plant pathogens. Plant Dis. 2007;91(4):336-45.

[99] Madden LV, Raccah B, Pirone TP. Modeling plant disease increase as a function of vector numbers: nonpersistent viruses. Researches on population ecology. 1990;32(1):47-65.

[100] Chappell TM, Beaudoin AL, Kennedy GG. Interacting virus abundance and transmission intensity underlie tomato spotted wilt virus incidence: an example weather-based model for cultivated tobacco. PloS one. 2013;8(8):e73321.

[101] Madden LV, Knoke JK, Louie R. The statistical relationship between aphid trap catches and maize dwarf mosaic virus inoculation pressure. The statistical relationship between aphid trap catches and maize dwarf mosaic virus inoculation pressure. 1983:159-68.

[102] Morsello SC, Kennedy GG. Spring temperature and precipitation affect tobacco thrips, Frankliniella fusca, population growth and tomato spotted wilt virus spread within patches of the winter annual weed Stellaria media. Entomol Exp Appl. 2009;130(2):138-48.

[103] Morsello SC, Beaudoin AL, Groves RL, Nault BA, Kennedy GG. The influence of temperature and precipitation on spring dispersal of Frankliniella fusca changes as the season progresses. Entomol Exp Appl. 2010;134(3):260-71.

[104] Ogada PA, Moualeu DP, Poehling H. Predictive Models for Tomato Spotted Wilt Virus Spread Dynamics, Considering Frankliniella occidentalis Specific Life Processes as Influenced by the Virus. PloS one. 2016;11(5):e0154533.

[105] Gillespie DL. No title. The effectiveness of biological control of Frankliniella occidentalis in prevention of the spread of Tomato spotted wilt virus. 2009.

[106] Nachappa P, Margolies DC, Nechols JR, Whitfield AE, Rotenberg D. Tomato spotted wilt virus benefits a non-vector arthropod, Tetranychus urticae, by modulating different plant responses in tomato. PLoS One. 2013;8(9):e75909.

[107] Maris PC, Joosten NN, Goldbach RW, Peters D. Tomato spotted wilt virus infection improves host suitability for its vector Frankliniella occidentalis. Phytopathology. 2004;94(7):706-11.

[108] Ogada PA, Maiss E, Poehling H. Influence of tomato spotted wilt virus on performance and behaviour of western flower thrips (Frankliniella occidentalis). J Appl Entomol. 2013;137(7):488-98.

[109] Sakimura K. Frankliniella fusca, an additional vector for Tomato spotted wilt virus, with notes on Thrips tabaci, another vector. Phytopathology. 1963;53(4).

[110] Wijkamp I, Goldbach R, Peters D. Propagation of tomato spotted wilt virus in Frankliniella occidentalis does neither result in pathological effects nor in transovarial passage of the virus. Entomol Exp Appl. 1996;81(3):285-92.

[111] Fasulo TR, Denmark HA. Two-spotted spider mite. Featured Creatures. University of Florida Institute of Food and Agricultural Sciences. 2009.

[112] Nachappa P, Margolies DC, Nechols JR, Campbell JF. Variation in predator foraging behaviour changes predator–prey spatio-temporal dynamics. Funct Ecol. 2011;25(6):1309-17.

[113] Chakraborty A, Singh M, Lucy D, Ridland P. A numerical study of the formation of spatial patterns in twospotted spider mites. Math Comput Model. 2009;49(9):1905-19.

[114] Sabelis MW, Van der Weel, J J. Anemotactic responses of the predatory mite, Phytoseiulus persimilis Athias-Henriot, and their role in prey finding. Exp Appl Acarol. 1993;17(7):521-9.

[115] Osborne LS, Ehler LE, Nechols JR. Biological control of the twospotted spider mite in greenhouses. Bulletin/Agricultural Experiment Stations, University of Florida (USA). 1985.

[116] Holling CS. The functional response of predators to prey density and its role in mimicry and population regulation. Mem Entomol Soc Can. 1965;97(S45):5-60.

[117] Fan M, Kuang Y. Dynamics of a nonautonomous predator–prey system with the Beddington–DeAngelis functional response. Journal of Mathematical Analysis and applications. 2004;295(1):15-39.

[118] Haque M. A detailed study of the Beddington–DeAngelis predator–prey model. Math Biosci. 2011;234(1):1-16.

[119] Chattopadhyay J, Chatterjee S. Cross diffusional effect in a Lotka-Volterra competitive system. NONLINEAR PHENOMENA IN COMPLEX SYSTEMS-MINSK-. 2001;4(4):364-9.

[120] Tian C, Lin Z, Pedersen M. Instability induced by cross-diffusion in reaction–diffusion systems. Nonlinear Analysis: Real World Applications. 2010;11(2):1036-45.

[121] Wang X, Cai Y. Cross-diffusion-driven instability in a reaction-diffusion Harrison predator-prey model. Abstract and Applied Analysis; Hindawi Publishing Corporation; 2013.

[122] Van den Boom C, Van Beek TA, Dicke M. Attraction of Phytoseiulus persimilis (Acari: Phytoseiidae) towards volatiles from various Tetranychus urticae-infested plant species. Bull Entomol Res. 2002;92(06):539-46.

[123] Maeda T, Takabayashi J. Production of herbivore-induced plant volatiles and their attractiveness to Phytoseius persimilis (Acari: Phytoseiidae) with changes of Tetranychus urticae (Acari: Tetranychidae) density on a plant. Appl Entomol Zool. 2001;36(1):47-52.

[124] De Boer JG, Dicke M. Information use by the predatory mite Phytoseiulus persimilis (Acari: Phytoseiidae), a specialised natural enemy of herbivorous spider mites. Appl Entomol Zool. 2005;40(1):1-12.

[125] van Wijk M, De Bruijn PJ, Sabelis MW. Predatory mite attraction to herbivore-induced plant odors is not a consequence of attraction to individual herbivore-induced plant volatiles. J Chem Ecol. 2008;34(6):791.

[126] Shi Z, Chapes SK, Ben-Arieh D, Wu C. An Agent-Based Model of a Hepatic Inflammatory Response to Salmonella: A Computational Study under a Large Set of Experimental Data. PloS one. 2016;11(8):e0161131.

[127] Shi ZZ, Wu C, Ben-Arieh D. Agent-based model: a surging tool to simulate infectious diseases in the immune system. Open Journal of Modelling and Simulation. 2014;2014.

[128] Shi Z, Ben-Arieh D, Wu CJ. A preliminary study of sepsis progression in an animal model using agent-based modeling. International Journal of Modelling and Simulation. 2016;36(1-2):44-54.

[129] Zhao S, Kuang Y, Wu C, Ben-Arieh D, Ramalho-Ortigao M, Bi K. Zoonotic visceral leishmaniasis transmission: modeling, backward bifurcation, and optimal control. J Math Biol. 2016;73(6-7):1525-60.

[130] Ribas LM, Zaher VL, Shimozako HJ, Massad E. Estimating the optimal control of zoonotic visceral leishmaniasis by the use of a mathematical model. The Scientific World Journal. 2013;2013.

[131] Zhao S, Wu J, Ben-Arieh D. Modeling infection spread and behavioral change using spatial games. Health Systems. 2015;4(1):41-53.

[132] Lozano S, Arenas A, Snchez A. Mesoscopic structure conditions the emergence of cooperation on social networks. PLoS one. 2008;3(4):e1892.

[133] Santos FC, Pacheco JM, Lenaerts T. Evolutionary dynamics of social dilemmas in structured heterogeneous populations. Proc Natl Acad Sci U S A. 2006;103(9):3490-4.

[134] Britton NF. Spatial structures and periodic travelling waves in an integro-differential reaction-diffusion population model. SIAM J Appl Math. 1990;50(6):1663-88.

[135] Kuang Y, Ben-Arieh D, Zhao S, Wu C, Margolies D, Nechols J. Mathematical Model for Two-Spotted Spider Mites System: Verification and Validation. . 2017.

[136] All about Two-Spotted Spider Mites [Internet].; 2005 [].

[137] Saltelli A. Sensitivity analysis for importance assessment. Risk Analysis. 2002;22(3):579-90.

[138] Saltelli A, Ratto M, Andres T, Campolongo F, Cariboni J, Gatelli D, et al. Global sensitivity analysis: The primer John Wiley and Sons. Chichester, UK, ISBN 978&0&470&05997&S. 2008.

[139] Axelrod RM. The complexity of cooperation: Agent-based models of competition and collaboration. Princeton University Press; 1997.

[140] Wu J, Ben-Arieh D, Shi Z. An Autonomous Multi—Agent Simulation Model for Acute Inflammatory Response. Investigations Into Living Systems, Artificial Life, and Real-world Solutions. 2013:218.

[141] Fleming WH, Rishel RW. Deterministic and stochastic optimal control. Springer Science & Business Media; 2012.

[142] Brittlebank CC. Tomato diseases. Journal of the Department of Agriculture in Victoria. 1919;17:1348-52.

[143] Samuel G, Bald JG, Pittman HA. Investigations on" Spotted Wilt" of Tomatoes. Investigations on" Spotted Wilt" of Tomatoes. 1930(44).

[144] Sherwood JL, German TL, Moyer JW, Ullman DE. Tomato spotted wilt virus. Tomato spotted wilt virus. 2009.

[145] Plant viruses spread by thrips - Integrated virus disease management [Internet]. [].

[146] Zitter TA, Daughtrey ML, Sanderson JP. Tomato spotted wilt virus. . 1989.

[147] Nagata T, Peters D. An Anatomical Perspective of Tospovirus Transmission-Chapter 3.

[148] Ullman DE, Meideros R, Campbell LR, Whitfield AE, Sherwood JL, German TL. Thrips as vectors of tospoviruses. Adv Bot Res. 2002;36:113-40.

[149] Sether DM, DeAngelis JD. No title. Tomato spotted wilt virus host list and bibliography. 1992.

[150] Hobbs HA, Johnson RR, Story RN, Black LL. Weed hosts and thrips transmission of tomato spotted wilt virus in Louisiana. Tospoviruses and Thrips of Floral and Vegetable Crops 431. 1995:291-7.

[151] Johnson RR, Black LL, Hobbs HA, STORY RN, VALVERDE RA, Bond WP. Association of Frankliniella fusca and three winter weeds with tomato spotted wilt virus in Louisiana. Plant Dis. 1995;79(6):572-6.

[152] Chatzivassiliou EK, Boubourakas I, Drossos E, Eleftherohorinos I, Jenser G, Peters D, et al. Weeds in greenhouses and tobacco fields are differentially infected by Tomato spotted wilt virus and infested by its vector species. Plant Dis. 2001;85(1):40-6.

[153] Wu J, Zhao S, Kuang Y, Ben-Arieh D, Nechols J, Margolies D. New mathematical models for vector-borne disease: transmission of tomato spotted wilt virus. Bridging Research and Good Practices towards Patients Welfare: Proceedings of the 4th International Conference on Healthcare Ergonomics and Patient Safety (HEPS), Taipei, Taiwan, 23-26 June 2014; CRC Press; 2014.

[154] Ullman DE, Cho JJ, Mau RF, Westcot DM, Custer DM. A midgut barrier to tomato spotted wilt virus acquisition by adult western flower thrips. PHYTOPATHOLOGY-NEW YORK AND BALTIMORE THEN ST PAUL-. 1992;82:1333.

[155] Van De Wetering F, Goldbach R, Peters D. Tomato spotted wilt tospovirus ingestion by first instar larvae of Frankliniella occidentalis is a prerequisite for transmission. PHYTOPATHOLOGY-NEW YORK AND BALTIMORE THEN ST PAUL-. 1996;86:900-5.

[156] Nagata T, Inoue-Nagata AK, Smid HM, Goldbach R, Peters D. Tissue tropism related to vector competence of Frankliniella occidentalis for tomato spotted wilt tospovirus. J Gen Virol. 1999;80(2):507-15.

[157] de Assis Filho, F M, Deom CM, Sherwood JL. Acquisition of Tomato spotted wilt virus by adults of two thrips species. Phytopathology. 2004;94(4):333-6.

[158] Stafford-Banks CA, Rotenberg D, Johnson BR, Whitfield AE, Ullman DE. Analysis of the salivary gland transcriptome of Frankliniella occidentalis. PloS one. 2014;9(4):e94447.

[159] Allen CT, Kharboutli MS, McAllister CD, Coker CM, Cooper PE. Thrips, Weeds, and Tomato Spotted Wilt Virus. Arkansas Agricultural Experiment Station. 2000;475:11-6.

[160] Morsello SC, Kennedy GG. Spring temperature and precipitation affect tobacco thrips, Frankliniella fusca, population growth and tomato spotted wilt virus spread within patches of the winter annual weed Stellaria media. Entomol Exp Appl. 2009;130(2):138-48.

[161] Morsello SC, Beaudoin AL, Groves RL, Nault BA, Kennedy GG. The influence of temperature and precipitation on spring dispersal of Frankliniella fusca changes as the season progresses. Entomol Exp Appl. 2010;134(3):260-71.

[162] Jeger MJ, van den Bosch F, McRoberts N. Modelling transmission characteristics and epidemic development of the tospovirus–thrip interaction. Arthropod-Plant Interactions. 2015;9(2):107-20.

[163] Shalileh S, Ogada PA, Moualeu DP, Poehling H. Manipulation of Frankliniella occidentalis (Thysanoptera: Thripidae) by Tomato Spotted Wilt Virus (Tospovirus) Via the Host Plant Nutrients to Enhance Its Transmission and Spread. Environ Entomol. 2016;45(5):1235-42.

[164] Lozano S, Arenas A, Snchez A. Mesoscopic structure conditions the emergence of cooperation on social networks. PLoS one. 2008;3(4):e1892.

[165] Kirk WD, Terry LI. The spread of the western flower thrips Frankliniella occidentalis (Pergande). Agricult For Entomol. 2003;5(4):301-10.

[166] Managing Western Flower Thrips on Greenhouse Crops [Internet]. [].

[167] Robb KL, Parrella MP, Newman JP. Biology and control of the western flower thrips. . 1988.

Appendix A- Population Distribution of Two Spotted Spider Mites and its Predator in Experiment

Table A.1 Initial distribution of prey and predator presented as (*u*,v)

(*32*, **6**)	(*0*, **0**)	(*0*, **0**)
(*0*, **0**)	(*0*, **0**)	(*0*, **0**)
(*0*, **0**)	(*0*, **0**)	(*0*, **0**)
(*0*, **0**)	(*0*, **0**)	(*0*, **0**)
(*0*, **0**)	(*0*, **0**)	(*0*, **0**)
(*0*, **0**)	(*0*, **0**)	(*0*, **0**)
(*0*, **0**)	(*0*, **0**)	(*0*, **0**)
(32, **0**)	(*0*, **0**)	(*0*, **0**)

Table A.2 Distribution of prey and predator presented as (*u*,v) on day 6

(*60*, **5**)	(*24*, **1**)	(*0*, **0**)
(*14*, **0**)	(*12*, **0**)	(*0*, **0**)
(*0*, **0**)	(*0*, **0**)	(*0*, **0**)
(*0*, **0**)	(*0*, **0**)	(*0*, **0**)
(*0*, **0**)	(*0*, **0**)	(*0*, **0**)
(*0*, **0**)	(*0*, **0**)	(*0*, **0**)
(*0*, **0**)	(*0*, **0**)	(*0*, **0**)
(210, **0**)	(*130*, **0**)	(*2*, **0**)

Table A.3 Distribution of prey and predator presented as (*u*,v) on day 12

(*52*, **6**)	(20, **2**)	(*6*, **0**)
(32, **0**)	(*8*, **1**)	(*34*, **4**)
(*0*, **0**)	(*0*, **0**)	(*0*, **0**)
(*0*, **0**)	(*0*, **0**)	(*0*, **0**)
(*0*, **0**)	(*0*, **0**)	(*0*, **0**)
(*48*, **0**)	(*22*, **0**)	(*0*, **0**)
(*136*, **0**)	(*32*, **0**)	(*0*, **0**)
(56, **0**)	(*44*, **0**)	(*0*, **0**)

Table A.4 Distribution of prey and predator presented as (*u*,v) on day 18

(*48*, **2**)	(12, **8**)	(*28*, **4**)
(*64*, **5**)	(*24*, **9**)	(*76*, **8**)
(*80*, **3**)	(*84*, **9**)	(32, **6**)
(*76*, **3**)	(*70*, **2**)	(*12*, **0**)
(*260*, **6**)	(*76*, **0**)	(60, **0**)
(*220*, **0**)	(*0*, **0**)	(*368*, **0**)
(*0*, **0**)	(*156*, **2**)	(356, **0**)
(0, **0**)	(*0*, **0**)	(*136*, **0**)

Table A.5 Distribution of prey and predator presented as (*u*,v) on day 24

(*110*, **10**)	(80, **24**)	(*98*, **16**)
(*132*, **42**)	(*92*, **22**)	(*112*, **26**)
(*124*, **25**)	(*148*, **12**)	(*138*, **18**)
(*64*, **8**)	(*88*, **4**)	(*112*, **0**)
(*84*, **3**)	(*70*, **3**)	(*116*, **10**)
(*42*, **6**)	(*36*, **3**)	(30, **1**)
(*24*, **0**)	(*20*, **1**)	(32, **0**)
(48, **2**)	(*72*, **2**)	(*84*, **1**)

Appendix B- Infection Status of Tomato Plants in the Experiment of Spotted Wilt Virus and Western Flower Thrips System

Table B.1 Initial Status of tomato plants

	1	2	3	4	5	6	7	8	9	10
1	H	H	H	H	H	I	H	H	H	I
2	I	H	H	H	H	I	H	H	H	H
3	H	H	H	I	I	H	H	H	H	H
4	I	H	H	H	H	H	H	H	H	I
5	I	H	H	I	H	H	H	H	H	H
6	H	H	H	H	H	H	H	H	I	I
7	H	H	H	I	H	H	I	H	H	H
8	H	I	I	H	H	H	H	H	H	H

Table B.2 Infection status of tomato plants in week 2

	1	2	3	4	5	6	7	8	9	10
1	H	H	H	H	H	I	H	H	H	I
2	I	H	H	H	H	I	H	H	H	H
3	H	H	H	I	I	H	H	H	H	H
4	I	H	H	H	H	H	H	H	H	I
5	I	H	H	I	H	H	H	H	H	H
6	H	H	H	H	H	H	H	H	I	I
7	H	H	H	I	H	H	I	H	H	H
8	H	I	I	H	H	H	H	H	H	H

Table B.3 Infection status of tomato plants in week 3

	1	2	3	4	5	6	7	8	9	10
1	H	H	H	H	H	I	H	H	H	I
2	I	H	H	H	H	I	H	H	H	H
3	H	H	H	I	I	H	H	H	H	H
4	I	H	H	H	H	H	H	H	H	I
5	I	H	H	I	H	H	H	H	H	H
6	H	H	H	H	H	H	H	H	I	I
7	H	H	H	I	H	H	I	H	H	H
8	H	I	I	H	H	H	H	H	H	H

Table B.4 Infection status of tomato plants in week 4

	1	2	3	4	5	6	7	8	9	10
1	H	H	H	H	H	I	H	H	H	I
2	I	H	H	H	H	I	H	H	H	H
3	H	H	H	I	I	H	H	H	H	H
4	I	H	H	H	H	H	H	H	H	I
5	I	H	H	I	H	H	H	H	H	H
6	H	H	H	H	H	H	H	H	I	I
7	H	H	H	I	H	H	I	H	H	H
8	H	I	I	H	H	H	H	H	H	H

Table B.5 Infection status of tomato plants in week 5

	1	2	3	4	5	6	7	8	9	10
1	H	Q	Q	H	H	I	H	Q	Q	I
2	I	H	H	H	H	I	H	H	Q	Q
3	H	H	H	I	I	H	H	H	H	Q
4	I	H	H	H	H	H	H	H	H	I
5	I	H	H	I	H	H	Q	H	H	H
6	H	H	H	H	H	H	Q	Q	I	I
7	H	H	H	I	H	H	I	H	H	H
8	Q	I	I	Q	H	H	H	H	H	H

Table B.6 Infection status of tomato plants in week 6

	1	2	3	4	5	6	7	8	9	10
1	H	Q	Q	H	H	I	Q	Q	Q	I
2	I	H	H	Q	H	I	H	H	Q	Q
3	H	H	H	I	I	H	H	Q	Q	Q
4	I	H	H	Q	Q	Q	H	Q	Q	I
5	I	H	H	I	H	H	Q	Q	Q	Q
6	H	H	Q	Q	Q	H	I	I	I	I
7	H	H	H	I	Q	Q	I	H	H	H
8	Q	I	I	Q	Q	Q	Q	H	H	H

Table B.7 Infection status of tomato plants in week 7

	1	2	3	4	5	6	7	8	9	10
1	Q	I	I	Q	Q	I	I	I	I	I
2	I	Q	Q	I	Q	I	Q	Q	I	I
3	Q	Q	Q	I	I	Q	Q	I	I	I
4	I	Q	Q	I	I	I	Q	I	I	I
5	I	Q	Q	I	Q	Q	I	I	I	I
6	Q	Q	I	I	Q	I	I	I	I	I
7	Q	Q	Q	I	I	I	I	Q	Q	Q
8	Q	I	I	I	I	I	I	Q	Q	Q

Table B.8 Infection status of tomato plants in week 8

	1	2	3	4	5	6	7	8	9	10
1	I	I	I	I	I	I	I	I	I	I
2	I	I	I	I	I	I	I	I	I	I
3	I	I	I	I	I	I	I	I	I	I
4	I	I	I	I	I	I	I	I	I	I
5	I	I	I	I	I	I	I	I	I	I
6	I	I	I	I	I	I	I	I	I	I
7	I	I	I	I	I	I	I	I	I	I
8	I	I	I	I	I	I	I	I	I	I

(“H” is uninfected plants, “Q” is questionable infection plants, “I” is confirmed infection plants)